REACTIVE EXTRUSION OF PHOSPHATE CROSSLINKED POTATO STARCH

REACTIVE EXTRUSION OF PHOSPHATE CROSSLINKED POTATO STARCH

By

GANG WANG

A Thesis

Submitted to the School of Graduate Studies

In Partial Fulfillment of the Requirements

For the Degree

Master of Applied Science

McMaster University

MASTER   OF   APPLIED   SCIENCE   (2010)   McMaster   University

(Chemical Engineering)   Hamilton, Ontario

TITLE: Reactive extrusion of phosphate crosslinked potato starch

AUTHOR: Gang Wang

           B. Eng. (Liaoning Shihua University)

           B. Econ. (Liaoning Shihua University)

SUPERVISOR: Dr. Michael Thompson

NUMBER OF PAGES: xvii; 156

ABSTRACT

Biobased engineering materials from natural polymers such as potato starch and sisal fiber have increasingly attracted more attention compared with their petroleum counterparts due to biodegradability, environmental protection, and sustainable development. A novel biobased composite was developed based on phosphate crosslinked thermoplastic potato starch and sisal cellulose fiber aimed at improving mechanical properties and hydrophobicity.

First of all, potato starch has a much narrow processing window in extrusion machinery for manufacturing thermoplastic starch. Statistical analysis of differential scanning calorimetry data aided in extrusion processing design and optimization.

Then, bulk crosslinking of potato starch with sodium trimetaphosphate in the presence of rheological controlling additives (xanthan gum and glycerol) was investigated. Batch kinetics for the reaction was studied using in-situ attenuated total reflectance infrared spectroscopy monitoring. The spectra data were processed by multivariate analysis to reveal vibrational bands related to crosslinking and to identify important variables for reaction optimization. A kinetics model was created to facilitate developing a reactive extrusion process for bulk starch phosphate crosslinking. The effects of hydrocolloidal xanthan gum and glycerol on starch crosslinking reaction were also evaluated.

Furthermore, gelatinized starch with processing additives was crosslinked with and without natural sisal fiber using sodium trimetaphosphate within a co-rotating intermeshing twin screw extruder. The produced biocomposites were characterized using

infrared spectroscopy, sessile drop contact angle measurement, moisture content determination and tensile mechanical testing. Comparison of experiment data and calculated values from modified Tsai-Halpin model confirmed crosslinkages formed between the crosslinked starch matrix and sisal fibers. The mechanical properties of the biocomposites were significantly improved, but the moisture sensitivity was increased due to reduced crystallinity caused by crosslinking.

Finally, hydrophobicity of the starch biocomposite was improved by surface modification with Hydrores 266MB dispersion. Improvement of hydrophobicity is essential to maintaining superior mechanical properties of the biocomposites in surroundings with high relative humidity.

ACKNOWLEDGEMENTS

TABLE OF CONTENTS

INDEX OF FIGURES

Appendix Figures

INDEX OF TABLES

NOMENCLATURE

AGU	Anhydroglucose unit
AKD	Alkyl ketene dimmer
ASTM	American Society for Testing and Materials
ATR	Attenuated total reflectance
ASA	Alkenyl succinic anhydride
db	Dry starch weight basis
deg.	Degree
DG	Degree of gelatinization
DSC	Differential scanning calorimetry
E_c	Modulus of the composite
E_f	Modulus of the fiber
E_m	Modulus of the matrix
EC	Extent of crosslinking
EDS	Energy dispersive spectroscopy
FDA	United States Food and Drug Administration
FTIR	Fourier transform infrared spectroscopy
$I_{absorbance}$	Relative infrared absorbance intensity
IPN	Interpenetrating network
MGS	Mean granule size
Mw	Molecular weight

NMR	Nuclear magnetic resonance
PCL	Polycaprolactone
PHA	Polyhydroxyalkanoates
PHB	Polyhydroxybutyrate
PLA	Polylactic acid
PLS	Partial least squares
PSI	Pounds per square inch
RC	Rate constant
RH	Relative humidity
SEM	Scanning electron microscope
STMP	Sodium trimetaphosphate
T_c	Crystallization temperature, °C
T_g	Glass transition temperature, °C
T_{gel}	Gelatinization temperature, °C
T_m	Melting temperature, °C
TPS	Thermoplastic starch
TSE	Twin screw extruder
V_f	Volume fraction of the fiber
WAXS	Wide angle X-ray scattering
XRD	X- ray diffraction analysis
ΔH	Enthalpy, J/g
ξ	Constant related to aspect ratio and fiber orientation

CHAPTER 1 INTRODUCTION

Polymers derived from petroleum possess excellent durability, processability, mechanical, thermal, and electrical properties. Therefore, they dominate many application areas including packaging, construction, automotive, and healthcare. The consumption of these plastics has been growing astronomically around the world. For instance, 11 million tons of non-biodegradable plastic waste is generated each year in United States alone, which takes hundreds of years to decompose and causes a disastrous impact on our ecosystem (Siddique, Khatib, & Kaur, 2008). The looming energy crisis will deteriorate and petroleum reserves will be eventually depleted if dependency on petroleum continues.

The urgent issues of pollution and energy crisis need to be addressed immediately by gradually substituting petroleum feedstock with renewable natural resources and developing environmentally friendly bio-based polymers and composites. Novel bio-based materials from natural polymers have increasingly attracted much attention compared with their petroleum counterparts over the past decade due to biodegradability, environmental protection, and sustainable development (Huda *et al.*, 2005; Mohanty, Misra, & Drzal, 2002; Rosentrater & Otieno, 2006; Yu *et al.*, 2007). Potato starch is one of the most abundant renewable natural resources in Canada, which is ideal to be used as feedstock for manufacturing biodegradable materials suitable for not only packaging, but also engineering and pharmaceutical applications. Starch is usually gelatinized with water and other plasticizers under heat and shear to form a thermoplastic starch (TPS) for the

purposes of reducing brittleness and improving processability (Bonacucina *et al.*, 2006; F. W. Xie *et al.*, 2006). TPS has been blended with various other polymers with superior properties, such as poly (lactic acid) (PLA) or Polyhydroxyalkanoates (PHA), to extend its usefulness (Park *et al.*, 2000; N. Wang, Yu, & Ma, 2007; X. L. Wang, Yang, & Wang, 2003). These bio-based materials with environmental benefits are considered as the next generation of materials for future commodity markets because they have the potential to compete against and gradually replace non-biodegradable petroleum based polymers. However, weak mechanical properties and high water sensitivity of starch based materials limit their usage in many applications at present and make replacement of petroleum based polymers difficult (Huneault & Li, 2007; X. L. Wang, Yang, & Wang, 2003).

One of the most important approaches to improving the weak mechanical properties of bio-based polymers is the incorporation of reinforcing fillers into the matrix. Natural fibers (jute, flax, hemp, sisal, etc.) have been widely utilized as reinforcement to improve mechanical properties of TPS and other biodegradable polymers because they are not only as renewable, biodegradable, and abundant as starch, but also have superior specific mechanical properties (Averous & Boquillon, 2004; Alvarez & Vazquez, 2006; Belhassen et al., 2009; Canigueral et al., 2009; Corradini et al., 2009; Curvelo, de Carvalho, & Agnelli, 2001; Graupner, 2008; Guimaraes et al., 2010; Huneault & Li, 2007; Saiah et al., 2009). Interfacial interactions via hydrogen bonding play an important role in a composite of starch and sisal cellulose fiber. Covalent interaction via crosslinking is believed to reinforce existing hydrogen bonding between the sisal fiber filler and the

starch matrix in this thesis, requiring study to determine if the mechanical and water absorption properties of the composite could be further improved. In addition, crosslinking contributes to increasing stability of the starch matrix towards high shear, temperature, and acidity due to the reinforcing effect of crosslinking on the existing hydrogen bonding between molecular chains (Nabeshima & Grossmann, 2001).

This thesis focuses on reactive extrusion of crosslinked potato starch and its novel biocomposite reinforced by natural sisal fiber in the presence of rheological control additives, such as hydrocolloidal xanthan gum and glycerol. The crosslinking reaction was monitored by in-situ attenuated total reflectance Fourier transform infrared spectroscopy (ATR/IR) in order to understand the kinetics of starch crosslinking reaction in the presence of the additives. Then, a reactive extrusion process of bulk phosphate crosslinking of potato starch was developed. Water absorbance and mechanical properties of the extrusion products were investigated. Finally, surface modification to the biocomposites was fulfilled to reduce water sensitivity and to maintain superior mechanical properties in surroundings with high relative humidity. The sisal fiber reinforced crosslinked starch biocomposite has the potential to be widely applied in packaging, construction, medical, and automotive industries.

1.1 Research objectives

The objectives of the project were to investigate reactive extrusion of thermoplastic potato starch, to examine the bulk kinetics of starch crosslinking in the presence of rheology controlling additives such as hydrocolloidal xanthan gum and glycerol, and to develop an extrusion process for producing biodegradable natural sisal fiber reinforced biocomposite based on crosslinked starch. The main tasks performed in the project were as follows:

- to investigate the optimal condition of gelatinization and the crosslinking reaction of potato starch suitable for reactive extrusion processing;

- to study the kinetics of starch bulk crosslinking reaction in the presence of hydrocolloidal xanthan gum and glycerol by in-situ ATR/IR monitoring;

- to explore the synergetic effects of both colloidal xanthan gum and glycerol on starch crosslinking reaction with STMP using multivariate analysis;

- to develop a bulk crosslinking process for potato starch modification in a twin screw extruder with suitable screw design and liquid dispersion;

- to generate a biocomposite formed by crosslinking starch and sisal fiber and to evaluate its mechanical and water absorption properties;

- to improve hydrophobicity of thermoplastic starch by modifying the composite surface with Hydrores 266MB emulsion (an alkyl ketene dimer) and thus improve water resistance and maintain superior mechanical properties in high relative humidity surroundings.

1.2 Outline of thesis

This thesis based on potato starch research project funded by ABIP BioPotato Network of Agriculture and Agri-Food Canada. The thesis is organized into 9 chapters. The framework of the potato starch research thesis is outlined as follows:

Chapter 1 presents a brief introduction to the research, objectives of the project, and a brief structure of this thesis. Chapter 2 presents a pertinent literature review. Background of potato starch research and previous work on starch gelatinization, crosslinking, production, characterization, properties of colloidal xanthan gum, and biodegradable natural polymer composites are discussed in this chapter. Chapter 3 describes the morphology and gelatinization behavior of potato starch. Statistical analysis of the DSC data lays a foundation for further extrusion work. Chapter 4 is a sandwiched paper accepted by the 2010 Annual Technical Conference (Orlando, FL) sponsored by the Society of Plastics Engineers. Extrusion of gelatinized potato starch and related process optimization are discussed in this chapter. Chapter 5 is a sandwiched paper submitted to Carbohydrate Polymers (2010). Influences of hydrocolloidal xanthan gum and glycerol on the kinetics of bulk phosphorylation of potato starch is examined in this chapter. Chapter 6 is another sandwiched paper submitted to Carbohydrate Polymers (2010). Properties of crosslinked starch biocomposites reinforced with sisal cellulose fiber are explored in this chapter. Chapter 7 discusses surface modification of the biocomposites and its effect on hydrophobicity. Chapter 8 summarizes the conclusions on the potato starch research. To facilitate future research work, some recommendations are presented in Chapter 9.

CHAPTER 2 LITERATURE REVIEW

2.1 Structure and properties of native and gelatinized potato starch

2.1.1 Morphology and chemical structure of native potato starch

Potato starch is one of the most abundant natural polymer resources. According to recent research, potato starch is considered as an ideal raw material for producing biodegradable materials suitable for not only engineering (Yu, Dean, & Li, 2006), but also pharmaceutical applications such as excipients (Braz, Hechenleitner, & Cavalcanti, 2007; Dumoulin et al., 1998). However, potato starch has disadvantages regarding its high amylopectin content and low granule porosity, leading to a narrow processing window in extrusion operations dealing with the preparation of biodegradable materials (DellaValle et al., 1995).

Potato starch granules have the largest sizes among various types of starches including wheat, rye, maize, oat, rice, sago, and cassava starch. As shown in Figure 2.1, potato starch usually has ellipsoidal or spherical granules with sizes ranging from 15 to 121 microns, and starch with larger average size is favored for certain applications (Moss, 1976). Amylose (a linear polysaccharide) and amylopectin (a branched polysaccharide) coexist in potato starch. The amylopectin content in potato starch is ~79 %, which is higher than that in common corn starch (72 %) and wheat starch (72 %) (BeMiller & Whistler, 1996). The structures of linear amylose and branched amylopectin are illustrated in Figure 2.2. Amylose molecules are composed of α (1-4) glycosidic bonded D-glucose and tend to form hydrogen-bonded structure, while amylopectin molecules are

α (1-4)-linked D-glucose chains joined by α (1-6)-linkage, forming a highly branched structure (Martin & Smith, 1995). There are mainly three types of amylopectin chains. *A-chain* does not carry other chains through C-6 linkage; *B-chain* carries other A/B-chains; *C-chain* carries the only reducing end of the macromolecule (Bertoft, 2004). A schematic illustration of the structures in a starch granule at varied length scales is represented in Figure 2.3.
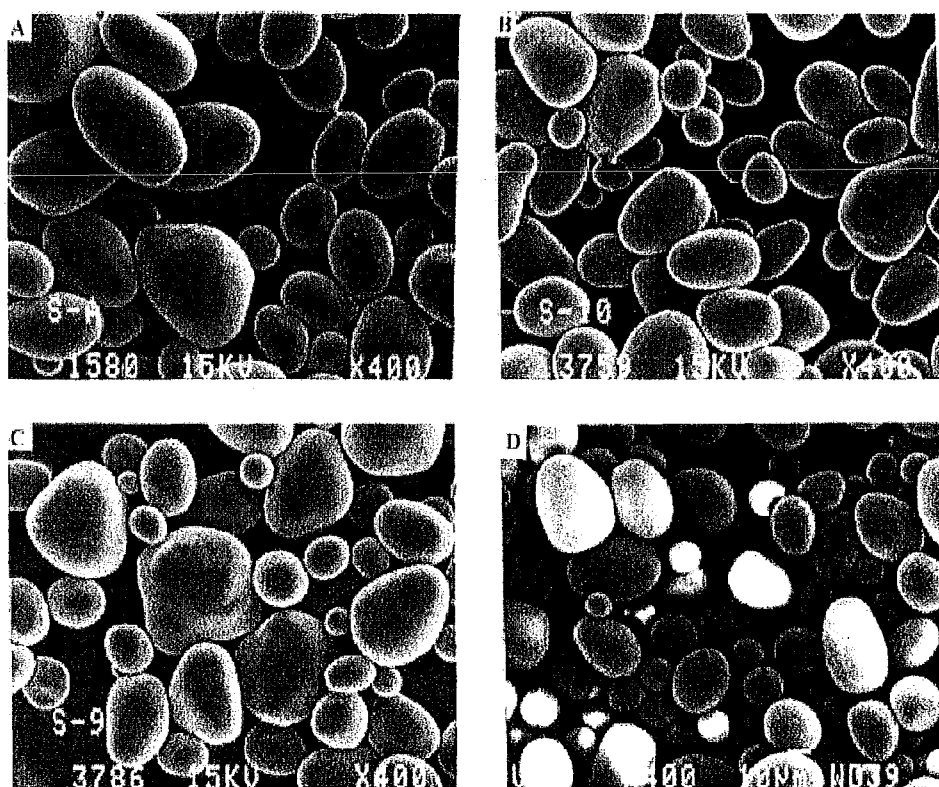
Figure 2.1. SEM images of (A) Kufri Jyoti, (B) Kufri Sindhuri, (C) Kufri Sutlej and (D) Kufri Chandermukhi native potato starches (400x magnification, bar = 10 μm) (N. Singh & Kaur, 2004).

A

B
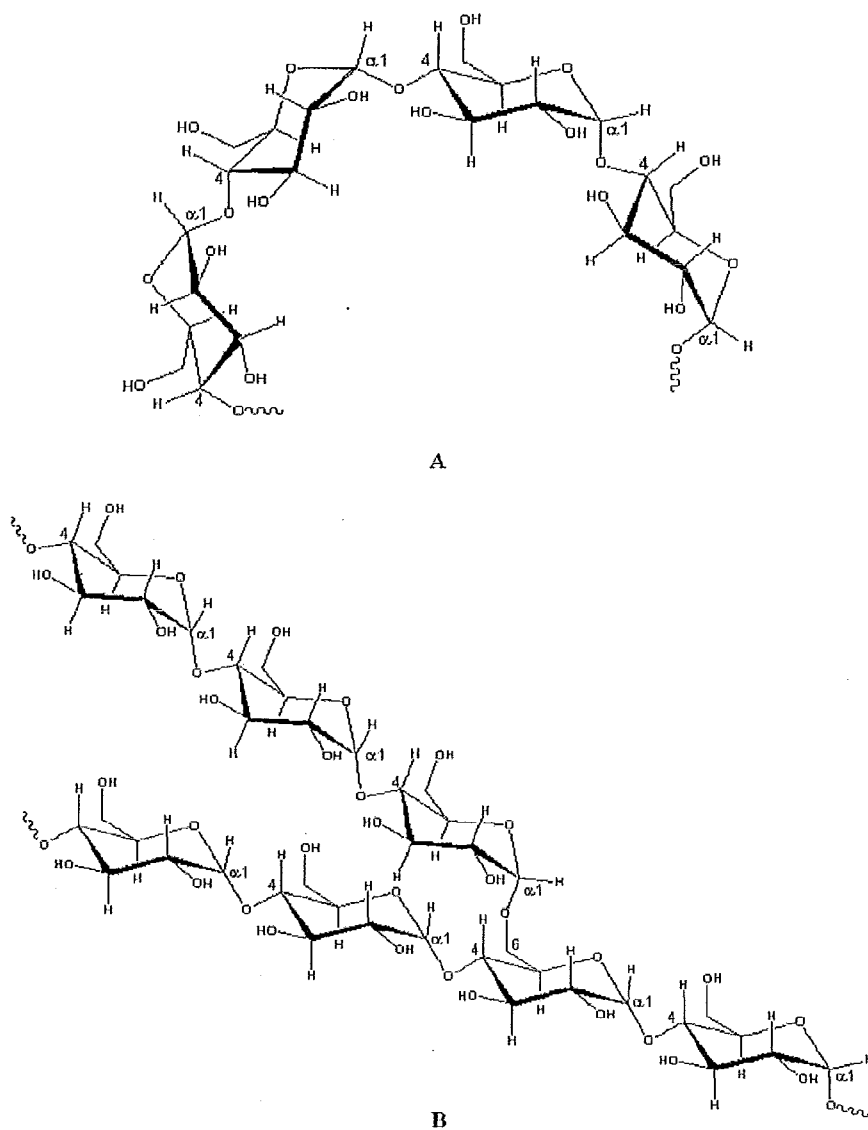
Figure 2.2. The structures of linear amylose (A) and branched amylopectin (B) (Denardin & da Silva, 2009).
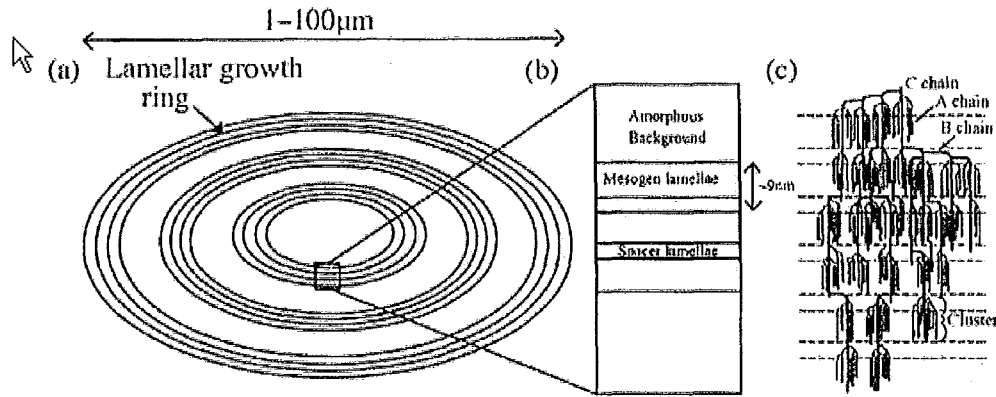
Figure 2.3. A schematic illustration of the structures in a starch granule at varied length scales (J. P. J. Jenkins, Cameron, & Donald, 1993).

2.1.2 Crystallinity of the native potato starch

A starch granule shows growth rings with alternating semicrystalline and amorphous regions (Figure 2.3). The semicrystalline region is composed of crystalline and amorphous lamellae. The crystalline lamellae are formed by clustering of about 9 nm long amylopectin A-chain branches with double helix structure as shown in Figure 2.4, while the amorphous lamellae consist of both amylose and amylopectin B-chains (Martin & Smith, 1995). A, B, and C type crystalline structures are usually identified by wide angle X-ray scattering. A-type crystallinity is related to short A-chains that form crystalline clusters. B-type crystallinity is associated with longer A-chains. C-type crystallinity is due to A-chains with medium length (P. J. Jenkins & Donald, 1995).
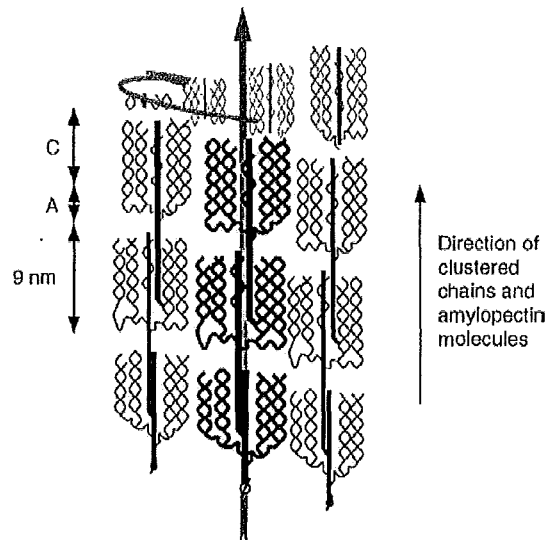
Figure 2.4. The super-helix structure of amylopectin based upon the cluster model (Bertoft, 2004).

2.1.3 Gelatinization and retrogradation of potato starch

Application of starch to engineering materials usually involves converting raw starch into gelatinized starch containing various plasticizers, i.e. thermoplastic starch (TPS), which has been widely utilized in preparing thermoplastic blends with other biodegradable polymers such as poly (lactic acid) (PLA) or Polyhydroxyalkanoates (PHA) (Park *et al.*, 2000). Gelatinization or water-assisted melting is the phenomenon of disrupting starch crystalline structure by heating starch together with water (Parker & Ring, 2001). Intact native starch granules display birefringence as Maltese crosses under microscope with polarized illumination, while gelatinized starch granules lose the characteristic birefringence, indicating irreversible swell and disintegration of starch granules into macromolecules (Singh & Singh, 2003). Starch gelatinization phenomenon can be conveniently detected by differential scanning calorimetry (DSC) at varied water

contents (Steeneken & Woortman, 2009). The gelatinization temperature of native starch varies among different species, which may be affected by varied mean granule size (MGS) (Puncha-Arnon et al., 2008). Puncha-Arnon reported that gelatinization temperature of canna, potato, mung bean and rice starches was 72.4 °C, 65.8 °C, 70.1 °C, and 75.2 °C respectively, the gelatinization temperature of potato starch being the lowest among the four starch species. The gelatinization temperature range for a single granule is narrow, but the range becomes wider for a granule population due to minor compositional variation between particles. Integrity of swollen granules is usually maintained without shear force below 100 °C (Parker & Ring, 2001). Gelatinization causes starch to partially solubilize in water via amylose leaching under mild shear and heating conditions. Total molecular dissolution occurs when the temperature increases beyond 130 °C (Steeneken & Woortman, 2009).

Freely dissociated starch molecule chains present after gelatinization may once again form crystalline structures during storage via hydrogen bonding. The phenomenon is called retrogradation (Biliaderis & Zawistowski, 1990). Both amylopectin content and structure variations contribute to retrogradation. The retrogradation rate constant increased at lower storage temperatures (Kim, Wiesenborn, & Grant, 1997). Retrograded potato starch showed broader endothermic curve and 10-20 °C lower onset and peak temperatures in DSC thermogram than before the original gelatinization process (Kim, Wiesenborn, & Grant, 1997). This is because re-associated molecules generate crystallite with weaker structure, the disruption of which occurs at lower energy level (White, Abbas, & Johnson, 1989).

2.2 Structure, production, and properties of crosslinked starch

2.2.1 Introduction to crosslinked starch and its applications

Native starch is not resistant to shear, acidity, and high temperature, making it unstable for specific purposes. To extend its applications, starch is crosslinked to form chemical bonds between molecular chains. The crosslinking bonds function as bridges to reinforce the existing hydrogen bonds between the molecular chains, which imparts crosslinked starch with increased stability towards high shear, temperature, and acidity (Nabeshima & Grossmann, 2001). Crosslinked starch has traditionally been used as thickener, adhesive, and texturizer in the food industry (Thomas & Atwell, 1999). Atichokudomchai and Varavinit (2003) reported that crosslinked Tapioca starch could be used in pharmaceutical tablets after acid hydrolysis modification (Atichokudomchai & Varavinit, 2003). In Dumoulin et al's work (1998), crosslinked starch was applied to excipients for controlled drug release (Dumoulin *et al.*, 1998). The drug release time was found to be affected by degree of crosslinking. Crosslinked starch can also be applied to biodegradable packaging and engineering materials such as fiber-reinforced crosslinked starch composites, though there is no mention in the literature yet for it.

2.2.2 Structure and characterization of crosslinked starch

The structural analysis of crosslinked starch was investigated using both X- ray diffraction analysis (XRD) and Fourier Transform Infrared (FT-IR) spectroscopy by Dumoulin (Dumoulin *et al.*, 1998). The high amylose starch was crosslinked by 6 wt %, 11 wt %, and 20 wt % (based on starch weight) epichlorohydrin respectively. XRD

results showed that the diffraction pattern of crosslinked starch shifted from B-type to V-type with the increased extent of crosslinking, indicating a high extent of crosslinking contributed to more disordered structure, while low to moderate extent of crosslinking helped form highly ordered structure. This was because higher extent of crosslinking hindered the mobility of chains, disrupted double helix structure, and reduced hydrogen-bonding, leading to more expanded and disordered structure (Dumoulin *et al.*, 1998).

Indirect characterization of the crosslinked starch granule produced by solution reaction has been done by measuring the degree of swelling, sedimentation time, and calculation of water solubility/absorption indices (Dubois *et al.*, 2001; Dulong *et al.*, 2004; Li *et al.*, 2009; Luo *et al.*, 2009; Mao *et al.*, 2006; Nayouf, Loisel, & Doublier, 2003; Seker & Hanna, 2005) However, these methods are not applicable to bulk modified samples since the end-product of an extruder must be pelletized or ground and therefore, their values bear little relationship to the native starch for comparison. Spectroscopic techniques are generally more informative for both solution and bulk reactions. Nuclear magnetic resonance techniques (^{13}C, ^{1}H, ^{31}P NMR) have been used to establish the reaction pathways through structural changes to the starch (Cury *et al.*, 2009; Delval *et al.*, 2004; Le Bail, Morin, & Marchessault, 1999; Sang, Prakash, & Seib, 2007; Shalviri *et al.*, 2010; Simkovic *et al.*, 2004). Similarly, Fourier transform infrared spectroscopy (FT/IR) has been employed to verify the characteristic chemical structure in solution-crosslinked starch samples (Zhang and Wang, 2009; Shalviri, et al., 2010). A strong adsorption peak appeared at about 1000 cm^{-1} in FT/IR spectrum, which was attributed to the characteristic vibration of P-O-C bond (Zhang & Wang, 2009). Shalviri et al. (2010)

a) low-moderate cross-linking degree; most contracted network and high hydrogen - bonding.

b) high cross-linking degree; much more interchain glyceric bridges; hydrogen-bonding is hindered, more expanded and more disordered network.
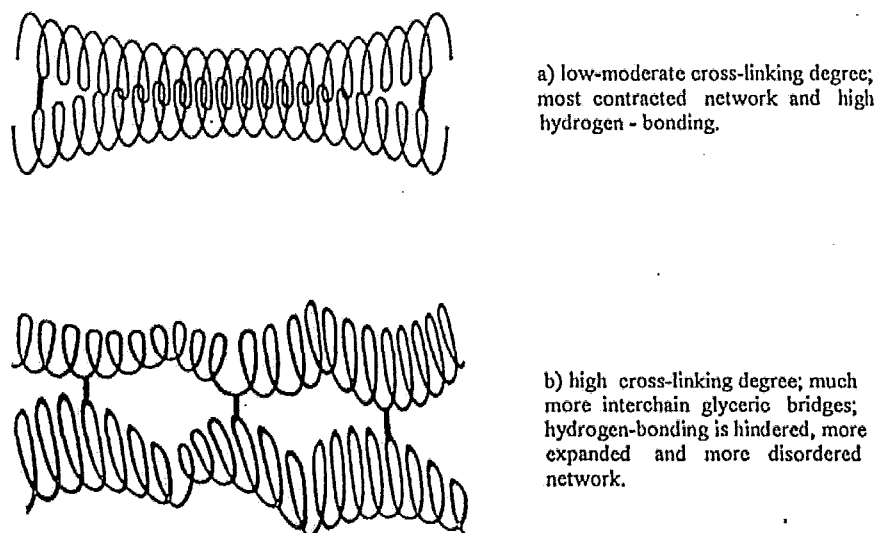
Figure 2.5. Hypothetical representation of the covalent and H-bonding stabilization of crosslinked starch for (a) low/moderate and (b) high degree of crosslinking (Dumoulin et al. 1998).

also reported a newly emerged peak at around 1266 cm^{-1} in FT/IR spectrum that was a characteristic peak of P=O bonds in crosslinked polysaccharides (Shalviri *et al.*, 2010).

2.2.3 Mechanism of starch crosslinking reaction

Though various crosslinking agents such as tetraethylene glycol diacrylate could be used for starch crosslinking (Marques *et al.*, 2006), the most commonly used crosslinking agents for starch are epichlorohydrin and sodium trimetaphosphate (STMP) (Demirgoz *et al.*, 2000; Dubois *et al.*, 2001). The former is normally avoided by starch manufacturers due to its carcinogenic nature (S. X. Xie, Liu, & Cui, 2005). The mechanism of starch crosslinking with multifunctional reagent sodium trimetaphosphate was proposed by Lim and Seib as shown in Figure 2.6 (Lim & Seib, 1993). They proposed that the starch crosslinking involved ring-opening of STMP to form starch

tripolyphosphate and the latter further reacted with starch to produce distarch phosphate, i.e. crosslinked starch, at the condition of pH above 8 (Lim & Seib, 1993). The pH of the system plays a major role in the formation of diesters in solution reactions, but in bulk processes, with reduced mobility of ions, processors favor the inclusion of other catalytic species as well. Catalytic species like sodium sulphate and sodium carbonate have been demonstrated to improve conversion towards the distarch phosphate (Mao *et al.*, 2006; Woo & Seib, 1997). Sodium sulphate not only promotes absorption of alkali and crosslinking reagents into starch granules, but also creates ionic strength that facilitates crosslinking reaction between negatively charged starch alkoxide and phosphoryl reactant species (Woo & Seib, 1997).
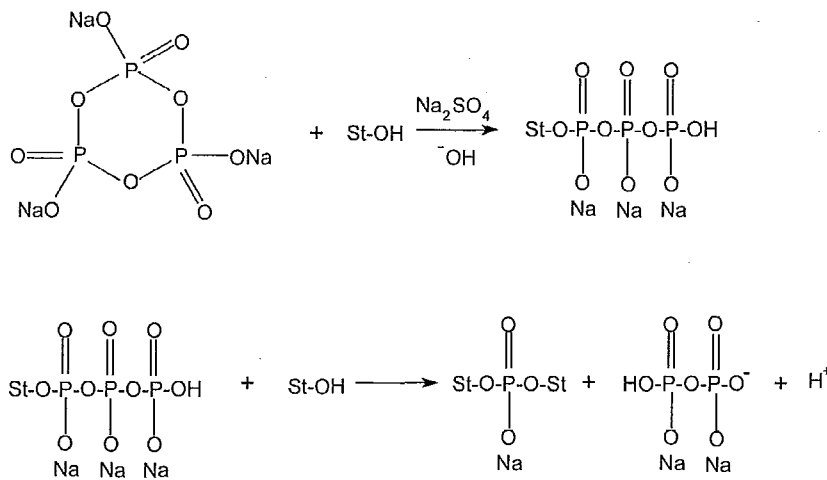
Figure 2.6. Proposed mechanism of starch crosslinking reaction with sodium trimetaphosphate by Lim & Seib (1993).

2.2.4 Extrusion of crosslinked starch

Extrusion technique has been applied to various types of starch modification including crosslinking using either single screw extruder or twin screw extruder (TSE) (Murua-Pagola, Beristain-Guevara, & Martinez-Bustos, 2009; Nabeshima & Grossmann, 2001; Seker & Hanna, 2005, 2006). Traditional starch crosslinking is generally performed in aqueous solution (Cury, Klein, & Evangelista, 2008; Demirgoz *et al.*, 2000; Dulong *et al.*, 2004; Le Bail, Morin, & Marchessault, 1999; Li *et al.*, 2009), and most of them are applied to starch films prepared by solution casting (Marques *et al.*, 2006; Rioux *et al.*, 2002). However, crosslinking starch with excess water is not suitable for reactive extrusion process. Therefore, a modification to the traditional method of crosslinking starch in an aqueous solution is necessary. The bulk phosphate crosslinking reaction is performed in a semi-solid state to avoid solution leaking and to facilitate efficient mass transport in a twin screw extruder in this thesis. The TSE functions as a two-stage bioreactor in which starch gelatinization happens at the first stage and phosphate crosslinking reaction occurs at the second stage. The reaction rate of acetylation reaction for raw granular formed starch is believed to be more than 100 times slower compared to gelatinized starch (deGraaf *et al.*, 1995). The benefit of crosslinking starch immediately after its gelatinization in a TSE is considerable reduction of reaction time while achieving desired extent of crosslinking, making extrusion technique suitable for starch modification by phosphate crosslinking.

2.3 Structure and properties of colloidal xanthan gum

2.3.1 Structure of xanthan gum

Xanthan gum is a bacterium *Xanthomonas campestris* generated extracellular polysaccharide (Dumitriu, Vidal, & Chornet, 1996). Xanthan gum is a cream-colored powder when in solid state. Xanthan gum is soluble in water, but insoluble in ethanol. The main functional applications are thickener, stabilizer, emulsifier, and foaming agent (FAO/WHO, 1999). The chemical structure of xanthan gum is shown in Figure 2.7. Xanthan gum consists of repeating pentasaccharide units containing two glucose units, two mannose units, and one glucuronic acid unit. The main backbone structure of xanthan gum is composed of (1-4)-linked β-D-glucose units (Garcia-Ochoa *et al.*, 2000). The hydroxyl groups in xanthan gum have the potential to be crosslinked with starch.
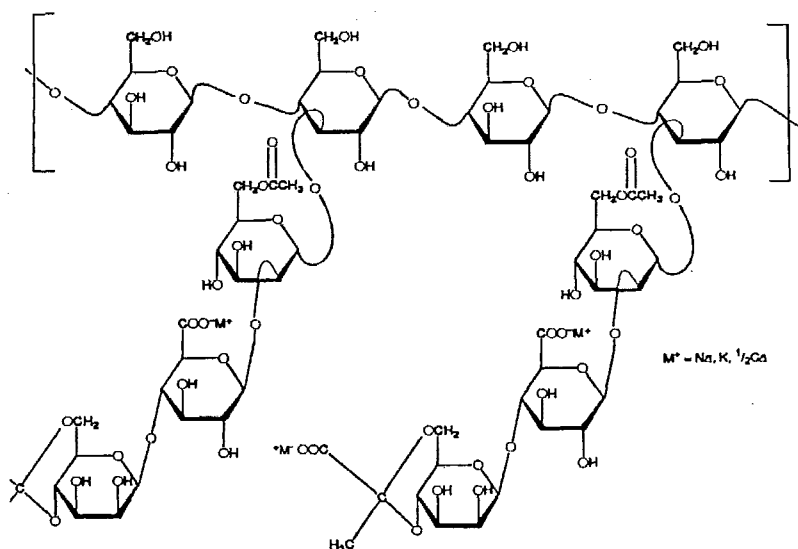
Figure 2.7. The chemical structure of xanthan gum generated by *Xanthomonas campestris* (Garcia-Ochoa *et al.*, 2000).

2.3.2 Application and properties of xanthan gum

Xanthan gum has been used for improving the viscosity in drilling mud and in the oil-recovery industry. Xanthan gum has also been utilized as a food additive due to its non-toxic nature according to United States Food and Drug Administration (FDA). Xanthan gum functions as thickener, emulsion stabilizer, temperature stabilizer, food ingredient compatibilizer, and rheological modifier (Garcia-Ochoa et al., 2000). Xanthan solutions are highly viscous and show pseudoplastic behavior at moderate temperatures. Xanthan gum possesses helix and random coil conformations that are dictated by dissolution temperature. Concentration positively affects the viscosity of xanthan solutions due to molecular entanglement and interaction, while temperature negatively influences viscosity. The pH value does not affect viscosity of xanthan solutions (Garcia-Ochoa et al., 2000).

2.3.3 Effect of xanthan gum on starch/xanthan gum blends

The addition of xanthan gum to various blending systems has been widely practiced. Xanthan gum and other gums like guar gum have been utilized to modify rheological properties and freeze-thaw stability of starch (Achayuthakan & Suphantharika, 2008; Nagano, Tamaki, & Funami, 2008; Pongsawatmanit & Srijunthongsiri, 2008; Ptaszek & Grzesik, 2007). The peak viscosity of xanthan/starch paste increases with increased xanthan gum content. It is believed that the accessible volume for xanthan gum decreases when starch granules swells, leading to increase of xanthan gum concentration, and thus sharply increase its viscosity in solution (Achayuthakan & Suphantharika, 2008). The

syneresis of starch gels was reduced from 74.45 % to 66.43 % by incorporation of 1 % xanthan gum, indicating a cryo-protective functionality of xanthan gum (Weber, Queiroz, & Chang, 2008).

The addition of xanthan gum to starch crosslinked with adipoyl chloride in a conical twin-screw extruder was reported by Miladinov and Hanna (Miladinov & Hanna, 1995). But they did not explore the possibility of the gum participating in the reaction, nor consider what synergetic effects of both hydrocolloidal xanthan gum and glycerol could have on starch crosslinking with STMP in bulk. So the present work has been carried out to generate knowledge in this area.

2.4 Biodegradable biocomposites

2.4.1 Introduction to biodegradable polymers

Biodegradability refers to being able to decompose by biological sources in dump sites after required service lifetime (Mohanty, Misra, & Drzal, 2002). The conventional feedstock in chemical engineering is mainly petroleum and natural gas. Traditional plastic products based on petroleum and natural gas are not normally biodegradable on a short time scale (i.e. months) and thus have caused serious pollution to our environment. Moreover, petroleum reserves are finite and not renewable, the formation of petroleum requiring millions of years. In addition, starch and natural fiber have advantages of relatively low cost and wide availability. Therefore, natural polymers such as starch and cellulose are ideal alternatives to traditional petroleum-based resins as feedstock in the modern plastics industry mainly due to their environmentally friendly and renewable nature.

2.4.2 Biodegradable biocomposites containing natural cellulose

Biocomposites, i.e. composite materials containing natural fibers and either petroleum based polymers (polypropylene) (Doan, Gao, & Mader, 2006; Qiu *et al.*, 2003; Xu *et al.*, 2008) or biodegradable polymers (PLA, PHA etc.), have attracted much recent attention due to the awareness of consumers to environment protection (Graupner, 2008; John & Thomas, 2008). Biocomposites have become a promising business. They have been applied to window and door frames, packaging, furniture sections, and automotive parts (Xu *et al.*, 2008). The wide application of fiber reinforced biocomposites is summarized in Figure 2.8.

Natural cellulose fibers have been investigated in recent years (George, Sreekala, & Thomas, 2001). Natural cellulose fibers include bast (jute, flax, hemp), leaf (sisal, pineapple), and seed/fruit fibers (cotton, oil palm) (George, Sreekala, & Thomas, 2001). Natural cellulose fiber is composed of (1-4)-β glycosidic linked D-anyhydroglucose units with degree of polymerization of about 10,000 (John & Thomas, 2008). The hydroxyl groups help create crystalline structure via hydrogen bonding to strengthen physical
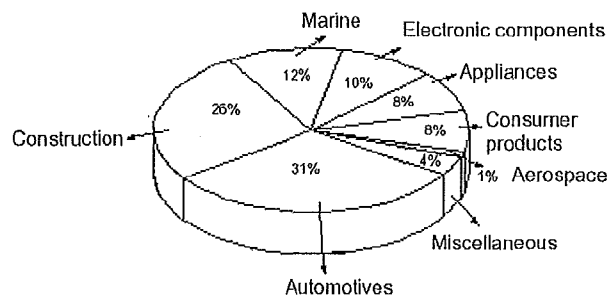
Figure 2.8. The application of fiber reinforced biocomposites (John & Thomas, 2008).

properties. The hydroxyl groups have the potential to be crosslinked (Seo *et al.*, 2009) or participate in hydrogen bonding to further strengthen the overall structure of a hydrophilic matrix. Natural cellulose fibers have replaced aramide, carbon, or glass fibers as reinforcing components in polymeric composites because natural cellulose fibers are renewable, biodegradable, abundant, and have higher specific mechanical properties (Trejo-O'Reilly, Cavaille, & Gandini, 1997). For example, the specific mechanical properties of sisal fiber are comparable to glass fiber due to its low density (Table 2.1) (Eichhorn *et al.*, 2001). Natural fibers are less brittle compared to more commonly employed inorganic fibers (like glass or carbon fibers) and thus are able to survive the harsh conditions of an extrusion or injection molding process with minimal attrition. They also help minimize wear damage to costly machinery due to their reduced abrasiveness compared to other reinforcement fibers used in polymer composites (Beckermann & Pickering, 2008). Since cellulose fibers are hydrophilic and polar, while the traditional polymer composite matrix such as polypropylene is hydrophobic and non-polar, the interfacial adhesion can be improved by introducing a compatibilizer such as maleic anhydride-polypropylene copolymer (Bledzki & Faruk, 2006), cellulose ester (Takatani *et al.*, 2008), lysine based diisocyanate (John & Thomas, 2008), or natural lignin (Graupner, 2008). Compatibilizer is not required in natural fiber reinforced crosslinked starch because that cellulose and starch have similar chemical structure and hydrophilicity.

There are various methods of producing starch/fiber composites in literatures. Film stacking, i.e. laminating multiple layers of thermoplastic starch film and natural

Table 2.1.Mechanical properties of sisal fiber and glass fiber (Eichhorn et al., 2001)

Fiber	Density (g cm^{-3})	Elongation at break (%)	Tensile strength (MPa)	Young's modulus (GPa)
Sisal	1.5	2.0-2.5	511-635	9.4-22.0
E-glass	2.5	2.5	2000-3500	70.0

fiber alternatingly followed by hot pressing, was employed to produce thermoplastic starch/flax fiber composites (Romhany, Karger-Kocsis, & Czigany, 2003). A batch mixer has also been used to prepare natural fiber/thermoplastic starch composites (Belhassen *et al.*, 2009; Canigueral *et al.*, 2009; Corradini *et al.*, 2009; Curvelo, de Carvalho, & Agnelli, 2001; Guimaraes *et al.*, 2010). Extrusion processing has been found to be effective not only in starch modification, including starch thermomechanical treatment (DellaValle *et al.*, 1995), plastification (VanderBurgt, VanderWoude, & Janssen, 1996), enzymatic hydrolysis and saccharification (Govindasamy, Campanella, & Oates, 1997), phosphorylation (Murua-Pagola, Beristain-Guevara, & Martinez-Bustos, 2009), and crosslinking (Murua-Pagola, Beristain-Guevara, & Martinez-Bustos, 2009; Nabeshima & Grossmann, 2001; Seker & Hanna, 2005, 2006), but also in manufacturing natural fiber/thermoplastic starch composites (Averous & Boquillon, 2004; Saiah *et al.*, 2009). Bulk production of crosslinked starch/natural fiber biocomposites in a twin extruder have not been discussed in open literature so far. Therefore, our work mainly focuses on developing a bulk process to manufacture biodegradable sisal fiber reinforced crosslinked starch biocomposites in a twin screw extruder and investigating how crosslinking and fiber loading affect mechanical properties of the biocomposites.

2.5 Surface modification

Natural fiber reinforced polymer composites, especially natural fiber reinforced crosslinked starch, are susceptible to high moisture surroundings. Water incorporation negatively affects mechanical properties and durability over the expected service lifetime of the composites, which necessitates surface modification in order to generate more hydrophobic behaviour. Paraffin can improve surface hydrophobicity, but it weakens bonding strength and lacks durability (Hundhausen, Militz, & Mai, 2009). Low molecular weight phenol formaldehyde resin was utilized to improve water resistance of chip boards (Kajita & Imamura, 1991). Alkyl ketene dimer (AKD) and alkenyl succinic anhydride (ASA) have been used as sizing agents to enhance resistance to liquid and to increase wet strength of cellulose in the paper industry (Neimo, 1999). The hydroxyl groups react with ASA or AKD to form esters and thus hydrophobic properties are improved. The reaction mechanism of AKD with hydroxyl groups is shown in Figure 2.9. Similarly, hydroxyl groups of crosslinked starch can also combine AKD through esterification to achieve hydrophobic surface and water resistance ability. AKD has been used for improving hydrophobicity of either starch or cellulose fiber in previous works, while in this thesis, a new type of AKD, Hydrores 266MB emulsion, is employed to modify the hydrophobicity of a novel crosslinked starch biocomposites reinforce by natural sisal fiber.
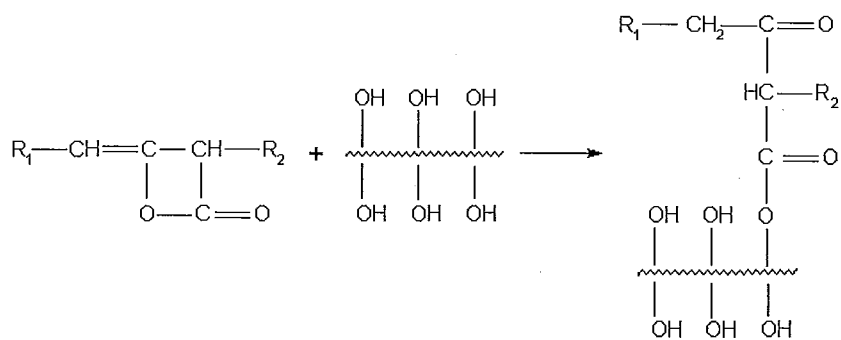
Figure 2.9. The reaction mechanism of AKD with hydroxyl groups to form β-keto-ester (Hundhausen, Militz, & Mai, 2009).

CHAPTER 3 MORPHOLOGY AND GELATINIZATION BEHAVIOR OF POTATO STARCH

3.1 Introduction

Study of potato starch morphology such as porosity and granule size distribution helps to understand the incorporation of water into starch granules for gelatinization and crosslinking reaction. Investigation of potato starch gelatinization behavior is important to determining water and glycerol content for the optimal starch gelatinization result during the extrusion process. The literature review regarding starch morphology and gelatinization is included in Chapter 2.

3.2 Experimental

3.2.1 Materials

Potato starch used in this research work was obtained from Manitoba Starch Products (Carberry, Manitoba, Canada). It is a food-grade unmodified potato starch. The analytical, microbiological, and nutritional properties are summarized in Table 3.1, Table 3.2, and Table 3.3 respectively, according to documents from the manufacturer.

Table 3.1 Analytical specifications of MSP potato starch (manufacturer data)

Analytical Specifications	Range	Method	Reference
Moisture	16-20%	MSP 05-02.4	
pH	6.0-8.0	MSP 05-02.1	CRA B-44-1
Ash	< 0.5%	MSP 05-02.2	CRA B-8-1
Particle Size	< 1.0% on a US100	MSP 05-02.3	

Table 3.2 Microbiological specifications of MSP potato starch (manufacturer data)

Microbiological Specifications	Range	Method	Reference
APC	< 10,000 cfu/g	MSP 05-03.1	AOAC Method 990.12
Yeast	< 250 cfu/g	MSP 05-03.2	AOAC Method 997.02
Mold	< 250 cfu/g	MSP 05-03.2	AOAC Method 997.02

Table 3.3 Nutritional specifications of MSP potato starch (manufacturer data)

Nutritional Specifications	Typical Sample
Moisture	17%
Calories	3.31 kcal/g
Total Carbohydrates	82.3%
Fat	0.2%
Protein	0.3%
Nitrogen	0.03%
Calcium	< 0.1%
Iron	< 0.01%
Magnesium	< 0.1%
Phosphorous	< 0.1%
Potassium	< 0.1%
Sodium	< 0.1%
Zinc	< 0.01%

3.2.2 Characterization

The morphology of selected samples was observed using a JEOL JSM-7000F (JEOL Ltd., Japan) scanning electron microscope (SEM). Starch granules were observed to facilitate granular size and pore size measurement. The starch granules were sputter coated with 5 nm platinum prior to observation in order to improve image quality. A relatively low accelerating voltage of 5kV was used to avoid damaging the delicate starch granules. The SEM image was analyzed using SigmaScan Pro 5 software (Systat Software Inc., USA). 186 raw starch granules in the image were traced and measured. The granular size was expressed using Feret's diameter, which is popular in biochemistry image analysis.

Raw potato starch porosity was measured by using Quantachrome high-pressure mercury intrusion porosimeter (Quantachrome Instruments, Florida, USA). The applied pressure was as high as 413.7 MPa so that pore size as small as 3 nm could be detected.

Differential scanning calorimetry (DSC) measurements were performed using a Q200 differential scanning calorimeter equipped with a refrigerated cooling system (TA Instruments, USA). Around 6.5 mg sample was sealed in an aluminum Tzero hermetic DSC pan and heated up from 20 °C to around 200 °C (depending on different purposes of the DSC tests) at 10 °C/min in the DSC chamber. A nitrogen flow of 150ml/min was applied during DSC tests. The TA Universal Analysis 2000 software was used to analyze the DSC curves and to identify thermal transition temperatures.

Statistical analysis of experimental data was conducted using Minitab 15 software obtained from Minitab Inc. (State College, PA, USA).

3.3 Results and discussion

3.3.1 Morphology of potato starch

Starch morphology was observed by SEM. The shape of potato starch granules was either spherical or ellipsoidal (Figure 3.1a). The granules of smaller size appeared as perfect spheres while larger granules showed more elongated shapes. The potato starch surface was generally smooth with only a small number of pores, as shown in the images. The starch granule size ranges from 11.6 to 57.1 microns in Feret diameter according to image analysis (Table 3.4 and Figure 3.2), while the pore size ranges from several nanometers to about 100 nanometers (Figure 3.1b). The size distribution of the raw potato starch granules was demonstrated by a histogram of Feret diameters shown in Figure 3.3. The majority of granule size was found between 17.5 to 37.5 microns.
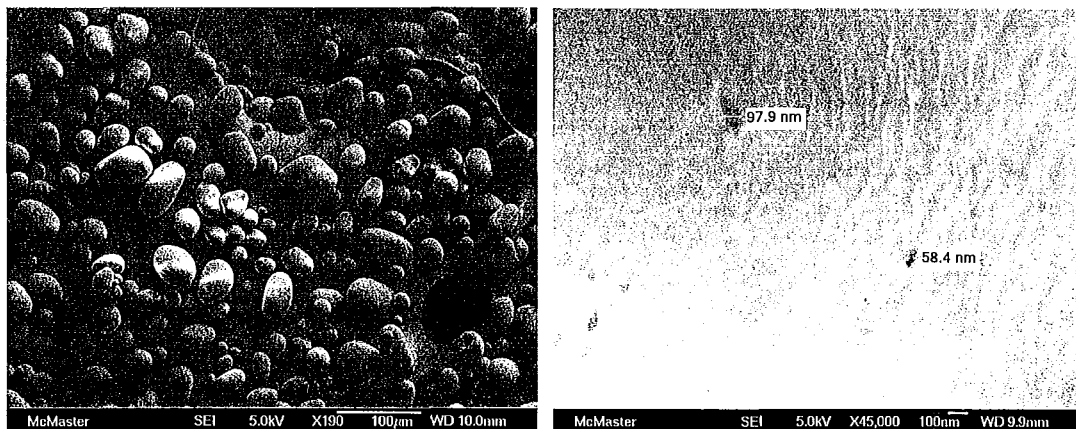
(a) 190 X magnification   (b) 45,000 X magnification

Figure 3.1 SEM images of raw potato starch

Table 3.4 Statistic data of granule diameter of potato starch

Stats	Feret Diameter (micron)	Minor Axis Length (micron)	Major Axis Length (micron)
Mean	28.2	24.9	32.3
Std Dev	10.2	8.2	13.5
Std Error	·0.8	0.6	1.0
95% Conf	1.5	1.2	2.0
99% Conf	2.0	1.6	2.6
# Nums	186	186	186
Min	11.6	10.7	12.1
Max	57.1	55.2	73.7
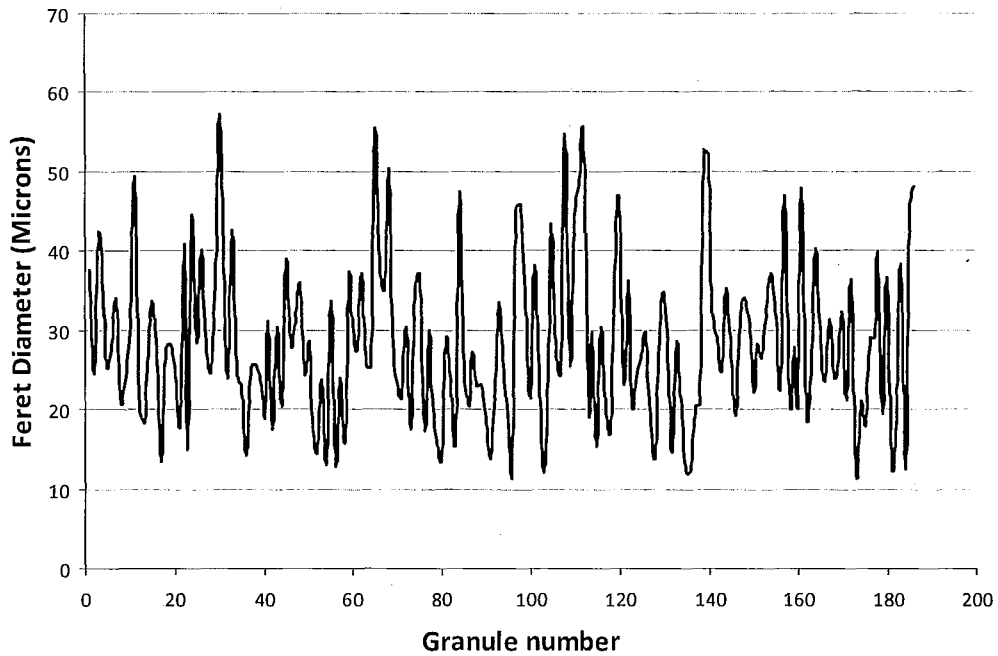
Figure 3.2 Granule diameter analyzed using SigmaPro Software.
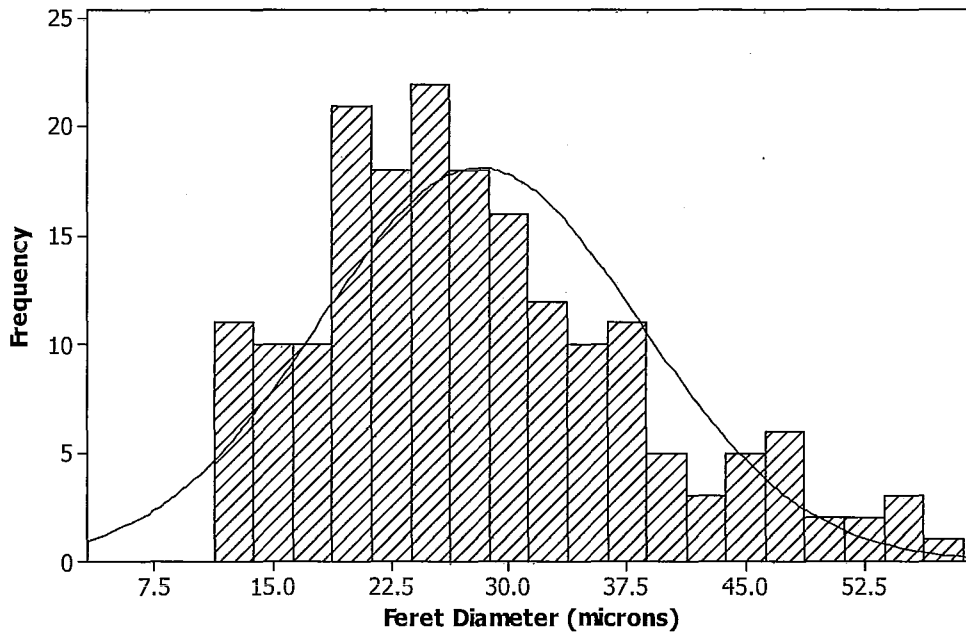
Figure 3.3 Histogram of Feret diameter showing size distribution of raw potato starch granules. Frequency refers to number of granules in a given granular size range.

The inter-particle, intra-particle, and total porosity were 0.77 %, 1.57 %, and 2.34 % respectively, based on porosimetry. Starch granules with higher porosity should be more easily penetrated by plasticizer or crosslinking agents, which would better facilitate starch gelatinization and crosslinking. But intra-particle porosity of raw potato starch is relatively low, which was expected to impede liquid diffusivity in this project and have adverse effects on potato starch processing.

3.3.2 Gelatinization of potato starch

Starch must be plasticized in order to be processed by an extruder and hence detailed work was initially required to determine suitable conditions. The

starch/glycerol/water mixture was thoroughly mixed and stabilized at room temperature for 30 minutes to equilibrate before DSC testing. The DSC thermograms of starch gelatinization are arranged in Appendix A. The starch images of raw starch and gelatinized starch (collected from the DSC pans) were made by an optical microscope with and without polarized illumination are shown in Figure 3.4. The raw starch displayed characteristic birefringence under polarized light, while the gelatinized starch can be seen to no longer have any indications of crystallinity.

(a)   (b)

(c)   (d)
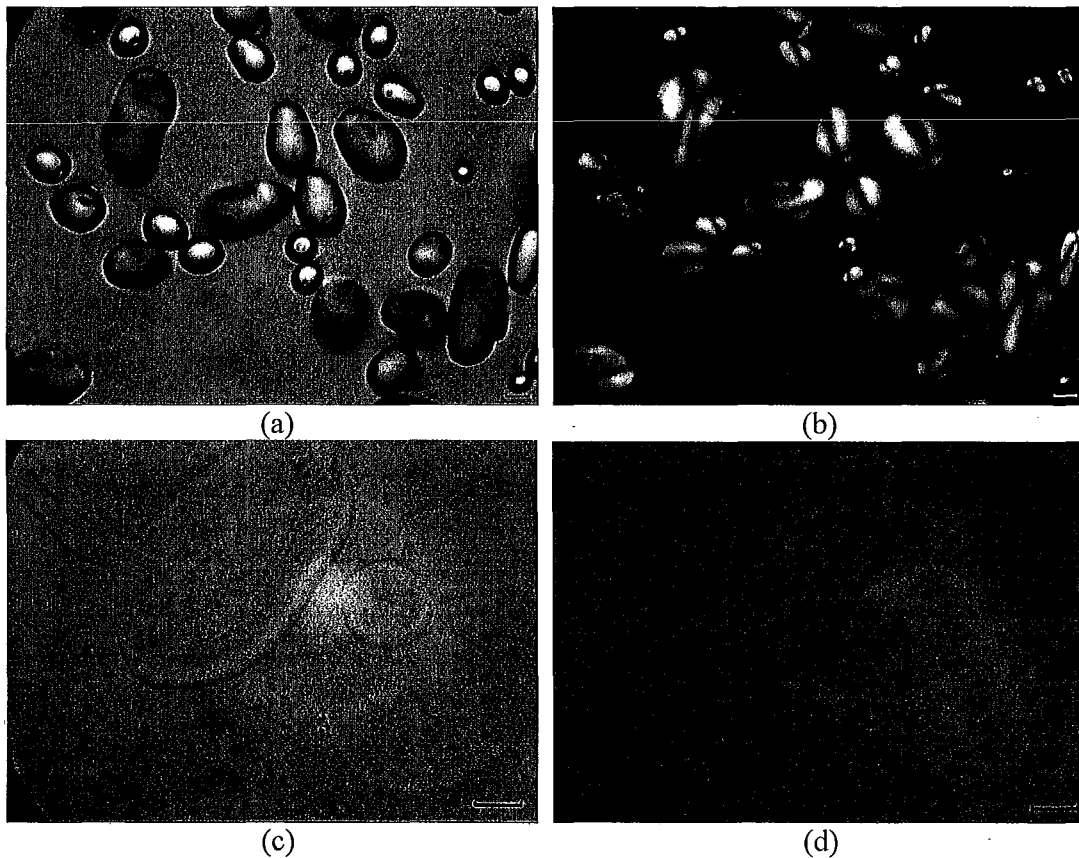
Figure 3.4 Raw starch (a, b) and gelatinized starch (c, d) observed under optical microscope with polarized light (b, d) and without polarized light (a, c) (bar = 10 micron).

3.3.2.1 Effect of glycerol content on gelatinization temperature of starch/glycerol/water mixtures

Table 3.5 and Figure 3.5 suggested that the gelatinization temperature increased with increased glycerol content when water content remained constant, all based on starch weight. This was because glycerol competed against starch for water so that there was less water available and more energy required for starch gelatinization.

Table 3.5 Effect of glycerol content on gelatinization temperature of starch/glycerol/water mixtures

Water (starch%)	Water (total%)	Glycerol (starch%)	Glycerol (total%)	T_o	T_{gel}	T_c	ΔH_{gel} (J/g)
35.6%	21.0%	33.9%	20.0%	81.1	84.2	94.8	1.32
35.6%	18.5%	56.5%	29.4%	89.0	92.0	104.9	2.97
35.6%	16.6%	79.1%	36.8%	94.0	98.6	130.0	7.79
58.2%	30.3%	33.9%	17.6%	73.6	76.7	109.2	9.17
58.2%	27.1%	56.5%	26.3%	81.3	85.1	112.1	7.77
58.2%	24.5%	79.1%	33.3%	83.2	89.9	99.3	3.19
80.8%	37.6%	33.9%	15.8%	71.4	74.5	103.0	8.68
80.8%	34.0%	56.5%	23.8%	73.8	77.2	99.3	6.55
80.8%	31.1%	79.1%	30.4%	78.8	82.2	103.5	7.81

T_o - onset temperature; T_{gel} – gelatinization temperature; T_c – conclusion temperature, ΔH_{gel} – enthalpy of gelatinization.
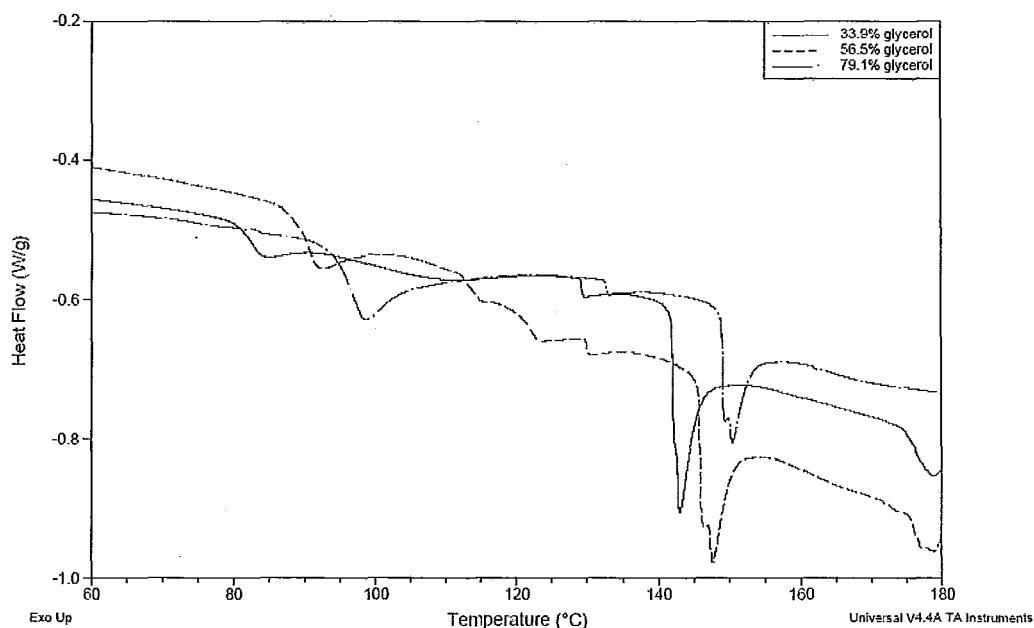
Figure 3.5 DSC thermograms of starch/glycerol/water mixture. Water content was 35.6 % based on starch weight. Glycerol contents based on starch weight are 33.9 %, 56.5 %, and 79.1 %, respectively.

3.3.2.2 Effect of water content on gelatinization temperature of starch/glycerol/water mixtures

From Table 3.6 and Figure 3.6 we see that the gelatinization temperature decreased with increased water content when glycerol content remained constant based on starch weight. The reason was that more available water helped dissociate crystalline structure of starch, requiring lower thermal energy to gelatinize the sample.

3.3.2.3 Starch gelatinization in the presence of excess water

The starch could gelatinize at lower temperature without shear at the presence of excess water, as shown in Figure 3.7. The onset, peak, and conclusion temperature of gelatinization were 56.6 °C, 60.6 °C, and 83.8 °C, respectively. The gelatinization enthalpy was 15.14 J/g. If starch with excess water can be considered as being fully

Table 3.6 Effect of water content on gelatinization temperature of starch/glycerol/water mixtures

Water (starch%)	Water (total%)	Glycerol (starch%)	Glycerol (total%)	T_o	T_{gel}	T_c	ΔH_{gel} (J/g)
35.6%	21.0%	33.9%	20.0%	81.1	84.2	94.8	1.32
58.2%	30.3%	33.9%	17.6%	73.6	76.7	109.4	9.17
80.8%	37.6%	33.9%	15.8%	71.4	74.5	103.0	8.68
35.6%	18.5%	56.5%	29.4%	88.9	92.0	104.9	2.97
58.2%	27.1%	56.5%	26.3%	81.3	85.1	112.8	7.77
80.8%	34.0%	56.5%	23.8%	73.8	77.2	99.2	6.55
35.6%	16.6%	79.1%	36.8%	94.0	98.6	123.0	7.79
58.2%	24.5%	79.1%	33.3%	83.2	89.9	99.3	3.19
80.8%	31.1%	79.1%	30.4%	78.8	82.2	103.8	7.81

T_o - onset temperature; T_{gel} – gelatinization temperature; T_c – conclusion temperature, ΔH_{gel} – enthalpy of gelatinization.
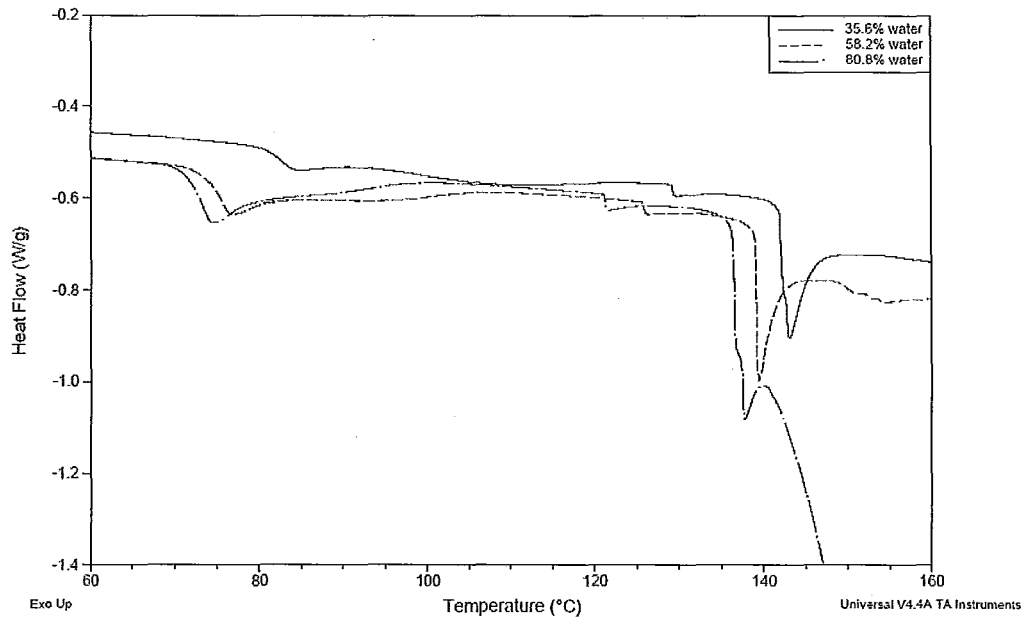
Figure 3.6 DSC thermograms of starch/glycerol/water mixture. Glycerol content was 33.9 % based on starch weight. Water contents based on starch weight are 35.6 %, 58.2 %, and 80.8 %, respectively.

gelatinized, its gelatinization enthalpy can be used as a reference to determine the degree of gelatinization under other experimental conditions. The degree of gelatinization can be calculated by the following equation:

$$DG = \frac{\Delta H_{gel,partial}}{\Delta H_{gel,full}} \times 100\% \qquad (1)$$

i.e.

$$DG = \frac{\Delta H_{gel,partial}}{15.14 \text{ J/g}} \times 100\% \qquad (2)$$

where DG is degree of gelatinization, $\Delta H_{gel, partial}$ is enthalpy of partial gelatinization, and $\Delta H_{gel, full}$ is the enthalpy of starch gelatinization with no previous disruption to the crystallinity prior to testing with excess water in the DSC.
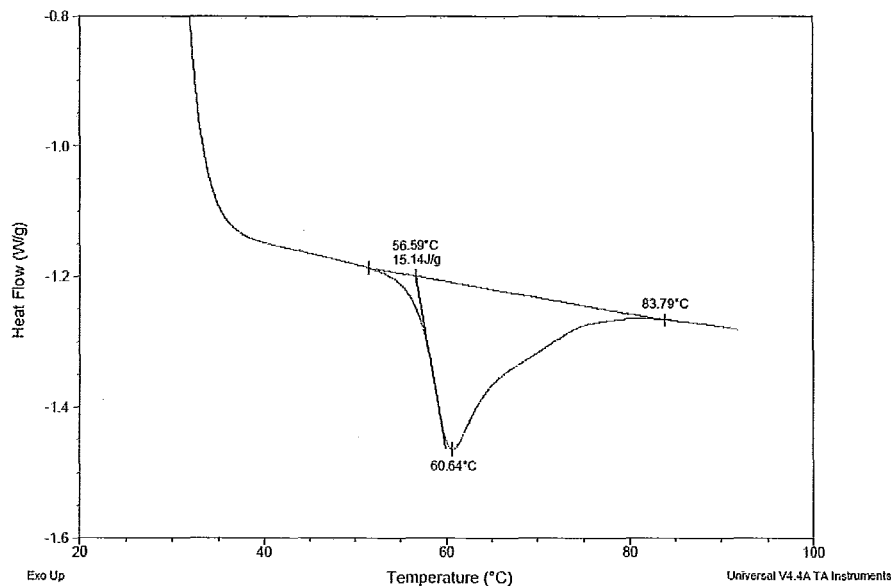
Figure 3.7 DSC thermogram of potato starch gelatinization in the presence of excess water.

3.3.2.4 Statistical analysis of starch gelatinization data

Gelatinization enthalpy was converted into degree of gelatinization (DG) according to Equation (2) in Section 3.3.2.3. Regression analysis using Minitab software (Minitab Inc., Pennsylvania, USA) revealed the relationship between the degree of gelatinization and composition of plasticizers in the starch/glycerol/water mixtures. The regression result was as follows:

DG (%) = 0.107 + 0.534 × water content (starch wt%) - 0.023 × glycerol content (starch wt%)

The optimal composition to achieving a higher degree of gelatinization could be
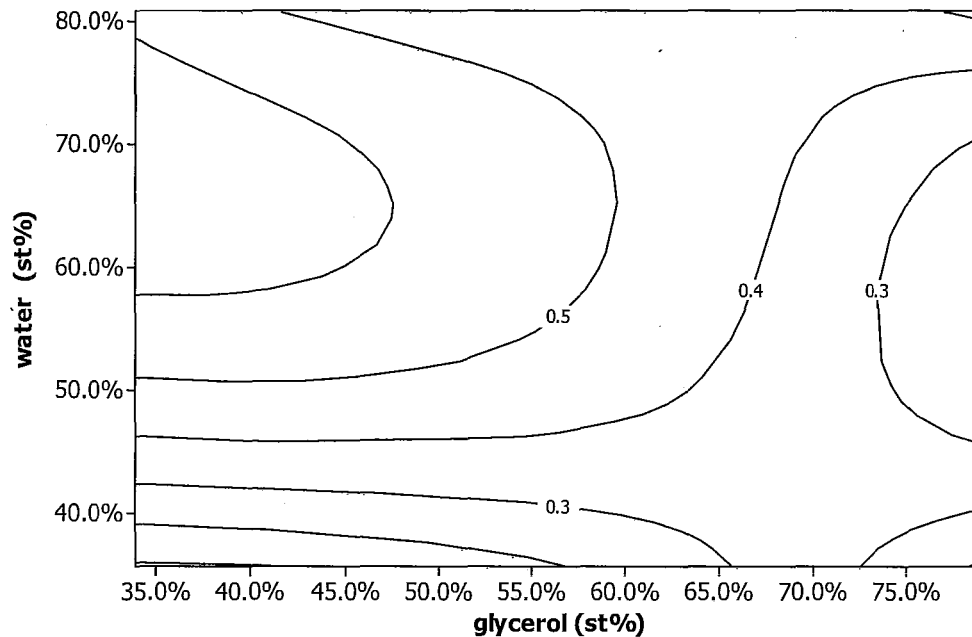
Figure 3.8 Contour plot of degree of gelatinization vs. water (starch %), glycerol (starch %) showing that 70 % water and 30 % glycerol led to a higher degree of gelatinization. The labels on the contour lines indicate percentage of gelatinization (For example: 0.5 = 50% gelatinization).

found in the contour plot of degree of gelatinization vs. water (starch %) and glycerol (starch %) content (Figure 3.8). Approximately 70 % water and 30 % glycerol was found to be the optimal composition for potato starch when rapid gelatinization is required, such as in the case of reactive extrusion where gelatinization and crosslinking must be completed in less than 2 minutes. All percentages of plasticizers were based on dry starch weight.

Further regression analysis also revealed the relationship between gelatinization temperature (T_{gel}) and plasticizer contents was as follows:

T_{gel} (°C) = 87.2 - 30.1 × water (starch wt%) + 26.4 × glycerol (starch wt%)

A second contour plot looking at gelatinization temperature (T_{gel}) vs. water (starch %) and glycerol (starch %) content indicated that the gelatinization temperature increased with increased glycerol content, and decreased with increased water content (Figure 3.9).
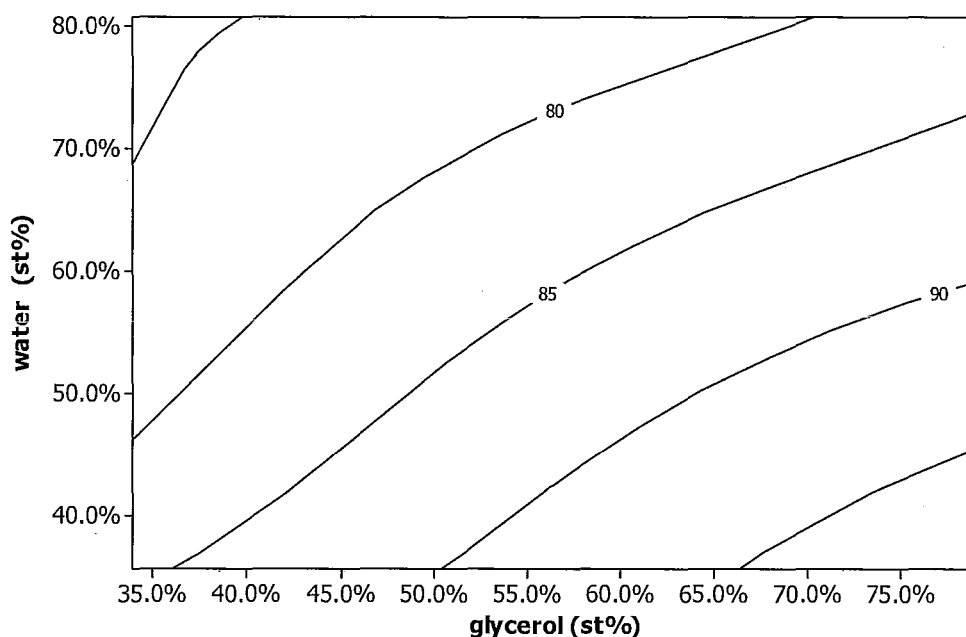
Figure 3.9 A contour plot of gelatinization temperature (T_{gel}) vs. water (starch %) and glycerol (starch %) content.

3.4 Conclusions

The size distribution of potato starch granules was determined by statistical image analysis of SEM graphs. The majority of potato starch granule size ranged from 17.5 to 37.5 microns. The total porosity of potato starch was 2.34 % as determined by mercury intrusion porosimeter. The low intra-particle porosity of raw potato starch was anticipated to be an impediment to water and reactant diffusivity and likely to negatively impact

starch gelatinization and crosslinking reaction. A statistical analysis of DSC experiment data suggested that higher water content contributed to lower gelatinization temperature and a higher degree of gelatinization, while higher glycerol content had the opposite effects. The optimal composition of glycerol and water for gelatinization could be determined by the contour plots, which should help improve starch gelatinization during twin screw extrusion processing. The optimal composition for potato starch gelatinization was found to be approximately 70 % water and 30 % glycerol (based on dry starch weight).

CHAPTER 4 TWIN SCREW EXTRUSION OF THERMOPLASTIC POTATO STARCH

D. Lawton, G. Wang, M.R. Thompson*

MMRI/ CAPPA-D
Department of Chemical Engineering, McMaster University
Hamilton, Ontario, Canada L8S 4L7
Tel: (905) 525-9140 x 23213
Fax: (905) 521-1350
mthomps@mcmaster.ca

and

[1] Q. Liu
[1] Guelph Food Research Centre, Agriculture and Agri-Food Canada,
Guelph, Ontario, Canada

The following chapter is based on a manuscript published in the ANTEC 2010 Conference Proceedings for the 2010 Annual technical conference held in Orlando, FL by the Society of Plastics Engineers. The manuscript was peer-reviewed. The work described was jointly done with Mr. David Lawton, an undergraduate student at the time in the group.

4.1 Abstract

Among starch species, potato tends to have a much narrower processing window in extrusion machinery for the preparation of thermoplastic starch compared to other common starch sources from corn or wheat. The present study demonstrates through a series of screw design refinements, a working approach to setting up a reasonable processing window of this starch type and discusses the issues involved. Finally the paper demonstrates through a series of trials with one of the optimal screw configuration, the influence of shear and formulation on final properties for the thermoplastic product.

4.2 Introduction

The field of bioplastics is generally considered to be in its infancy though several researchers and companies have been working in the area for decades already. Just as when petroleum-based plastics emerged, processor and machinery manufacturers are now being required to build up an understanding on the performance of these bio-source materials and adjust their operations accordingly. Thermoplastic starch (TPS) is an important material in this new revolution, having a well established supply chain for feedstock, good understanding of its structure, and an unfettered pathway for biodegradation. Neat TPS is brittle, exhibits excessive moisture sensitivity, and demonstrates weak mechanical properties. Yet with the addition of plasticizers like glycerol or urea (You et al., 2003), and/or blending with other host plastics like polylactic acid (PLA) (Huneault & Li, 2007; Wang, Yu, & Ma, 2007) or polyolefins (St Pierre et al.,

41

1997), the resulting material is suitable for packaging processes like blown film and thermoforming.

Native starch exists in granular form with particle sizes in range of 1-100 μm. Cereal and tuber starches are most commonly used in industrial applications, with corn (maize) being the most popular variety for thermoplastics but such selection depends on regional availability. For Canada, potato is an important crop source of starch due to its abundance and its starch yield being among the highest per cultivated acreage. To process starch in an extruder, the granule must disintegrate and the hydrogen bond associations of interior semi-crystalline structure must be disrupted. Heat-moisture gelatinization is the most common approach in food science to destructure starch. In excess water (>61% w/w) gelatinization is detected by differential scanning calorimetry (DSC) between 45-70°C for most species (61°C for potato). As the water content available decreases, both gelatinization and melting contribute to starch destructuring (Steeneken & Woortman, 2009). Other plasticizers like glycerol influence the transition in a complex manner as they compete with starch for water while also interfering with the hydrogen bonds between polysaccharide chains. Without shear, gelatinization of potato starch can take considerable time since the granules lack discernable porosity, and larger size or channelization for water to readily penetrate the granule. With the shear of an extruder bulk gelatinization can be done at low hydration very rapidly since the action of the screw minimizes the penetration time of water through starch granule. Shear tears the surface layer of starch and aids dissociation of the polysaccharide structure but often at the cost of chain degradation.

The work in our research facilities is largely focused upon modification of TPS which constrains the use of plasticizers in the system. A screw design was sought to provide mixing suitable for reactive extrusion yet also match the processing window of potato starch. Potato starch has one of the narrowest processing windows and requires higher specific mechanical energy to process compared to most other starch varieties (DellaValle et al., 1995). This paper reports upon observations made during optimization trials related to finding a suitable screw design and provides analysis of the produced thermoplastic material based on that optimal setup.

4.3 Experimental

4.3.1 Materials

Potato starch was obtained from Manitoba Starch Products (Carberry, Manitoba). According to scanning electron microscopy (SEM) the granule size was 12-57 μm (Feret diameters) and had a maximum pore size of 50 nm which was confirmed by high pressure mercury porosimetry. Less than 5 pores/μm^2 were noted by SEM. The moisture content of the native starch was 17.25 wt%. The plasticizers used in the work were distilled water and glycerol (reagent grade, BD Chemicals).

4.3.2 Apparatus

A 40 L/D 27mm Leistritz ZSE-HP co-rotating intermeshing twin screw extruder (TSE) was used in all trials. The barrel temperature profile was kept constant as 55-75-110-130-130-130-115-95-90°C. The strand die was set to 90°C. Powders were fed at 2

kg/h by a Brabender DDSR20 twin-screw gravimetric feeder. Liquids were fed by a Teledyne ISCO 260D syringe pump. Collected thermoplastic samples were granulated using a 66SRE-Extreme from Rapid Granulators Inc and then reduce to powder using a benchtop grinder.

4.3.3 Procedure

A total of six screw designs were tested in this work, with Screw 1 (poor) and Screw 6 (optimal) shown in Figure 4.1. For the optimization trials, the thermoplastic starch formulation consisted of 55 wt% starch (dry basis), 20 wt% water and 25 wt% glycerol. Due to the narrow processing window of potato starch and the limits imposed by this study on plasticizer content in light of future use with reactive extrusion, only one screw design was successful in producing samples. For Screw 6, trials were conducted for a range of screw speeds (50-100 RPM) using two formulations contained 20 wt% water with varying content of starch (55-60 wt% dry basis) and glycerol (20-25 wt%).

4.3.4 Characterization

Moisture content was determined using 4 g of each powder samples in a Mettler-Toledo HG63 moisture analyzer. All samples were stored two weeks at 23°C and 53% relative humidity prior to testing. Testing used an isothermal heating method at 105°C for one hour. The sample viscosity was determined for a 6% aqueous solution of TPS. Solutions were prepared by first heating up to 95°C and then cooled down to room temperature. The solutions formed gel-like liquids with differing fluidity. The viscosity measurements of these gel-like liquid samples were performed using a StressTech HR

Figure 4.1 Screw designs for preparing thermoplastic potato starch. Screw 1 gave poor performance where as Screw 6 represents an optimal configuration.

rheometer (ATS RheoSystems, USA) with the concentric cylinders (CC25) configuration. A heating cell was employed to maintain a constant temperature of 25°C for all measurements. Shear rates was varied up to 700 s^{-1}. DSC measurements were performed using a Q200 differential scanning calorimeter equipped with a refrigerated cooling system (TA Instruments, USA). A single-pass thermal scan from 20-200°C was performed at a ramp rate of 10 °C/min.

4.4 Results and discussion

4.4.1 Influence of screw element selection

The work in this section focuses on the performance of difference screw elements in the preparation of thermoplastic starch by twin screw extrusion. The authors could find no thorough examination in the open literature explaining the issues surrounding suitable screw designs, particularly for potato varieties.

In progressing through the six variants of screw designs many attributes of starch feeding and mixing along with additive metering were discovered. The first screw design, shown in Figure 4.1 as Screw 1, highlights an unsuccessful configuration demonstrating problems with both feeding and shear gelatinization. In regards to feeding starch powder into the TSE, the use of double-flighted self-wiping conveying elements (GFA-type) underneath the feed opening was found to be problematic. These elements exhibited difficulty taking in the fed powder, even with use of a large lead (40 mm). Native starch possesses an inherently high equilibrium moisture content (17 wt%) and as a result, the powder displays cohesive properties. The starch was often being pushed back into the

feed throat, or caking on the walls of the feed opening. The eventual outcome was arching above the extruder screws if left unattended. Single-flighted square-pitched conveying elements (GFF-type) were found to achieve adequate uptake of the starch due to their larger available volume (particularly in the nip region between adjacent screws) and the flights acted more as paddles than simple separators of incoming material.

For shear gelatinization and mixing, kneading blocks were the obvious choice in a screw design. Powders were plastically deformed over the kneading disc tip, to a higher extent in the intermeshing region between adjacent elements but also against the barrel wall. The offset angle of the kneading block had no observable influence while the starch remained granular since the parameter neither affected the available volume of the element nor the frequency of deformation events over the tips. For downstream kneading events after the first, the gelatinized starch had a more thermoplastic appearance and $30°$ or $60°$ elements were recommended as they offered a good balance of mixing and metering. Kneading blocks with a $90°$ offset were not recommended due to surging and longer residence time. Conversely, with distributive-type mixing elements (GLC-type and GFM-type) it was difficult to maintain prolonged operation of the extruder. With the inclusion of reversing-style GLC elements in the screw, the motor load steadily increased with operating time and the screws routinely seized; reversing-style refers to a drag flow contribution in the direction of the feed zone. Pulling the screws revealed densely packed, fully degraded TPS in these elements. No further attempts were made with any reversing-style element, neither mixing type nor conveying type. Between the forwarding-style distributive mixing elements, GFM is more aggressive than the GLC; forwarding-style

elements offer a positive drag contribution aiding flow towards the die. With both forwarding-style distributive mixing elements, the motor load no longer increased with time as found with the reversing GLC but similar seizing issues were reported. Seizing occurred most often when the mixing element was too close in proximity to an upstream kneading block (i.e. too many high mechanical energy zones in succession). Well isolated from other mixers along the screw, forwarding-style GLC and GFM mixing elements are excellent distributive mixers but lack self-wiping attributes for controlling residence time and remained difficult to use without flow surging. More easily processed starches like corn or wheat may possibly accept these distributive mixing elements in their screw design, but for potato starch, it was recommended that they be avoided.

4.4.2 Method of plasticizer addition

Our trials looking at plasticizer addition began with preblended mixtures of starch and plasticizers. The liquid content of water and glycerol were blended with starch and allowed to sit overnight, following the typical procedure mentioned in the open literature for extruding thermoplastic starch. The cohesive nature of the wetted solids decreased the calibration accuracy (feed factor) of our gravimetric feeder, with metering variance as great as 10 % (well above the 0.4 % found with polymer pellets). The starch-plasticizer mixture agglomerated readily and would become highly compacted in the dispensing throat of the feeder. Moreover, bridging occurred in the feeder bin which needed to be frequently dislodged manually despite an agitator being present inside. As a result of these difficulties the PID controller that operated the feeder often became unstable with the drive command reaching its maximum eventually. For these reasons, the authors were

encouraged to seek a direct liquid injection method, as well as to show operations with an industrially relevant processing system. Converting to only native starch in the gravimetric feeder brought about steady rates with metering variances less than 2 %.

Transitioning to a direct injection system for the plasticizers necessitated a reduction in the number of mixers in the screw design from five to three due to limited space; no aggressive action could occur to the starch until plasticized by the liquid additives. Reducing the number of intense shear regions was also beneficial in minimizing the light-brown coloring of the extrudate that was otherwise observed at high screw speeds (>150 RPM). Direct liquid addition into an open barrel section, whether in the feed zone or downstream (i.e. Zone 3 in our case) produced poor results with starch powder building up on the opening walls till the screws became blocked. The style of conveying screw elements in the injection zone, either GFF or GFA had no effect on the problem. Injection via a barrel port was found more suitable but with a standard low-pressure (<0.7 MPa) displacement pump there were great difficulties in maintaining unhindered liquid addition. Starch within the screw would routinely block the port due to localized rapid agglomeration of the oversaturated powder which either caused the screws to seize or the die to freeze off as the remaining powder in the screw dried and became densely packed. A high pressure pump (ISCO 260D) overcame the issue of the wetted starch pushing up into the injection lines; pressures greater than 2.8 MPa were intermittently generated by the pump to displace starch blockages.

The original thinking regarding setting up a screw for liquid injection was to maintain a zero pressure, partially filled conveying zone under the injection port so as to

minimize blockage by the solids. This proved to be the incorrect approach. The liquids and solids became segregated in the screw during trials rather than being intimately mixed (and still blocked the injector). The exiting material at the die appeared only partially gelatinized and intermittently liquid exited ranging in color from caramel-like to tar-like. To maintain intimate contact between starch and plasticizer in the injection zone, that region of the screw needed to fill completely but without creating an obstruction which would cause the still dry powder to compact and block the process. Using a mixing element like a kneading block or GLC under the injection port only caused the screw to seize. The most successful design used only spacers directly under the injector for a length of 20 mm, creating a pressure-driven annular flow region. With this setup, Screw 6 as shown in Figure 4.1, steady operation was achieved with a high rate of consistency in pressure readings and good quality melt exiting at the die.

4.4.3 Starch trials

Using the optimal screw design determined for continuous, steady processing from the previous section, a set of experimental trials followed to investigate the quality of thermoplastic potato starch produced. Two formulations with constant water content but differing glycerol content were studied. Series A formulation contained 20 wt% glycerol and 20 wt% water for plasticizers of potato starch whereas Series B contained 25% glycerol and 20 wt% water. The thermal transitions for these low hydrated formulations (unprocessed) were first determined by DSC, and the data is summarized in Table 4.1. Whereas potato starch with excess water produces only a single broad

Table 4.1 Thermal transitions for low hydrated potato starch with plasticizers (no shear) by DSC

Series	Starch* (wt%)	Water (wt%)	Glycerol (wt%)	T_{p1} (°C)	H_1 (J/g)	T_{p2} (°C)	H_2 (J/g)	T_{p3} (°C)	H_3 (J/g)
A	60%	20%	20%	86.0	2.41	127.6	0.496	143.3	2.22
B	55%	20%	25%	92.1	1.87	131.7	0.574	145.4	5.57

T_p – peak transition temperature, H – enthalpy of transition
* dry basis

transition at 61°C, low hydrated samples display a complex profiles with three transition peaks. The lowest temperature transition (T_{p1}) is a gelatinization endotherm; T_{p2} and T_{p3} are melting transitions (Steeneken & Woortman, 2009). With shear to aid melting and concerns regarding degradation, the barrel temperatures of the extruder were set just above the T_{p2} transition.

A total of six runs were conducted using Screw 6 and the operating data collected is shown in Table 4.2. Melt temperature and melt pressure were lower for the more highly plasticized formulation, Series B. Correspondingly, the specific mechanical energy of the process was slightly lower for the same formulation. Figure 4.2 shows the viscosity curves determined for each series. At low screw speeds the rheology of samples A50, A75 and B50 were all similar, exhibiting greater flow resistance compared to other samples. Both materials produced at 100 RPM exhibited the lowest viscosity, most notably for A100 which possessed less plasticizer to retard chain degradation compared to B100. According to Figure 4.3, water affinity by thermoplastic starch increased with increasing viscosity and higher glycerol content. Though the measurement techniques

differ, this trend regarding chain size and plasticizer seems to follow the water solubility

index (WSI) data of Van der Burgt (Van der Burgt, Vander Woude, & Janssen, 1996). In

general, processing by this screw design would appear to favor screw speeds below 100

RPM in order to minimize degradation of TPS.

Table 4.2 Operating conditions for thermoplastic starch

Sample Name	Screw Speed (RPM)	Output (kg/h)	Melt Press (MPa)	Melt Temp (°C)	SME* (kW/kg)
A50	50	2.80	0.55	85	0.098
A75	75	2.80	0.56	87	0.176
A100	100	2.81	0.60	88	0.261
B50	50	3.02	0.45	73	0.091
B75	75	3.03	0.46	72	0.163
B100	100	3.01	0.47	71	0.229

* SME – specific mechanical energy
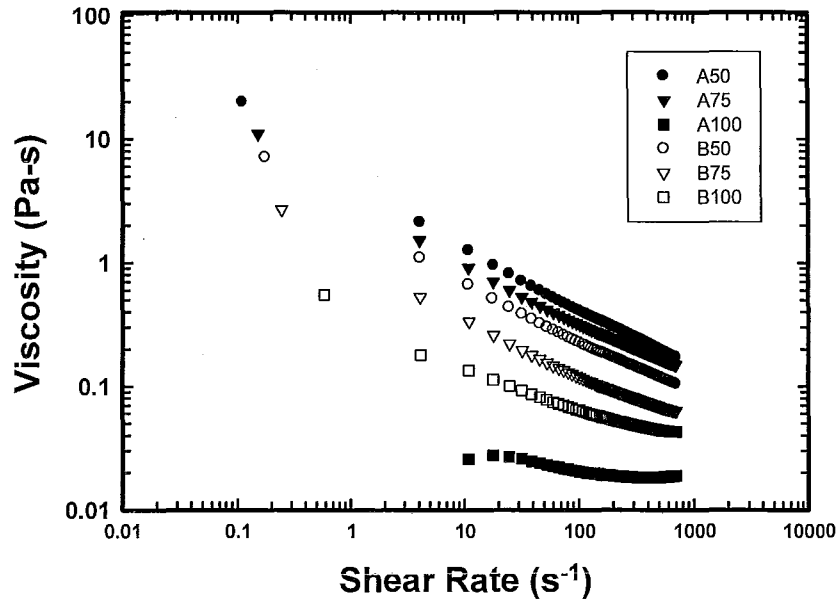
Figure 4.2 Viscosity curves for different thermoplastic starch samples prepared with Screw 6.
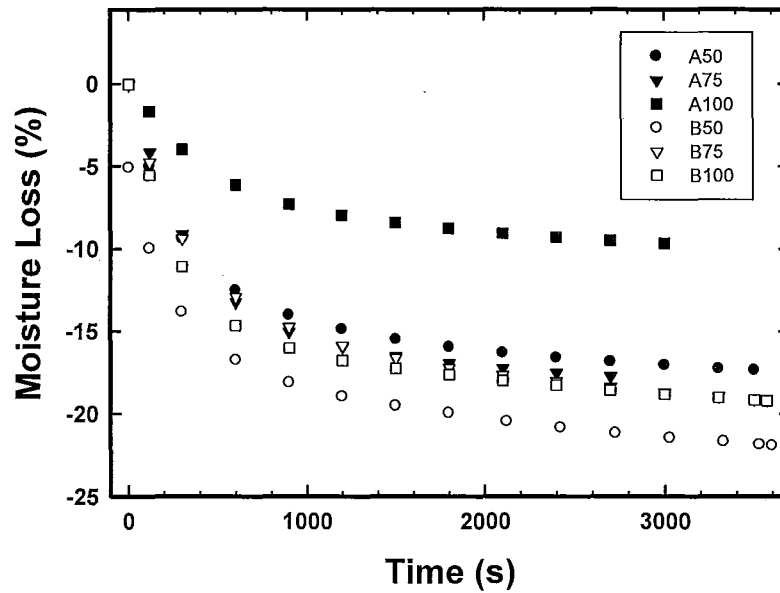
Figure 4.3 Moisture desorption curves for different thermoplastic starches prepared with Screw 6.

Finally, while the exiting materials appeared homogenous, the samples were analyzed by DSC to quantify the degree of destructuring. Figure 4.4 presents thermograms for Series A and B materials, showing only an endotherm transition related to TPS without lower transitions indicative of gelatinization by residual native starch. The melting peak appears shifted to a lower temperature with higher glycerol content (~180°C for 20 wt% glycerol to ~160°C for 25 wt% at the 50 RPM condition), following the results of other researchers (Liu, Yi, & Feng, 2001). It is also apparent that increasing screw speed decreased the peak temperature of the melting transition. The trend is consistent with degradation of a polymer. The broad endotherm transition found for B75, A75 and B100 was not fully understood in relation to the process but was suspected to be related to the final molecular weight distribution.
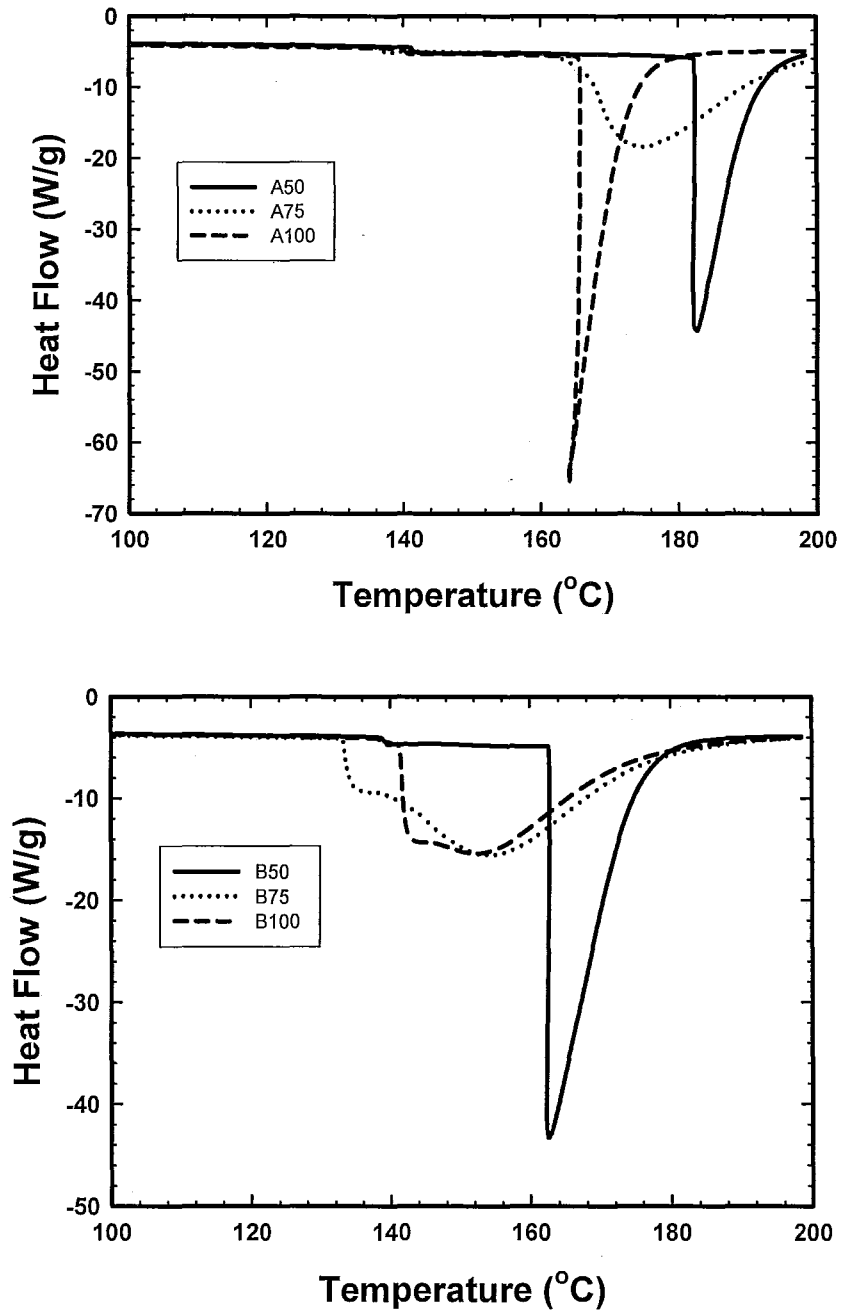
Figure 4.4 DSC thermograms of different thermoplastic starches prepared with Screw 6.

4.5 Conclusions

A suitable screw design and operational layout was determined for the extrusion of thermoplastic potato starch. Continuous, steady operation was achieved with good stability noted for the output material. The samples were found to exhibit significant degradation only at a screw speed of 100 RPM, affecting both rheology and water absorption capacity. The final product exhibited no gelatinization transitions indicating full disruption of the semi-crystalline structure of starch by the extrusion process.

4.6 Acknowledgements

The authors would like to thank the Agricultural Bioproduct Innovation Program (ABIP) Biopotato Network and Agriculture and Agri-Food Canada (AAFC) for their funding of this research. Additionally, the authors are grateful to Manitoba Starch for providing materials to the project.

4.7 References

Della Valle, G., Boche, Y., Colonna, P., & Vergnes, B. (1995). The extrusion behaviour of potato starch. *Carbohydrate Polymers*, 28, 255-264.

Huneault, M. A., & Li, H. B. (2007). Morphology and properties of compatibilized polylactide/thermoplastic starch blends. *Polymer*, 48, 270-280.

Liu, Z. Q., Yi, X. S., & Feng, Y. (2001). Effects of glycerin and glycerol monostearate on performance of thermoplastic starch. *Journal of Materials Science*, 36, 1809-1815.

Steeneken, P. A. M., & Woortman, A. J. J. (2009). Identification of the thermal transitions in potato starch at a low water content as studied by preparative dsc. *Carbohydrate Polymers*, 77, 288-292.

St Pierre, N., Favis, B. D., Ramsay, B. A., Ramsay, J. A., & Verhoogt, H. (1997).
    Processing and characterization of thermoplastic starch/polyethylene blends.
    Polymer, 38, 647-655.

Van der Burgt, M. C., VanderWoude, M. E., & Janssen, L. (1996). The influence of
    plasticizer on extruded thermoplastic starch. *Journal of Vinyl & Additive
    Technology*, 2, 170-174.

Wang, N., Yu, J. G., & Ma, X. F. (2007). Preparation and characterization of
    thermoplastic starch/pla blends by one-step reactive extrusion. *Polymer
    International*, 56, 1440-1447.

You, X. D., Li, L., Gao, J. P., Yu, J. G., & Zhao, Z. X. (2003). Biodegradable extruded
    starch blends. *Journal of Applied Polymer Science*, 88, 627-635.

CHAPTER 5 INFLUENCES OF HYDROCOLLOIDAL GUM AND GLYCEROL ON KINETICS OF BULK PHOSPHORYLATION OF POTATO STARCH

G. Wang, M.R. Thompson

MMRI/ CAPPA-D
Department of Chemical Engineering, McMaster University
Hamilton, Ontario, Canada L8S 4L7
Tel: (905) 525-9140 x 23213
Fax: (905) 521-1350
mthomps@mcmaster.ca

and

[1] Q. Liu
[1] Guelph Food Research Centre, Agriculture and Agri-Food Canada,
Guelph, Ontario, Canada

The following chapter is based on a manuscript submitted to the journal Carbohydrate

Polymers, July 2010. The contents are the sole work of the Master's candidate.

5.1 Abstract

This work studies the bulk modification of potato starch using sodium trimetaphosphate (STMP) in the presence of rheological controlling additives, namely xanthan gum and glycerol. Batch kinetics for the reaction was investigated using a novel in-situ technique based on attenuated total reflectance infrared (ATR-IR) spectroscopy for monitoring the extent of crosslinking. Multivariate analysis of the spectral data revealed important vibrational bands related to crosslinking for monitoring as well as identified significant variables for optimizing the reaction. Native potato starch was used in in-situ ATR-IR monitoring to develop a kinetic model of the bulk reaction. The kinetic model was examined in usefulness for developing a reactive extrusion process. The higher extent of crosslinking in the extruder than predicted by the model indicates the importance of advective mass transfer. The effect of crosslinking in the presence of the hydrocolloidal xanthan gum and glycerol on the crosslinking of potato starch was also investigated in this study.

5.2 Introduction

Value added products based on modified starch are important to the pharmaceutical, food, adhesive, paper and most recently, the polymer packaging sectors (Braz et al., 2007; Dumoulin et al., 1998). The chief benefits of starch as an industrial material are its abundance, low cost, safety, sustainability, and negligible impact on the existing food supply chain. Various kinds of chemical modification of starch are traditionally

conducted in aqueous solution so that its granular structure is maintained intact. In solution, the microstructure of the starch granule (i.e. porosity of its surface membrane and extent of channelization within its interior)· imposes diffusional control over the reactant ingredients, thereby slowing conversion of interior constituents. This is particularly true of potato starch which possesses very limited porosity and channelization, and hence functionalities produced by the reaction remain localized to the peripheral regions (Fannon et al., 2004). Maintaining an intact starch particle is important in some product cases where granule characteristics influence its usefulness such as in cooking or tabletting, but where such limits are not present it is far more economical and efficient to generate these chemistries in the bulk phase. Bulk phase modification for polymers is often known as *reactive extrusion* in reference to the machinery most commonly used as it offers excellent control over dosing and mixing of reactants with vastly different viscosities. The field evolved in the synthetic polymer and rubber industries (Tzoganakis, 1989), but Carr (1991, 1992, 1994) was quick to demonstrate its potential in the area of modified starch. The major advantage of bulk modification is the absence of solvents requiring costly recovery and disposal, as well as rapid exposure of the interior polysaccharides in starch through mechanical shear to improve the extent of reaction achievable for low porous matter like potato starch.

Bulk crosslinking of starch via phosphorylation has been studied by several authors in recent years (Murua-Pagola et al., 2009; Nabeshima & Grossmann, 2001; Seker & Hanna, 2005, 2006). Though various crosslinking agents such as tetraethylene glycol

diacrylate could be used for starch crosslinking (Marques et al., 2006), the most

commonly used reagents are epichlorohydrin and sodium trimetaphosphate (STMP)
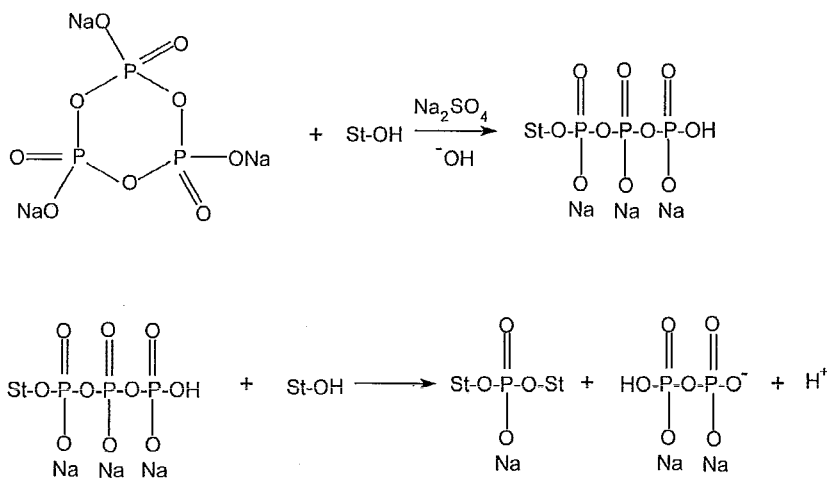
Figure 5.1 Crosslinking mechanism proposed by Lim and Seib (1993).

(Demirgoz et al., 2000; Dubois et al., 2001); epichlorohydrin is more generally avoided

in industry due to its carcinogenic nature (Xie et al., 2005). The mechanism of starch

crosslinking with STMP was proposed by Lim and Seib (1993), as shown in Figure 5.1.

The reaction involves ring-opening of STMP to form starch tripolyphosphate which

further reacts with starch to produce distarch phosphate, i.e. crosslinked starch, at a

condition of pH > 8. The pH of the system plays a major role in the formation of diesters

in solution during reaction, but in bulk processes, with reduced mobility of ions,

processors favor the inclusion of other catalytic species as well. Catalytic species like

sodium sulphate and sodium carbonate have been demonstrated to improve conversion

towards the distarch phosphate (Mao et al., 2006; Woo & Seib, 1997). Sodium carbonate causes starch molecules to swell by interfering with hydrogen bonding and thus activates hydroxyl reaction sites (Mao et al., 2006). Sodium sulphate not only promotes absorption of alkali and crosslinking reagents into starch granules, but also improves the ionic strength of the system to facilitate crosslinking reaction between negatively charged starch alkoxides and phosphoryl reactant species (Woo & Seib, 1997).

Xanthan gum and other gums like guar gum have been utilized to modify rheological properties and the freeze-thaw stability of starch (Achayuthakan & Suphantharika, 2008; Nagano et al., 2008; Pongsawatmanit & Srijunthongsiri, 2008; Ptaszek & Grzesik, 2007). The addition of xanthan gum to starch crosslinked with adipoyl chloride in a conical twin-screw extruder was reported by Miladinov and Hanna (1995). However, their work never considered that the hydrocolloidal gum could participate in the reaction, which has been recently proven to occur (Shalviri et al., 2010; Chung et al., 2007). Glycerol is a plasticizer routinely added to bulk processes to aid the gelatinization and flow of starch within extrusion machinery. Neither gum nor glycerol has been studied till now for their effect on the reaction, particularly in terms of rate and extent of conversion.

This paper presents an in-situ ATR-IR analysis technique to follow the extent of reaction for phosphate crosslinking in bulk starch and uses the new method to better understand the impact of additives like xanthan gum and glycerol on the kinetics and extent of reaction. The work first examines the bulk crosslinking of potato starch on the batch scale and then applies the technique to samples prepared by reactive extrusion.

5.3 Experimental

5.3.1 Materials

Potato starch (MSP Grade) was provided by Manitoba Starch Products (Carberry, Manitoba, Canada). It is a food-grade potato starch. The typical moisture content was 17% based on measurement using a Mettler-Toledo HG63 moisture analyzer. The reagents, sodium trimetaphosphate ($Na_3P_3O_9$, > 99.5 % purity) and sodium sulphate (Na_2SO_4, > 99.0% purity) were purchased from Sigma-Aldrich Canada (Oakville, ON, Canada). Glycerol (> 99.5% purity) was provided by Caledon Labrotories Ltd (Georgetown, ON, Canada) while xanthan gum was obtained from Sigma-Aldrich Ltd (St. Louis, MO, USA). The aqueous sodium hydroxide (0.1 N standardized) solution was purchased from LabChem Inc. (Pittsburgh, PA, USA). All water used was de-ionized.

5.3.2 Bulk kinetic trials

The crosslinking kinetics was investigated in batch without the presence of shear by in-situ ATR-IR analysis. A series of starch crosslinking experiments were carried out at two different temperatures of 90 °C and 120 °C. The concentrations of all reactants for each run are listed in Table 5.1, given on a dry starch basis. A constant weight fraction of Na_2SO_4 (2.7% w/w) was used for all experiments.

A 15 g sample was mixed according to the listed formulations and NaOH was added to adjust the alkalinity of the mixture to a pH of 11, then by tumble blending for 10 minutes. The total water content in the sample was 87 wt% on a dry starch basis. The relatively high water content minimized damage to the starch during processing and

Table 5.1 Percentage of reactants in starch crosslinking reaction under in-situ ATR/IR monitoring

Experiment No.	STMP (wt% starch[a])	Xanthan gum (X) or Glycerol (G) (wt% starch)
1[b]	20	0
2	10	0
3	5.0	0
4	2.7	0
5	1.6	0
6	0.7	0
7	0	0
8	2.7	10 (G)
9	2.7	30 (G)
10	2.7	1 (X)
11	2.7	2 (X)
12[c]	5.0	0
13	2.7	0
14	1.6	0
15	0.7	0
16	0	0
17	2.7	10 (G)
18	2.7	30 (G)
19	2.7	1 (X)
20	2.7	2 (X)

a. Percentage in the table is based on dry starch weight.
b. Temperature for experiments 1-11 is 120 °C.
c. Temperature for experiments 12-20 is 90 °C

improved dispersion of the reactants in the continuous phase without creating a dilute

solution inside the extruder. Each experiment was conducted with a ReactIR™ 1000

infrared system (Mettler-Toledo) scanning the mid-range infrared bands between 600-

4000 cm^{-1} at a resolution of 4 cm^{-1}. A test specimen (0.5 g) was enclosed with the

infrared probe using aluminum foil and sealed to avoid any losses of water by

dehydration during the trial. A temperature-controlled heater maintained the reaction

temperature and applied pressure, minimizing air entrainment of the test specimen against

the window of the IR probe. The flexible probe arm of the unit allowed positioning of the

reactant system above it for in-situ monitoring. Consecutive infrared spectra were

collected every 20 seconds for a duration of 3600 seconds. An example of the spectral

dataset for a completed experimental run is shown in Figure 5.2.
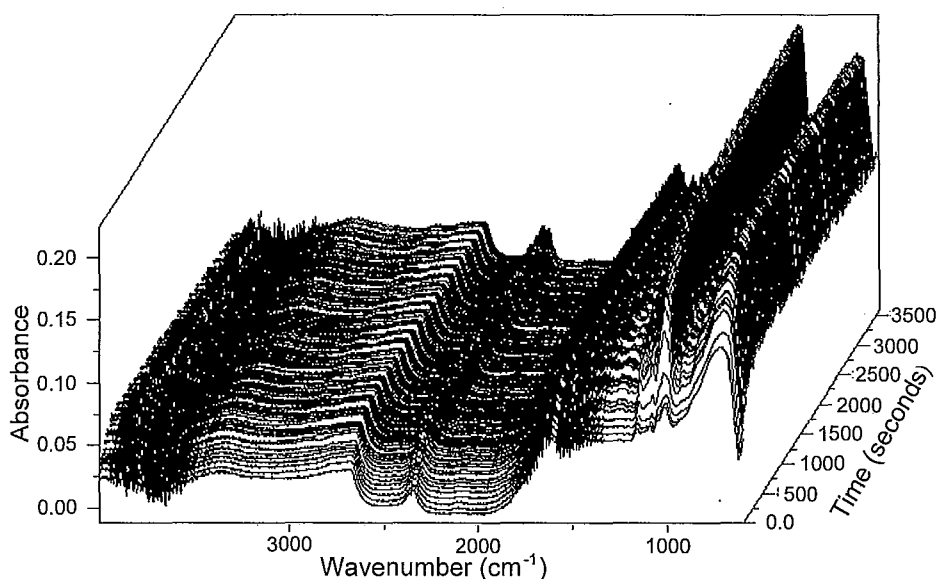
**Figure 5.2 Time series of infrared spectra collected by the ATR/IR probe for the
crosslinking reaction using 2.7 wt % STMP (based on dry starch weight) at 120 °C.**

It was found important that the water concentration within the starch sample remained constant throughout the test. Otherwise, important vibrational bands in the IR spectra related to phosphorylation were affected as the sample dehydrated. Enclosing the test specimen with the infrared probe using an aluminum foil envelope was found the most effective approach to avoid this issue and still allowed excellent heat transfer from the heater to the material.

5.3.3 Extrusion trials

A 40 L/D 27 mm co-rotating intermeshing twin screw extruder (Model ZSE27-HP from American Leistritz Extruder Corporation, Somerville, NJ) was employed to modify starch via reactive extrusion. The screw design used for these experiments was determined from an evaluation of six different configurations (Lawton et al., 2010). The chosen screw design for the trials, shown in Figure 5.3, produced fully transparent, only slightly yellowed mass indicative of a fully gelatinized thermoplastic starch with little shear degradation. The short distance from the point where the solution of reactants and plasticizer were added into the starch and the first kneading block in the screw design is considered as a gelatinization zone before which there was negligible crosslinking reaction occurring according to the results of previous kinetic study. Therefore, the extruder screw can be designated into two consecutive zones: gelatinization and reaction, as shown in the figure of the optimal screw design.

The screw speed of the extruder was constant at 20 RPM to minimize shear damage to the crosslinked starch network and provide a reasonable residence time for the crosslinking reaction. The barrel temperature profile of the extruder was 60-70-70-90-90-
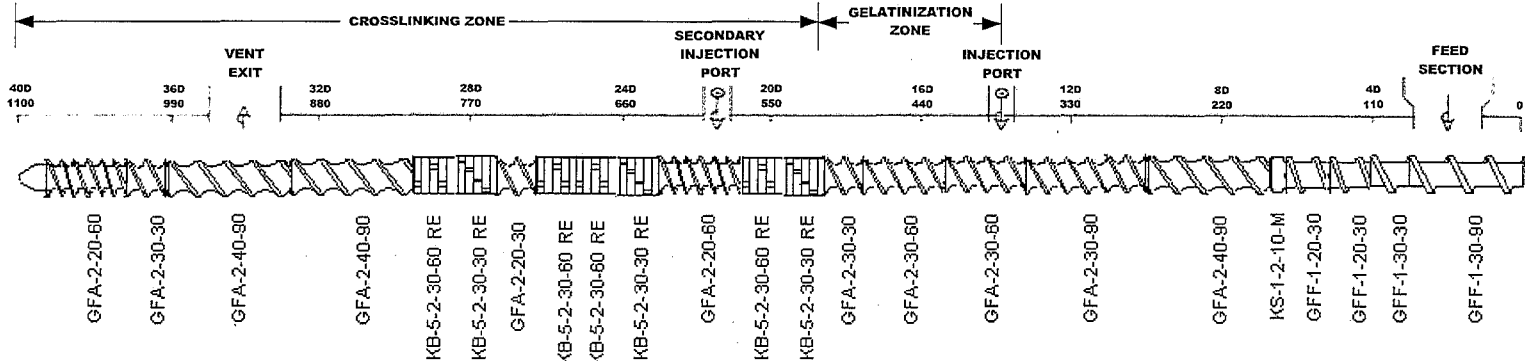
Figure 5.3 Tested screw design for starch modification representing optimal processing performance.

100-120-120-100 °C and 95 °C for the die. Liquid dosing of the aqueous solution containing dissolved STMP, glycerol and Na_2SO_4 (adjusted to a pH of 11 by NaOH) was done using a B Series chemical metering pump from LMI Roy Milton Inc. (Ivyland, Pennsylvania) to an injection port located at the third barrel zone (12 L/D from the feed opening). Native starch powder was fed at a rate of 1 kg/h into the feeding port of the extruder barrel by a Brabender DDSR20 twin-screw gravimetric feeder (Brabender Technologie, Brampton, ON.). The starch was not previously dried before use but the water content in the extruder was adjusted for consistency based on moisture analysis (Mettler HG63 moisture analyzer) of the feedstock. The total water content on a dry starch basis was 87%. Appropriate amount of water is necessary to avoid seizing of the extruder screws and overloading of the extruder motor while maintaining bulk state reaction with higher localized concentration of reactants than reaction in aqueous solution. Xanthan gum was premixed (when used) and fed together with the starch.

Concentrations of the reactants in the reactive extrusion trials are listed in Table 5.2. Similar to the kinetics trials, all percentages were based on a dry starch basis. The crosslinked extrudates were immediately chilled by cool water (15 ± 5 °C) and then washed repeatedly with deionized water/ethanol to remove residual reactants so that a reasonable estimate of the extent of crosslinking could be obtained.

5.3.4 Characterization

Elemental analysis of the phosphorus in the prepared samples was performed using JOEL 7000 with Energy Dispersive X-ray Spectroscopy (EDS) (JEOL Ltd., Japan).

Table 5.2 Percentage of reactants in potato starch formulations prepared by reactive extrusion

Experiment[a]	STMP[b] (wt% starch)	Na$_2$SO$_4$ (wt% starch)	Xanthan gum (wt% starch)	Glycerol (wt% starch)
E1-1	2.7	2.7	0	10
E1-2	2.7	2.7	0	30
E2-1	2.7	2.7	1	0
E2-2	2.7	2.7	2	0
E3-1	1.6	2.7	0	0
E3-2	2.7	2.7	0	0
E4	0	0	0	0
E5-1	2.7	2.7	1	10
E5-2	2.7	2.7	1	30
E6-1	2.7	2.7	2	10
E6-2	2.7	2.7	2	30

a. Water content for all experiments is 87 wt%.

b. Percentages in the table are based on dry starch weight.

The lower detection threshold of EDS for phosphorus was 0.1% on a total weight basis, preventing measurement of the naturally occurring low phosphorous content (~0.02%) in native starch. Before analysis, the crosslinked samples were washed repeatedly with deionized water/ethanol (till its chemical fingerprint remained constant by infrared analysis) and then dried under vacuum at 40 °C overnight. The phosphorous content detected by EDS was used in collaboration with the infrared analysis, as an indicator of the extent of crosslinking. Infrared spectroscopy was used to measure the extent of crosslinking for each extruded sample using the same ATR-IR apparatus mentioned in section 5.3.2 for the in-situ kinetics study.

To rheologically quantify the extent of crosslinking, granulated samples of the extrudate were prepared using a mechanical granulator (Model 66SRE, Rapid Granulator Inc., Sweden) followed by a bench-top grinder to obtain a fine powder. A hydrogel was prepared from the starch sample by heating a suspension of 6 wt% starch sample in deionized water to 95 °C and then cooling down to room temperature. Rheological measurements were conducted using a StressTech HR rheometer (ATS RheoSystems, USA) with concentrical cylinders (CC25) configuration. A temperature cell was employed to maintain a constant temperature of 25°C for all the measurements. Shear rates varying from 0-700 s^{-1} were evaluated.

Statistical analysis for the kinetics study was conducted using a multivariate software package (ProSensus, Inc., Canada). Multivariate analysis of the infrared data in the 900-1400 cm^{-1} region was used to reveal the effects of reaction time, crosslinking agent, xanthan gum, and glycerol content on the extent of crosslinking.

5.4 Results and discussion

5.4.1 Evaluating crosslinking by in-situ IR analysis

Evaluating the extent of crosslinking during phosphorylation of potato starch is quite often difficult due to the already presence of phosphorus in native species and the low extent of conversion allowed for in certain products (i.e. foods and pharmaceuticals). By solution reaction the granules remain largely intact and so particle attributes are often used to characterize the extent of reaction. Indirect characterization of the crosslinked starch granule has been done by measuring the degree of swelling, sedimentation time,

and calculation of water solubility/absorption indices (Dulong, et al., 2004; Dubois, et al., 2001; Li, et al., 2009; Luo, et al., 2009; Mao, et al., 2006; Nayouf, et al., 2003; Seker & Hanna, 2005). However, these methods are not applicable to bulk modified samples since the end-product of an extruder must be pelletized or ground and therefore, their values bear little relationship to the native starch for comparison. Spectroscopic techniques are generally more informative for both solution and bulk reactions. Nuclear magnetic resonance techniques (^{13}C, ^{1}H, ^{31}P NMR) have been used to establish the reaction pathways through structural changes to the starch (Shalviri, et al., 2010; Cury, et al., 2009; Sang, et al., 2007; Delval, et al., 2004; Le Bail, Morin, & Marchessault, 1999; Simkovic, et al., 2004). Similarly, infrared analysis has been used to verify the presence of P-O-C bonds in solution-crosslinked starch samples (Zhang and Wang, 2009; Shalviri, et al., 2010). Infrared analysis was selected for the kinetic study in the present work due to its rapid responsiveness and sensitivity to changing sample conditions in the solid state. The challenge was to establish a reliable analysis technique at or above the boiling point of water since dehydration of the starch sample affected many of its vibrational bands during the in-situ studies.

To establish the important vibrational bands for the crosslinking reaction multivariate statistics was applied to the infrared spectral data. A selection of IR spectra in the 600-1400 cm^{-1} range from different stages of the reaction are shown in Figure 5.4, for the conditions of 2.7 wt% STMP at 120 °C while in the *in-situ* batch heating apparatus. An intense series of peaks in the range of 950-1200 cm^{-1} were witnessed to develop before 1200 seconds and then remained mostly constant in their intensity. Those bands

were significantly affected by the state of gelatinization for potato starch. Based on the time to reach plateau for the peak intensities of these vibrational bands, complete gelatinization was estimated within 700 seconds at 120 °C and 1100 seconds at 90 °C. Using Principle Components Analysis on the 2800 infrared spectral datasets collected over each 1 h run revealed that the baseline corrected absorbance of the characteristic peaks at 1001 cm^{-1} and 1269 cm^{-1} preferentially increased as the reaction progressed. Based on the assignments of Coates (2000), the former band corresponded to ester stretching (v_{as} P-O-C) while the latter band was assigned to stretching vibrations of organic phosphates (v_{as} P=O). Based on concerns regarding confounding of the peak at
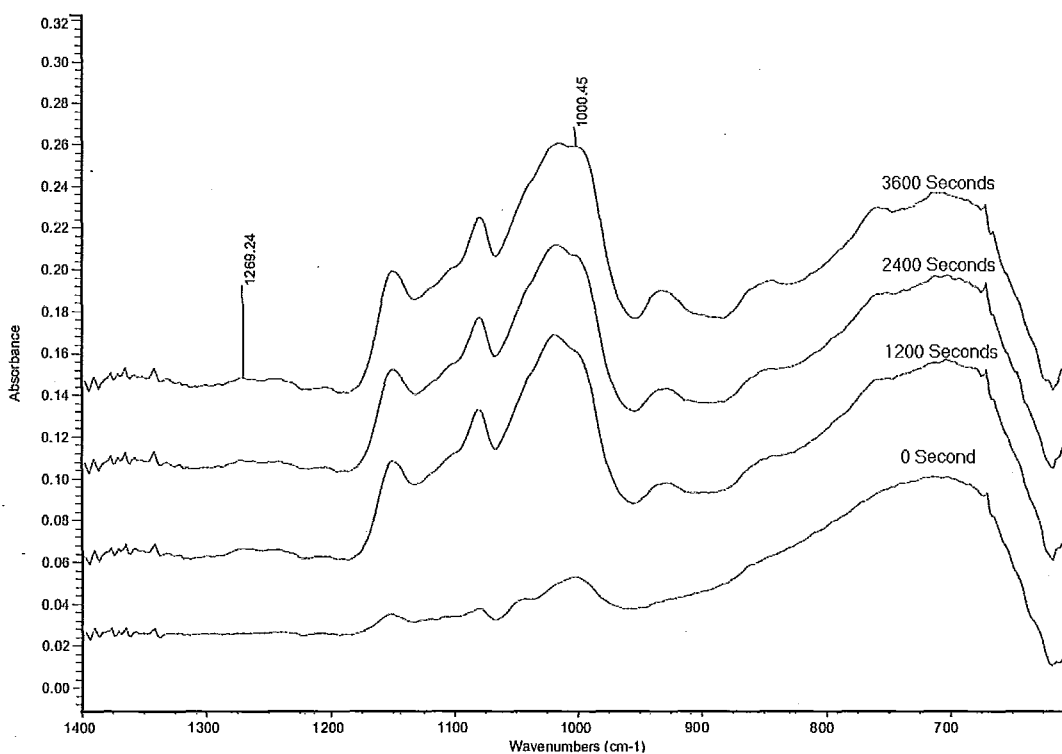
Figure 5.4 Infrared spectra plot of relative absorbance of the peaks at 1001 cm^{-1} (P-O-C bond) and at 1269 cm^{-1} (P=O bond) changing with reaction time of starch crosslinking reaction at STMP percentage of 2.7 wt % (based on dry starch weight) at 120 °C.

1001 cm^{-1} with gelatinization, only 1269 cm^{-1} was used to quantify the reaction though

the other was routinely monitored and generally found a good indicator of the

phosphorylation as well. Absorbance of the peak at 1269 cm^{-1} was felt to be a significant

indicator of the reaction as the peak continued to progressively increase in intensity even

once other peaks related to gelatinization ceased to change. Later mentioned rheology

testing in this thesis confirmed that the samples of starch were crosslinked over this span

of time and differed in their extent of crosslinking based on concentration of STMP.

A plot of the reaction progression at 120 °C based on the band intensity at 1269 cm^{-1}

is shown in Figure 5.5 for STMP concentrations up to 20 wt% without gum or glycerol.
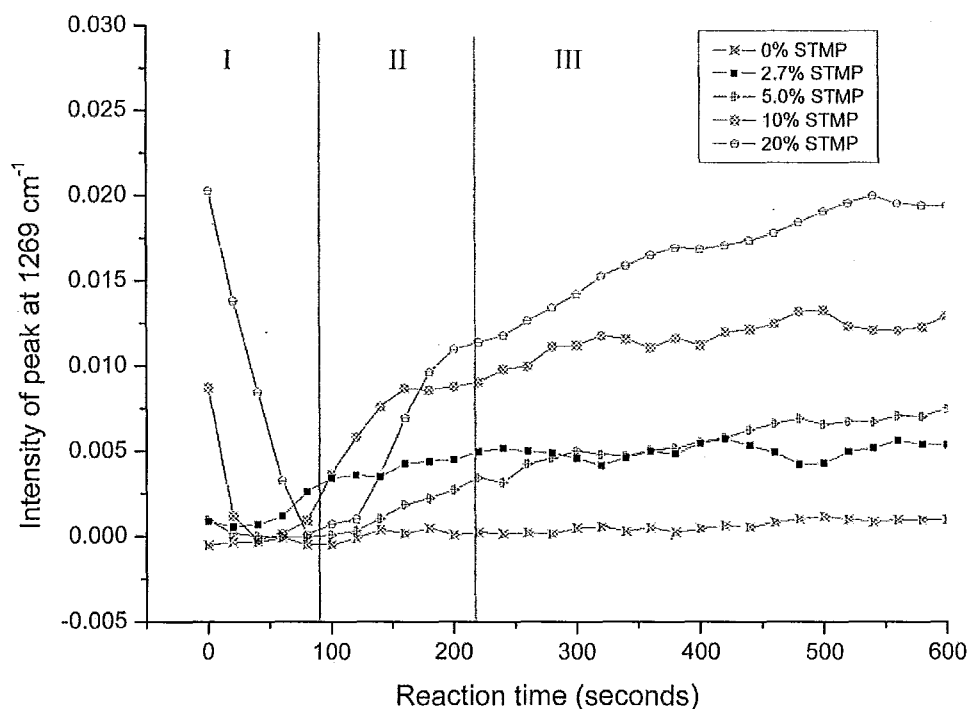
Figure 5.5 Profile curve of the peak at 1269 cm^{-1} (P=O bond) changing with reaction time of starch crosslinking reaction at STMP percentage of 0 wt%, 2.7 wt%, 5.0 wt%, 10 wt%, 20 wt% respectively (based on dry starch weight) at 120 °C in 600 seconds.

The figure includes the control sample (0 wt% STMP), shown to indicate the peak remained unchanged from the baseline when phosphorylation did not occur. There are three characteristic regions observable in the figure over the duration of the experiment. Region I covers approximately the first 100 s of the reaction where at low concentrations, < 10 wt% STMP, the peak intensity remained effectively indistinguishable from the baseline. The region shows an induction period in the bulk reaction related to ring-opening of the STMP in the presence of the hydroxyl ion of NaOH giving the tripolyphosphate reactant. Assuming a high dissociation constant for starch at pH 11, the supposition of a nucleophilic attack by starch alcoholate ion of the trimetaphosphate ring cannot be reconciled by this finding, though differences may occur in initiation due to the bulk state of the reaction. According to Sang et al. (2007) further hydrolysis may occur with the possibility of pyro- and ortho-phosphates also being present during the reaction. At higher concentrations of STMP, 10 wt% and above, the excess reactant was thought to form complexes initially which produced the non-zero value for the band at 1269 cm^{-1}. At these higher concentrations, the phosphate complexes took longer to undergo ring-opening and for this peak intensity to drop to zero, but for all concentrations tested the peak intensity did finally drop to a baseline value of zero before commencement of Region II. Over the following ~100 s which we considered Region II, the rapid increase in intensity for the peak pointed to a shifted equilibrium driving the formation of starch tripolyphosphate once sufficient ring-opened reactant species were present. The onset of Region III was determined by the concentration of STMP originally present but more or less corresponded to a time of 200-280 s from once the reaction started, taking longer to

reach for lower amounts of the reactant. The third region was denoted by a significant reduction in the reaction rate, continuously becoming slower till the reaction effectively stopped between 600-1000 s, taking longer for lower STMP content. The formation of distarch phosphate appears here to be the rate-controlling step in the bulk modification of potato starch. Considering the maximum reaction time within a twin screw extruder is reasonably estimated to be 120-200 s (after all reactants were added to the process), this data points out that the primary product of reactive extrusion would be tripolyphosphate starch unless shear contributions were noteworthy (particularly to gelatinization).

5.4.2 Extent of crosslinking

The quoted *extent of crosslinking,* calculated for the subsequent sections of this work, used elemental analysis of phosphorus content to generate a calibration curve with the infrared band at 1269 cm^{-1}. The five reacted samples previously shown in Figure 5.5 with concentrations of STMP from 0-20% (w/w) relative to dry potato starch were characterized by EDS for their phosphorus content. The determined final phosphorus content (weight percentage) of these samples was 0%, 0.44%, 0.82%, 1.14%, 1.36%, and 2.28% corresponding to conditions using 0%, 1.6%, 2.7%, 5.0%, 10% and 20% STMP, respectively. The standard deviation in this measurement was ±0.11%. The earlier noted detection threshold of the EDS technique was apparent in this data as it could not distinguish the phosphorus content of native potato starch (~0.02% P; Lim and Seib, 1993) from the baseline. The data from the EDS showed linear correlation with the infrared band ($R^2 = 0.99$) when fitted by regression analysis. The established correlation for estimation of the extent of crosslinking (EC) derived from phosphorus content was:

$$EC = 529.93 \cdot I_{absorbance} \tag{1}$$

where EC has the units of number of phosphate crosslinkages (N_{P-O-C}) per 100 anhydroglucose unit (AGU) and $I_{absorbance}$ was the relative infrared absorbance intensity at 1269 cm^{-1} compared to the baseline case at 0% STMP.

5.4.3 Batch reaction kinetics

The phosphate crosslinking reaction was considered to follow pseudo first-order kinetics due to the excess starch in the presence of STMP. The conversion data calculated using Eqn (1) was found to give a reasonable fit to the generalized equation given as:

$$r = k[starch]^0[STMP] = k'[STMP] \tag{2}$$

where r is the reaction rate [N_{P-O-C} (100 AGU)$^{-1}$ s^{-1}], and k' is the pseudo first-order rate constant [s^{-1}] which is a function of the excess starch content. The averaged k' calculated for 0.6-5% STMP content at 90 °C and 120 °C was 0.00109 s^{-1} and 0.00138 s^{-1} respectively, based on the slope of the plot of Ln (N_{P-O-C}) versus reaction time. The error in the determined rate constants was 0.1%. In comparison to the value of 0.0189 h^{-1} given by Hirsch and Kokini (1998) for the reaction in solution at 90°C, the calculated rate here demonstrated improved conversion achievable by reactions in bulk. The activation energy calculated from the averaged k' and using the Arrhenius equation was 9.33 x 10^3 J/mol.

Bulk modification of starch often requires inclusion of a plasticizer like glycerol in order to convey the material without burning or prevent exceeding the power capacity of the machinery. Conversely, hydrocolloidal gums like xanthan gum are added to starch

Table 5.3 Pseudo first-order rate constants (RC) for the different batch systems

STMP[a] (wt%)	Additves[b] (wt%)	RC (s^{-1}) at 90 °C	RC (s^{-1}) at 120 °C
2.7	n/a	0.00112	0.00144
2.7	10% G	0.00130	0.00157
2.7	30% G	0.00059	0.00110
2.7	1% X	0.00115	0.00145
2.7	2% X	0.00118	0.00150

a. Percentages in the table are based on dry starch weight.
b. G – glycerol, X – xanthan gum.

mass to increase its viscosity during processing. These rheological controlling additives when present increase the content of hydroxyl species in the phosphorylation reaction but have not been considered in the literature as participants in crosslinking. To ascertain the effect of these additives on the reaction kinetics, a PLS model analyzed the extent of crosslinking for bulk reactions where these two species were individually added. The concentrations examined for these species were chosen according to reasonable variance in the bulk viscosity, xanthan gum having a much greater impact compared to glycerol. The coefficient plot from the model showing the extent of influence by each factor is given in Figure 5.6 while the actual rate data at fixed 2.7% STMP is shown in Table 5.3. The coefficient plot according to multivariate analysis shows that STMP had the most significant effect on the crosslinking reaction; glycerol significantly increased the rate while xanthan gum has a smaller but still positive effect. The reaction rate at 90 °C increased by 2.7% and 5.4% with the inclusion of 1% and 2% xanthan gum, respectively and 16.1% and -47.3% for 10% and 30% glycerol, respectively. Glycerol was most

effective at its lower concentration of 10% whereas xanthan gum had a persistent positive

effect on the rate up to its highest tested concentration of 2% (w/w). The chemical

structure of xanthan gum consists of repeating pentasaccharide units (Garcia-Ochoa et al.,

2000) capable of forming alkoxide ions during the reaction. Xanthan gum and glycerol

contributed in the reaction by increasing the concentration of alkoxide ions present and

enhanced the ionic strength of the system. Both outcomes helped to shift the equilibrium

in the direction of creating diester phosphates, and thus positively influenced the

crosslinking reaction. The diminishing effectiveness of glycerol on the reaction is

indicative of its interactions formed with starch. Glycerol is a known anti-plasticizer at

higher concentrations (van Soest et al., 1996) forming strong associations with starch
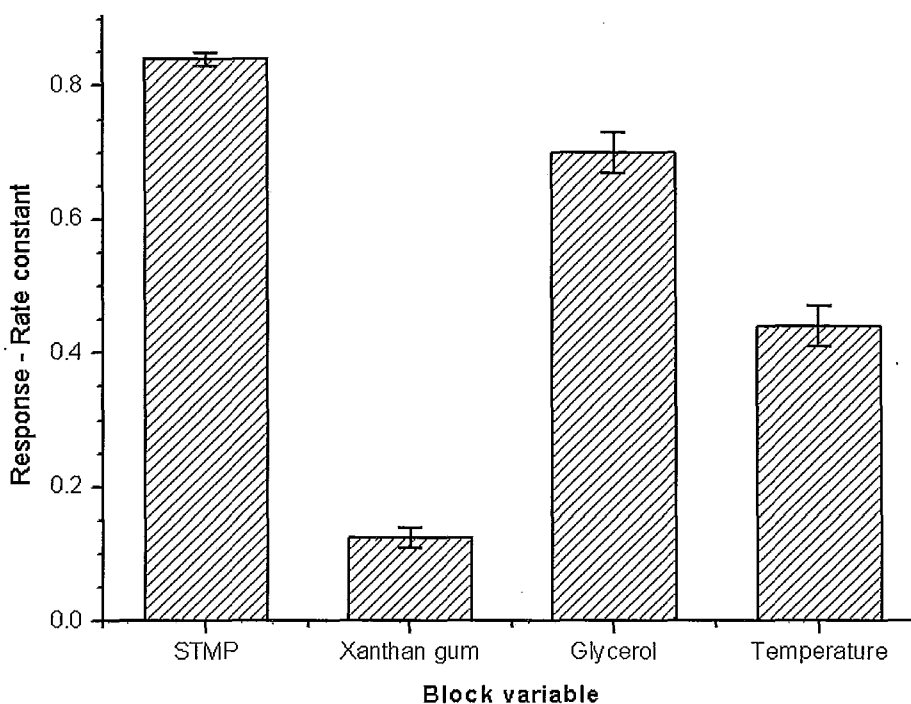
Figure 5.6 Coefficient plot of the PLS model showed the effect of variables on the crosslinking reaction.

which inhibits both gelatinization and retrogradation. At its higher concentration of 30%, glycerol hindered diffusion of the reactants within potato starch by competing for water and likely for the crosslinking agent as well.

5.4.4 Extent of crosslinking of extrusion samples

The extent of crosslinking based on infrared analysis of the extruded samples is summarized in Figure 5.7. The samples were analyzed immediately upon exiting from the die of the extruder. From the point of reactant addition into the extruder up to the die exit the mean residence time was estimated to be 200 s. This measurement was based upon colorimetric tracer studies for residence time determination; a review of tracer techniques
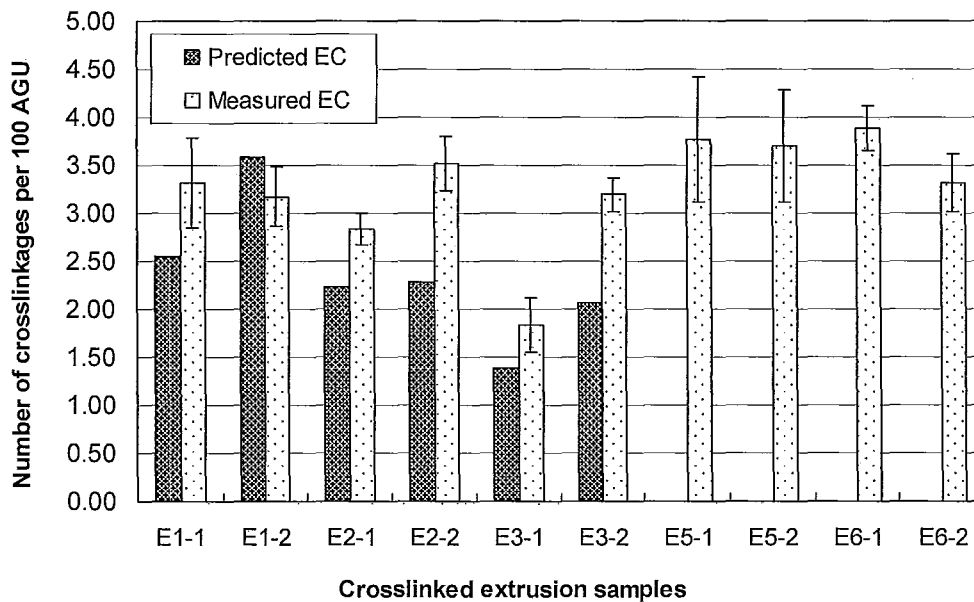
Figure 5.7 Extent of crosslinking (EC, number of phosphate crosslinkages per 100 AGU) of crosslinked extrusion products compared with predicted EC.

used in extruders is given in Thompson et al. (1995). The residence time and corresponding rate constant from the kinetic study were used to predict the extent of crosslinking for each extruded sample in order to evaluate the effect of intensive shear mixing upon the reaction system; predicted values calculated for 120 °C based on measured extrudate temperature. The results in the figure show that the measured extent of crosslinking after extrusion was significantly greater in almost all cases compared to the predicted value, on average by 40%. However, the trends for each of the major reactants and additives in regards to the extent of crosslinking occurring remained the same as seen in the batch kinetics study. There were concerns that the rheology controlling additives would display different crosslinking trends in the flowing system as now their physical properties on the continuous phase would have a more significant role than in the batch experiments, but that does not appear to be the case.

A major reason for the difference between the two sets of values (i.e. batch versus extrusion) was the starch had already been gelatinized in the extruder prior to mixing with the sodium trimetaphosphate and other additives, and hence the system did not exhibit the same diffusion-limited reaction rate found when the granule wall membrane was intact. De Graf, et al. (1995) had noted in their kinetic study of acetylation for potato starch that granular state reactions were about 100 times slower compared to gelatinized starch. Unfortunately, pre-gelatinized starch could not be tested in our batch kinetics study since it was not possible to evenly mix the reactants into bulk gelatinized starch without shear, and such mechanical movement could not be used in direct proximity to our infrared probe. Hence, the work in the extruder stands alone, conducted to

demonstrate the barrier effect of the wall membrane on bulk crosslinking of starch. It is quite evident from the results in the figure that when STMP is concentrated in immediate proximity to the polysaccharide species of starch (as found in a well mixed bulk mixture), not diluted and largely segregated within a water phase or impeded by a granule wall, that the reaction rate is significantly higher.

The differences between predicted and measured EC values in Figure 5.7 were seen to increase as crosslinking increased with higher STMP content, higher gum content or low glycerol content. This can be readily explained when realizing that intact starch granules would be experiencing crosslinking primarily at their periphery (Fannon et al., 2004) which produces a steady reduction in membrane swellability and thus, a logically expected decrease in the diffusion of reactants into their interiors. An ever-decreasing rate of reaction would result for a granule due to its crosslinked exterior 'shell' and it was felt that the growing difference between the extruder and batch results with increased extent of crosslinking was cause by the fact that the reaction in the extruder would not suffer this phenomenon (at least not for the level of crosslinking in this study).

Figure 5.7 includes a set of runs (E5-1, E5-2, E6-1, E6-2) looking at the additivity of effects by xanthan gum and glycerol plasticizer on the extent of crosslinking. The results were once again in agreement with the trends shown by the PLS model and by the samples testing the rheology controlling additives individually. The increase in xanthan gum had again a positive effect on the extent of crosslinking but the negative effect of high glycerol content appeared to have a larger effect as the gum content increased. In fact, at 2% gum and 30% glycerol (E6-2) the extent of crosslinking was now comparable

to the sample with only 2.7% STMP and no additives (E3-2) (percentage based on dry starch weight). The results suggest the anti-plasticizing influence of glycerol mentioned earlier was unimpeded in this case by the inclusion of the gum.

5.4.5. Rheological properties of extrusion samples

Hydrogels made from crosslinked starch samples prepared on the extruder were characterized for their rheological changes. The viscosity curves of each extruded starch hydrogel based on differing amounts of STMP (without additives) are shown in Figure 5.8(a). Both cross-linked starch hydrogels and the gelatinized control showed pseudoplastic or shear-thinning behavior at lower shear rates and a terminal plateau above 400 s^{-1}. The plateau represents a deformational limit whereby the complex structure of starch offers no further disentanglement within the given medium, most probably due to water phase separation and migration to the high shear plane. The shear viscosities of the cross-linked species were lower than the control but showed little difference based on STMP content. The reduced viscosity was attributed to a lower capacity to swell by the crosslinked species and thus lower macromolecular entanglements were apparent to resist deformation. The shear thinning nature of the crosslinked polymers was less pronounced with a higher slope seen compared to the gelatinized control (0% STMP and 0% Na_2SO_4). With higher STMP content the sample exhibited slightly higher viscosity despite increased extent of crosslinking, possibly suggesting some shear damage during extrusion.
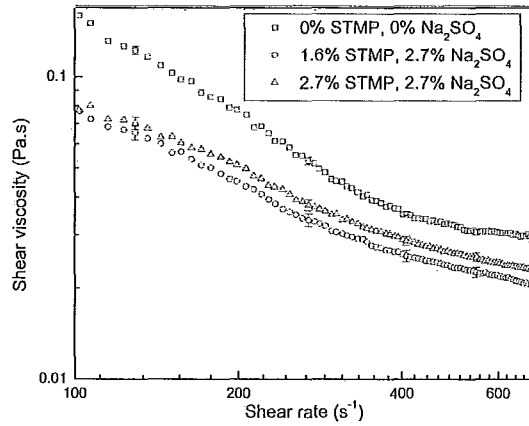
(a) with varied amount of crosslinking agents
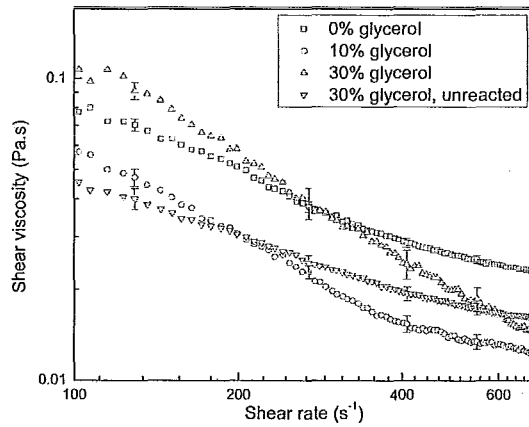
(b) with varied amount of glycerol
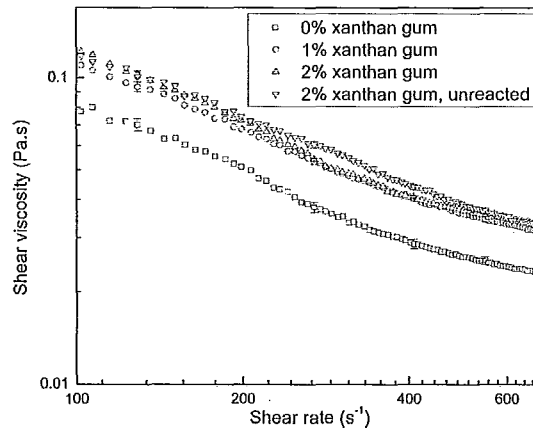
(c) with varied amount of xanthan gum

Figure 5.8 Viscosity curves of hydrogels made from crosslinked extrusion products containing different amount of reactants (based on weight percent of dry starch).

The influence of glycerol on viscosity is shown in Figure 5.8(b). The graph includes two controls to aid in our analysis. The 0% control shown corresponded to a crosslinked sample prepared without glycerol included during reactive extrusion. That same sample was also tested with 30% glycerol added into the hydrogel solution (i.e. unreacted glycerol). The unbound glycerol in that case was noted to shift the entire curve to a lower viscosity demonstrating the normally observed behavior of increased free volume by a plasticizer on a polymer system. With glycerol in the reacting material (E1-1 and E1-2) the slope of the viscosity curve was decreased indicating greater shear thinning – a behavior not seen with the unbound glycerol. Increased shear thinning is often related to branched polymer structures which we take to infer that the glycerol is participating in the phosphorylation reaction. Due to steric hindrance, only one hydroxyl group was likely capable of participation in the reaction, end-capping the starch-tripolyphosphate chain and preventing a distarch linkage from forming. With 10% glycerol content in the reaction, crosslinking between starch molecules remained the dominant influence on viscosity (with crosslinking likely improves slightly by its plasticizing effect); however, by 30% the higher content of glycerol in the system lead to significantly more branching in comparison to crosslinkage formation, corresponding to our reported drop in measured extent of crosslinking in Figure 5.7.

The rheological properties of cross-linked starch incorporating different amounts of xanthan gum are shown in Figure 5.8 (c). Similar to the analysis of glycerol, this graph includes two controls to aid in understanding the effect of the gum on the reacted samples. The 0% control was once again the sample crosslinked without any additives

present and that same sample was also tested with 2 % xanthan gum added into the hydrogel solution (i.e. unreacted) prior to viscosity measurement. In this case, the unreacted xanthan gum led to increased viscosity that was slightly higher than all other tested samples. The reason is that the unreacted xanthan gum molecules expanded and entangled without restriction by crosslinkages. The trisaccharide side chains of xanthan gum along with its backbone form a large exclusion volume in solution which produces high viscosity even at very low concentration. For the cases where the xanthan gum was present in the reaction, the effect on viscosity was little difference from the unreacted case. The viscous thickening attributes of xanthan gum were dominant in this case and there was little distinction in viscosity between the two concentrations of gum present. The analysis in this case does not aid in understanding the nature by which the additive participated in the reaction, though with the higher measured extent of crosslinking for both concentrations of gum it was felt that it was simply replacing starch molecules in some bimolecular linkages.

5.5 Conclusions

An in-situ ATR/IR monitoring technique was demonstrated for monitoring the kinetics of bulk crosslinking. Multivariate statistical analysis was used to extract the meaningful vibrational bands that changed over the course of the reaction. The intensity of absorbance bands at 1001 cm^{-1} and 1269 cm^{-1} (v_{as} P-O-C and v_{as} P=O) were found to be most readily affected as phosphorylation progressed. The presence of conventionally used rheology controlling additives such as hydrocolloidal xanthan gum and glycerol,

were noted to have an effect on the reaction rate. From the analysis in this paper it is reasonably surmised that the glycerol terminates a phosphoryl reaction leading to a branched microstructure while the gum simply replaced a starch molecule in a crosslinkage. Rheological tests showed the influence of either additive was minor on the final crosslinked structure and therefore it remains advisable to utilize additives of xanthan gum and glycerol in extrusion process to control processability. Extrusion trials for the bulk reaction highlighted the importance of gelatinization to the reaction rate. In comparison to the batch kinetics study, the samples produced by reactive extrusion showed a 40% higher extent of crosslinking. The result was attributed to the fact that gelatinization was rapidly achieved in the extruder and the crosslinking reaction proceeded without the mass transport barrier of the granule wall.

5.6 Acknowledgements

5.7 References

Achayuthakan, P., & Suphantharika, M. (2008). Pasting and rheological properties of waxy corn starch as affected by guar gum and xanthan gum. *Carbohydrate Polymers*, 71, 9-17.

Braz, R., Hechenleitner, A. A. W., & Cavalcanti, O. A. (2007). Extraction, structural modification and characterization of lotus roots polysaccharides (nelumbo

nucifera gaertn). Excipient with potential application in modified drug delivery systems. *Latin American Journal of Pharmacy*, 26, 706-710.

Carr, M. E. (1991). Starch-derived glycol and glycerol glucosides prepared by reactive extrusion processing. *Journal of Applied Polymer Science*, 42, 45-53.

Carr, M. E. (1992). Preparation and application of starch graft poly(vinyl) copolymers as paper coating adhesives. *Starch-Starke*, 44, 219-223.

Carr, M. E. (1994). Preparation of cationic starch containing quaternary ammonium substituents by reactive twin-screw extrusion processing. *Journal of Applied Polymer Science*, 54, 1855-1861.

Chung, H. J., Min, D., Kim, J. Y., & Lim, S. T. (2007). Effect of minor addition of xanthan on cross-linking of rice starches by dry heating with phosphate salts. *Journal of Applied Polymer Science*, 105, 2280-2286.

Coates,J. (2000). Interpretation of infrared spectra. In: R.A. Meyers, Editor, *Encyclopedia of Analytical Chemistry*, pp.10815–10837. John Wiley & Sons Ltd.: Chinchester, UK.

Cury, B. S. F., Castro, A. D., Klein, S. I., & Evangelista, R. C. (2009). Modeling a system of phosphated cross-linked high amylose for controlled drug release. Part 2: Physical parameters, cross-linking degrees and drug delivery relationships. *International Journal of Pharmaceutics*, 371, 8-15.

De Graf, R. A., Broekroelofs, G. A., Janssen, L. P. B. M., & Beenackers, A. A. C. M. (1995). The kinetics of the acetylation of gelatinised potato starch. Carbohydrate Polymers, 28, 137–144.

Delval, F., Crini, G., Bertini, S., Morin-Crini, N., Badot, P. M., Vebrel, J. L., et al. (2004). Characterization of crosslinked starch materials with spectroscopic techniques. *Journal of Applied Polymer Science*, 93, 2650-2663.

Demirgoz, D., Elvira, C., Mano, J. F., Cunha, A. M., Piskin, E., & Reis, R. L. (2000). Chemical modification of starch based biodegradable polymeric blends: Effects on water uptake, degradation behaviour and mechanical properties. *Polymer Degradation and Stability*, 70, 161-170.

Dubois, I., Picton, L., Muller, G., Audibert-Hayet, A., & Doublier, J. L. (2001). Structure/rheological properties relations of crosslinked potato starch suspensions. *Journal of Applied Polymer Science*, 81, 2480-2489.

Dulong, V., Lack, S., Le Cerf, D., Picton, L., Vannier, J. P., & Muller, G. (2004). Hyaluronan-based hydrogels particles prepared by crosslinking with trisodiurn trimetaphosphate. Synthesis and characterization. *Carbohydrate Polymers*, 57, 1-6.

Dumoulin, Y., Alex, S., Szabo, P., Cartilier, L., & Mateescu, M. A. (1998). Cross-linked amylose as matrix for drug controlled release. X-ray and ft-ir structural analysis. *Carbohydrate Polymers*, 37, 361-370.

Fannon, J. E., Gray, J. A., Gunawan, N., Huber, K. C., & BeMiller, J. N. (2004). Heterogeneity of starch granules and the effect of granule channelization on starch modification. *Cellulose*, 11, 247-254.

Garcia-Ochoa, F., Santos, V. E., Casas, J. A., & Gomez, E. (2000). Xanthan gum: Production, recovery, and properties. *Biotechnology Advances*, 18, 549-579.

Hirsch, J. B., Kokini, J.L. (1998). Kinetics of Starch Crosslinking. *Institute of Food Technologists Annual Meeting*, Atlanta.

Lawton, D., Wang, G., Thompson, M.R., & Liu, Q. (2010). Reactive extrusion of potato starch, *ANTEC conference paper*.

Le Bail, P., Morin, F. G., & Marchessault, R. H. (1999). Characterization of a crosslinked high amylose starch excipient. *International Journal of Biological Macromolecules*, 26, 193-200.

Li, B. Z., Wang, L. J., Li, D., Chiu, Y. L., Zhang, Z. J., Shi, J., et al. (2009). Physical properties and loading capacity of starch-based microparticles crosslinked with trisodium trimetaphosphate. *Journal of Food Engineering*, 92, 255-260.

Lim, S., & Seib, P. A. (1993). Preparation and pasting properties of wheat and corn starch phosphates. *Cereal Chemistry*, 70, 137-144.

Luo, F. X., Huang, Q., Fu, X., Zhang, L. X., & Yu, S. J. (2009). Preparation and characterisation of crosslinked waxy potato starch. *Food Chemistry*, 115, 563-568.

Mao, G. J., Wang, P., Meng, X. S., Zhang, X., & Zheng, T. (2006). Crosslinking of corn starch with sodium trimetaphosphate in solid state by microwave irradiation. *Journal of Applied Polymer Science*, 102, 5854-5860.

Marques, P. T., Lima, A. M. F., Blanco, G., Laurindo, J. B., Borsali, R., Le Meins, J. F., et al. (2006). Thermal properties and stability of cassava starch films cross-linked with tetraethylene glycol diacrylate. *Polymer Degradation and Stability*, 91, 726-732.

Miladinov, V. D., & Hanna, M. A. (1995). Apparent viscosity of starch and xanthan gum extruded with crosslinking agents. *Industrial Crops and Products*, 4, 261-271.

Murua-Pagola, B., Beristain-Guevara, C. I., & Martinez-Bustos, F. (2009). Preparation of starch derivatives using reactive extrusion and evaluation of modified starches as shell materials for encapsulation of flavoring agents by spray drying. *Journal of Food Engineering*, 91, 380-386.

Nabeshima, E. H., & Grossmann, M. V. E. (2001). Functional properties of pregelatinized and cross-linked cassava starch obtained by extrusion with sodium trimetaphosphate. *Carbohydrate Polymers*, 45, 347-353.

Nagano, T., Tamaki, E., & Funami, T. (2008). Influence of guar gum on granule morphologies and rheological properties of maize starch. *Carbohydrate Polymers*, 72, 95-101.

Nayouf, M., Loisel, C., & Doublier, J. L. (2003). Effect of thermomechanical treatment on the rheological properties of crosslinked waxy corn starch. *Journal of Food Engineering*, 59, 209-219.

Pongsawatmanit, R., & Srijunthongsiri, S. (2008). Influence of xanthan gum on rheological properties and freeze-thaw stability of tapioca starch. *Journal of Food Engineering*, 88, 137-143.

Ptaszek, P., & Grzesik, M. (2007). Viscoelastic properties of maize starch and guar gum gels. *Journal of Food Engineering*, 82, 227-237.

Sang, Y., Prakash, O., & Seib, P.A. (2007). Characterization of phosphorylated cross-linked resistant starch by ^{31}P nuclear magnetic resonance (^{31}P NMR) spectroscopy. *Carbohydrate Polymers*, 67, 201-212

Seker, M., & Hanna, M. A. (2005). Cross-linking starch at various moisture contents by phosphate substitution in an extruder. *Carbohydrate Polymers*, 59, 541-544.

Seker, M., & Hanna, M. A. (2006). Sodium hydroxide and trimetaphosphate levels affect properties of starch extrudates. *Industrial Crops and Products*, 23, 249-255.

Shalviri, A., Liu, Q., Abdekhodaie, M. J., & Wu, X. Y. Novel modified starch-xanthan gum hydrogels for controlled drug delivery: Synthesis and characterization. *Carbohydrate Polymers*, 79, 898-907.

Simkovic, I., Hricovini, M., Mendichi, R., & van Soest, J. J. G. (2004). Cross-linking of starch with 1, 2, 3, 4-diepoxybutane or 1, 2, 7, 8-diepoxyoctane. *Carbohydrate Polymers*, 55, 299-305.

Thompson, M.R., Puaux, J.P., Hrymak, A.N., Hamielec, A. E. (1995). Modeling the residence time distribution of a non-intermeshing twin screw extruder. *International Polymer Processing*, 10, 111-119

Tzoganakis, C. (1989). Reactive extrusion of polymers: A review. *Advances in Polymer Technology*, 9, 321-330.

van Soest, J.J.G., Bezemer, R.C., de Wit, D., & Vliegenthart, J.F.G. (1996). Influence of glycerol on the melting of potato starch. *Industrial Crops and Products*, 5, 1-9

Woo, K., & Seib, P. A. (1997). Cross-linking of wheat starch and hydroxypropylated wheat starch in alkaline slurry with sodium trimetaphosphate. *Carbohydrate Polymers*, 33, 263-271.

Xie, S. X., Liu, Q., & Cui, S. W. (2005). Starch modifications and applications. In: S. W. Cui, Editor, *Food carbohydrates: chemistry, physical properties, and applications*, pp. 359-382. Boca Raton: CRC press.

Zhang, J., & Wang, Z. W. (2009). Optimization of reaction conditions for resistant canna edulis ker starch phosphorylation and its structural characterization. *Industrial Crops and Products*, 30, 105-113.

CHAPTER 6 CROSSLINKED STARCH BIOCOMPOSITES REINFORCED WITH SISAL CELLULOSE FIBERS

G. Wang, M.R. Thompson

MMRI/ CAPPA-D
Department of Chemical Engineering, McMaster University
Hamilton, Ontario, Canada L8S 4L7
Tel: (905) 525-9140 x 23213
Fax: (905) 521-1350
mthomps@mcmaster.ca

and

[1] *Q. Liu*
[1] Guelph Food Research Centre, Agriculture and Agri-Food Canada,
Guelph, Ontario, Canada

The following chapter is based on a manuscript submitted to the journal Carbohydrate

Polymers, July 2010. The contents are the sole work of the Master's candidate.

6.1 Abstract

A novel bio-based composite was investigated in this study derived from a modified thermoplastic potato starch and sisal cellulose fibers in an attempt to address common deficiencies of weak mechanical strength and high moisture sensitivity in starch-based bioplastic sought for structural usage. A matrix comprised of gelatinized potato starch and processing additives of a hydrocolloidal gum and glycerol was covalently crosslinked with sisal fibers using sodium trimetaphosphate (STMP). The bulk modification was completed during compounding within a co-rotating intermeshing twin screw extruder (TSE). The biocomposite material was characterized using infrared spectroscopy, sessile drop contact angle measurement, moisture content determination and tensile mechanical testing. Through experimental testing and use of the Tsai-Halpin model, it was determined that crosslinkages formed between the starch matrix and sisal fibers, leading to substantial reinforcement of the thermoplastic matrix. While mechanical properties were shown to improve by this approach, the moisture sensitivity of the material was also increased. The increased crosslink density in the starch reduced crystallinity, giving more ready access for water to diffuse into the amorphous regions in this material.

6.2 Introduction

Biodegradable plastics refer to materials maintaining durability over a mandated service life but being able to naturally decompose in waste landfill facilities (Mohanty, Misra, & Drzal, 2002). The conventional feedstocks for polymer engineering are mainly

petroleum and natural gas. Plastic products from these sources lack a potential pathway toward biodegradation (though there are odd exceptions) and thus can negatively affect our environment because of their prolonged lifetime after disposal, resisting bacterial and oxidative degradation. Biological derived polymers are ideal alternatives to traditional petroleum as feedstock due to their environmentally friendliness and renewable nature. There are many emerging examples of bioplastics such as polylactic acid (PLA), poly-3-hydroxybutyrate (PHB), and lignin-based Arboform™. The major deficiencies to broad immediate use of starch based bioplastic in applications are weak mechanical properties and high moisture sensitivity, making replacement of conventional materials difficult (Huneault & Li, 2007). Thermoplastic starch (TPS) among other bioplastics has been widely utilized at this moment in time due to its ready availability in ample quantities and its well understood biodegradation pathway. TPS is made from a selected starch variety and requires substantial addition of plasticizers (ex. water, glycerol, triethyl citrate, urea) in its preparation in order to reduce brittleness and to improve processability (Bonacucina *et al.*, 2006; Wang et al., 2003).

One of the most important approaches to offsetting the low mechanical properties and moisture sensitivity of TPS is the incorporation of natural fibers into the matrix (Averous & Boquillon, 2004; Alvarez & Vazquez, 2006; Belhassen et al., 2009; Canigueral et al., 2009; Corradini et al., 2009; Curvelo, de Carvalho, & Agnelli, 2001; Graupner, 2008; Guimaraes et al., 2010; Huneault & Li, 2007; Saiah et al., 2009). Such biocomposites have improved marketability to a wide range of industries including construction, marine, electronics, consumer appliances, automotive and even aerospace

(John & Thomas, 2008). Cellulose is a particularly attractive example of natural fiber being readily isolated from a variety of biological sources including jute, flax, hemp, sisal, and cotton (George, Sreekala, & Thomas, 2001). This fiber is popular for reinforcing filler as they are similarly renewable, biodegradable, and abundant as the TPS matrix, and yet has comparable or even higher specific mechanical properties than aramide, carbon, or glass fibers on account of their low weight (Eichhorn et al., 2001; Trejo-O'Reilly, Cavaille, & Gandini, 1997); sisal fiber for example has an estimated tensile modulus of 450-700 MPa and density of only ~1450 kg/m^3 (Nair, Diwan, & Thomas, 1996; de Verney, Lima, & Lenz, 2008). However, often the extent of mechanical reinforcement afforded by these fibers remains inadequate for designers to view these biocomposites as replacement materials for existing polymers. With regards to moisture sensitivity, cellulose fibers do not feasibly reduce absorption since their chemical structure remains similar in hydrophilic nature to the starch matrix. Sisal has been shown to decrease the equilibrium moisture absorption capacity of a material (Curvelo, de Carvalho, & Agnelli, 2001; Corradini et al., 2009) but increase its hydrophilicity as determined by water contact angle measurement (Sreekumar, Leblanc, & Saiter, 2010).

Modification or treatment of sisal fibers can further improve the mechanical properties through better interfacial adhesion with the continuous polymer phase. Treatment with compatibilizers is often employed to make hydrophilic and polar fiber more hydrophobic and non-polar so that it becomes compatible with hydrophobic and non-polar matrix. However, in matrix systems based on starch which already possesses similar chemical structure to cellulose, such treatments generally offer little significant

benefit in terms of improving interfacial adhesion and mechanical properties. Alkaline treated and acetylated fibers compounded into MaterBi-Y, a starch based bioplastic, were tested by several researchers (Alvarez and Vazquez, 2006; Cyras, Vallo, Kenny, & Vazquez, 2004) but their reported data showed little improvement or even worse performance in regards to mechanical strength or moisture sensitivity compared to untreated fibers. Use of mercerized sisal fibers was equally unfavorable, found to significantly reduce the tensile mechanical behavior of a fiber-reinforced thermoplastic starch (Corradini, de Morais, Rosa, Mazzetto, Mattoso, & Agnelli, 2006). These chemical modification routes showed that optimal interfacial interactions via hydrogen bonding already existed for a system comprised of sisal cellulose fibers and starch. A covalent interaction via crosslinking with STMP was considered as an alternative in our work, requiring study to determine if the mechanical and water absorption properties of thermoplastic starch could be further improved. The addition of hydrocolloidal xanthan gum positively influenced crosslinking reaction as verified by our previous work (Wang, Thompson, & Liu, 2010). Moreover, introduction of xanthan gum into the system provided another means of rheological control over the extrusion process.

This paper is focused upon examining the performance of a sisal fiber-reinforced crosslinked potato starch developed by twin screw extrusion. The work investigates how crosslinking and fiber loading affect the final properties of this manufactured biocomposite.

6.3 Experimental

6.3.1 Materials

Potato starch was obtained from Manitoba Starch Products (Carberry, Manitoba, Canada). It was a food-grade unmodified potato starch with typical moisture content of 17% as measured by a Mettler-Toledo HG63 moisture analyzer. Sodium trimetaphosphate (STMP, > 99.5% purity) and sodium sulphate powder (> 99.0% purity) were supplied by Sigma-Aldrich Canada Ltd (Oakville, ON, Canada). Glycerol (> 99.5% purity) was provided by Caledon Laboratories Ltd (Georgetown, ON, Canada) while xanthan gum was obtained from Sigma-Aldrich Ltd (St. Louis, MO, USA). Aqueous sodium hydroxide solution (0.1 N) was obtained from LabChem Inc. (Pittsburgh, PA, USA). Natural cellulose fiber (Sisal, 0.12 ± 0.04 mm in diameter, 13 ± 3 mm in length) was provided by Espartos Santos (Murcia, Spain).

6.3.2 Extrusion preparation

A detailed description of the setup used for these experiments was given in a recent paper (Wang, Thompson, & Liu, 2010). Briefly, the materials were prepared on a 27 mm co-rotating intermeshing twin screw extruder with a strand die (Model ZSE27-HP, American Leistritz Extruder Corporation, NJ, USA) using the screw design shown in Figure 6.1. The temperature profile of the 9 zones along the extruder barrel was 60-70-70-90-90-100-120-120-100°C with the die temperature set to 95°C. An aqueous solution containing Na_2SO_4, glycerol, and sodium trimetaphosphate (STMP) (adjusted to a pH of
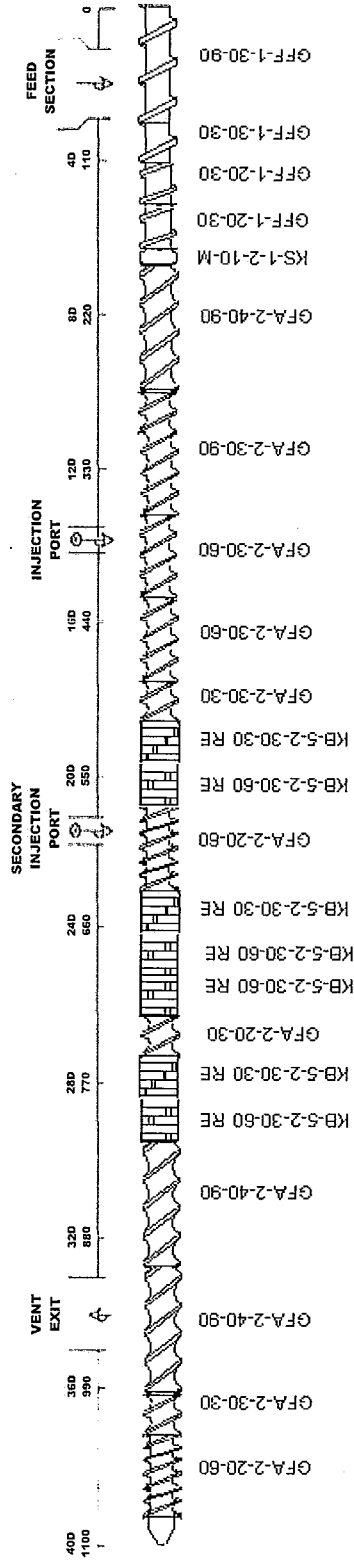
Figure 6.1 Optimal screw design for starch crosslinking modification by reactive extrusion.

11 by NaOH) was injected by a B series chemical metering pump from LMI Milton Roy

Inc. (Ivyland, Pennsylvania) through the first liquid injection port located at the third

barrel zone (12L/D from the feeding port). The total water content was constant for all

trials at 87 wt% (dry starch basis). The relative high water content was necessary to

minimize damage to any crosslinked structure formed under the mechanical shear

required to rapidly and uniformly disperse the reactants into the gelatinized matrix. The

solids, namely starch powder, xanthan gum, and sisal fiber were fed at 1 kg/hr into the

feeding port of the extruder barrel by a Brabender DDSR20 twin-screw gravimetric

feeder (Brabender Technologie, Brampton, ON). The feed rate and screw speed, 20 RPM,

were selected to give a residence time of ~200 s (based on colorimetric tracer studies)

which was suitable to forming diester linkages, according to our previously given kinetic

study for the bulk reaction (Wang, Thompson, & Liu, 2010). The low screw speed was

also suitable to minimize damaging the sisal fiber and crosslinked starch matrix. The

majority of water content of the extruded products was devolatilized at the extruder

through a vent zone open to atmosphere near the end of the machine and further water

loss occurred as the starch was extruded and compression molded. Additional oven

drying and storage under a fixed relative humidity (RH) was done according to the test

analysis performed, as indicated in the following characterization section.

The concentrations of reactants used to prepare crosslinked starch samples *without*

fibers are listed in Table 6.1. The formulation for the prepared biocomposites designated

as samples F1 through F6 is listed in Table 6.2. All percentages of reactants were

calculated on a dry starch weight basis.

Table 6.1 Concentrations of reactants in reactive extrusion of crosslinked starch

No.	STMP (wt%, db[a])	Na$_2$SO$_4$ (wt%, db)	Xanthan gum (wt%, db)	Glycerol (wt%, db)
E1-1	2.7	2.7	0	10
E1-2	2.7	2.7	0	30
E2-1	2.7	2.7	1	0
E2-2	2.7	2.7	2	0
E3-1	1.6	1.6	0	0
E3-2	1.6	2.7	0	0
E3-3	2.7	1.6	0	0
E3-4	2.7	2.7	0	0
E4	0	0	0	0
E5-1	2.7	2.7	1	10
E5-2	2.7	2.7	1	30
E6-1	2.7	2.7	2	10
E6-2	2.7	2.7	2	30

a.db - dry starch weight basis.

Table 6.2 Formulation for the prepared biocomposites

No.	Sisal fiber (wt%, db[a])	STMP (wt%, db)	Na$_2$SO$_4$ (wt%, db)	Xanthan gum (wt%, db)	Glycerol (wt%, db)
F1	2.5	2.7	2.7	2	10
F2	5.0	2.7	2.7	2	10
F3	10	2.7	2.7	2	10
F4	15	2.7	2.7	2	10
F5	20	2.7	2.7	2	10
F6	25	2.7	2.7	2	10

a.db - dry starch weight basis.

6.3.3 Characterization

To measure the mechanical properties, the extruded starch samples were compression molded into slabs with thickness of 3.2 mm right after extrusion and then die-cut into ASTM D 638-08 Type IV dumbbell shaped samples for tensile testing. All modified starch samples were dried under vacuum at 40°C overnight to remove excess moisture and then stored at 30 ± 5% RH in an environmental controlled room for 10 days prior to characterization. The biocomposite samples reinforced with fiber were conditioned for 30 ± 5% RH in the same manner while those prepared at 95 ± 5% RH were stored in a sealed container with excess water for 10 days before use. The tensile tests were carried out on Instron 3366 mechanical testing system (Instron Corporation, USA) at a crosshead speed of 5 mm/min according to ASTM D 638-08. Values of tensile modulus, tensile strength and elongation at break were determined. A minimum of five specimens were tested for each sample material.

The fiber-starch interface was examined by micrographs of cryogenically fractured samples to view the cross-section of an extruded rod sample. The analysis was done using JEOL JSM-7000F (JEOL Ltd., Japan) scanning electron microscope (SEM) at 15 kV. All samples were dried under vacuum at 40°C overnight to minimize moisture. The fractured surface was sputter coated with a 10 nm layer of gold to improve observations. Thermal analysis was performed using a Q200 differential scanning calorimeter (DSC) equipped with a refrigerated cooling system (TA Instruments, USA). A sample of 6.5 mg previously vacuum dried to ~5% moisture was sealed in aluminum

Tzero hermetic DSC pan and heated up from -20°C to 200°C at 10°C/min in the DSC chamber. A nitrogen flow of 150 ml/min was applied during testing.

In order to determine the extent of crosslinking, the modified starch and its biocomposite extrudates were analyzed by a ReactIR™ 1000 ATR-FTIR system (Mettler-Toledo) scanning the mid-range infrared bands between 600-4000 cm^{-1} at a resolution of 4 cm^{-1}. The samples had been previously washed repeatedly with deionized water/ethanol to remove free reactants and vacuum dried to a moisture content of ~5%. The relative absorbance of the spectra was converted into an estimate value for extent of crosslinking based on correlation with the measured phosphorous content found in the samples (determined by energy dispersive X-ray spectroscopy (EDS) on a JOEL 7000 SEM with EDS). Details on the correlation are given in our previous work (Wang, Thompson, & Liu, 2010). The expression for extent of crosslinking (EC) is:

$$EC = a \cdot I_{absorbance} \qquad (1)$$

where EC has the units of number of phosphate crosslinkages per 100 anhydroglucose unit (AGU); $I_{absorbance}$ was the relative infrared absorbance intensity at 1269 cm^{-1} compared to the baseline case at 0% STMP; Correlation factor a is 529.93 for the crosslinked starch samples (quoted in the previous paper) and 577.80 for the biocomposites samples reinforced with sisal fiber, respectively.

To prepare samples for contact angle tests, extruded starch samples were compression molded after extrusion and then die-cut into round pellets with diameter of 10 mm and thickness of 3.2 mm. The prepared pellets were vacuum dried and stored in sealed plastic bags at 30 ± 5% RH for 24 hrs before contact angle measurements. A

Model 100-00-115 goniometer (Rame-hart Inc., Mountain Lakes, NJ, USA) equipped with a Sanyo VCB-3512T NTSC CCD digital camera (Sanyo Electronic LTD, Japan) was employed to measure contact angles. FTA 32 software (Version 2.0, Build No.160, First Ten Angstroms Inc.) was used to process images in order to calculate contact angle of a water droplet. The contact angle was measured once every 20 seconds for 480 seconds. A micro-syringe was used to precisely control the volume of the water droplet. The moisture content of each sample after being stored at $30 \pm 5\%$ RH or $95 \pm 5\%$ RH for 10 days in this work was tested using a Mettler-Toledo HG63 moisture analyzer set to 105°C. The measured moisture content results are listed in Table 6.4.

Statistical analysis of experimental results was conducted using Minitab 15 software obtained from Minitab Inc. (State College, PA, USA).

6.4 Results and discussion

6.4.1 Properties of prepared crosslinked starch

The extent of crosslinking and thermal properties (i.e. transition temperature, T_m, and transition enthalpy, ΔH) for the crosslinked starch samples previously conditioned at $30 \pm 5\%$ RH for 10 days are summarized in Table 6.3. The extent of crosslinking was determined using an empirical correlation stated in our earlier work based upon the relative absorbance intensity of an infrared band sensitive to phosphorylation, namely $1269 \ cm^{-1}$ (Wang, Thompson, & Liu, 2010). Statistical analysis of this data showed that the extent of crosslinking increased with increasing STMP and xanthan gum but decreased for glycerol content greater than 10%. The peak endotherm temperature

Table 6.3 Extent of crosslinking and thermal properties of the crosslinked starch and its biocomposites

No.	Extent of crosslinking[a]	T_m (°C)	ΔH (J/g)[b]
E1-1	3.3	94.67	0.42
E1-2	3.2	86.50	0.57
E2-1	2.8	89.39	1.15
E2-2	3.5	87.87	0.51
E3-1	1.7	70.61	0.48
E3-2	1.8	110.68	0.34
E3-3	3.4	101.21	0.21
E3-4	3.2	107.17	0.94
E5-1	3.8	100.94	1.56
E5-2	3.7	87.01	0.82
E6-1	3.9	100.78	0.14
E6-2	3.3	75.59	2.24
F1	3.0	83.84	1.05
F2	2.9	87.94	0.50
F3	3.1	86.73	0.58
F4	3.3	87.00	0.80
F5	3.4	85.15	0.21
F6	4.1	97.95	0.48

a. Units of crosslinkages per 100 anhydroglucose repeat units.

b. The average standard error for extent of crosslinking, T_m, and ΔH are 6.0%, 0.8%, and 6.2% respectively.

determined by DSC showed a positive correlation with the extent of crosslinking, indicating the reduced chain mobility afforded by the reactively formed intermolecular

bridges affected the transition behavior. Considering the starch was fully gelatinized as a result of the extrusion process the endothermic peak was attributed to crystallinity from retrogradation of the partially crosslinked structure. The enthalpy of the transition decreased with increasing extent of crosslinking which follows as the partially formed interpenetrating network would retard crystalline reordering. In terms of parameters, the peak temperature T_m increased with STMP content but decreased with increasing xanthan gum and glycerol content. Glycerol is known to slow retrogradation in starch gels (Vansoest et al., 1994) as does xanthan gum (Yoshimura, Takaya, & Nishinari, 1999). While starch decomposition could be contributing to the transition behavior via rheological changes caused by crosslinking, the fact that xantham gum appeared to have the opposite effect despite being a viscosity enhancer suggests this effect was minor.

Table 6.4 highlights the moisture sensitivity of the different crosslinked starch materials based on measured moisture absorption content and contact angle determination. Statistical analysis showed that the moisture content response positively correlated with the concentration of STMP, xanthan gum, and glycerol used in the synthesis. For instance, the moisture content increased from 2.0 wt% to 3.8 wt% as STMP content increased from 1.6 wt% to 2.7 wt%. The moisture content also increased from 2.8 wt% to 11.4 wt% when glycerol content increased from 10 wt% to 30 wt%. The moisture content increased from 6.9 wt% to 15.4 wt% when xanthan gum content increased from 1 wt% to 2 wt% while glycerol content remained constant at 30 wt%. The lower crystallinity reported with increased extent of crosslinking allowed more ready incorporation of water within the polysaccharide matrix and both xanthan gum and glycerol offered increased sites for

coordination with water. Figure 6.2 shows plots for selected materials demonstrating

progression of the contact angle value over time. An equilibrium water contact angle

Table 6.4 Measurement of moisture adsorption content and contact angle data of crosslinked starch and its corresponding biocomposites

Sample	Moisture content (wt%)		Contact Angle[a]	Contact Angle
	30 ± 5% RH	95 ± 5% RH	(deg.)	Slope (deg/sec)
E1-1	2.8	-	22.8	-0.0195
E1-2	11.4	-	42.2	-0.0315
E2-1	6.6	-	47.2	-0.0262
E2-2	6.5	-	39.9	-0.0228
E3-1	2.0	-	27.6	-0.0166
E3-2	4.6	-	25.1	-0.0203
E3-3	3.8	-	24.1	-0.0189
E3-4	3.8	-	26.5	-0.0242
E4	2.4	-	35.7	-0.0188
E5-1	1.8	-	34.8	-0.0241
E5-2	6.9	-	25.7	-0.0274
E6-1	2.8	-	27.7	-0.0235
E6-2	15.4	-	31.3	-0.0304
F1	0.8	10.5	20.6	-0.0388
F2	0.6	13.6	15.6	-0.0343
F3	0.6	10.9	11.1	-0.0302
F4	1.3	11.2	16.3	-0.0368
F5	1.0	9.6	22.1	-0.0403
F6	1.5	8.7	32.0	-0.0541

a. The average standard error of moisture content and contact angle are 5.8% and 5.9% respectively.

value for this type of test is rarely achieved with strongly hydrophilic materials, at least within a reasonable span of time (i.e. hours). For this reason, the values stated in Table 6.4 correspond to 60 s after testing began, giving sufficient time for droplet stabilization but little for absorption. The values were similar in range to those reported by other researchers investigating additive effects on starch films (Demirgoz et al., 2000; Veiga-Santos et al., 2005). The table includes the contact angle slope (units of deg./sec) as well, which can be considered as a measurement of absorption kinetics. According to statistical analysis based on the tabulated contact angle values as well as the contact angle slope, the
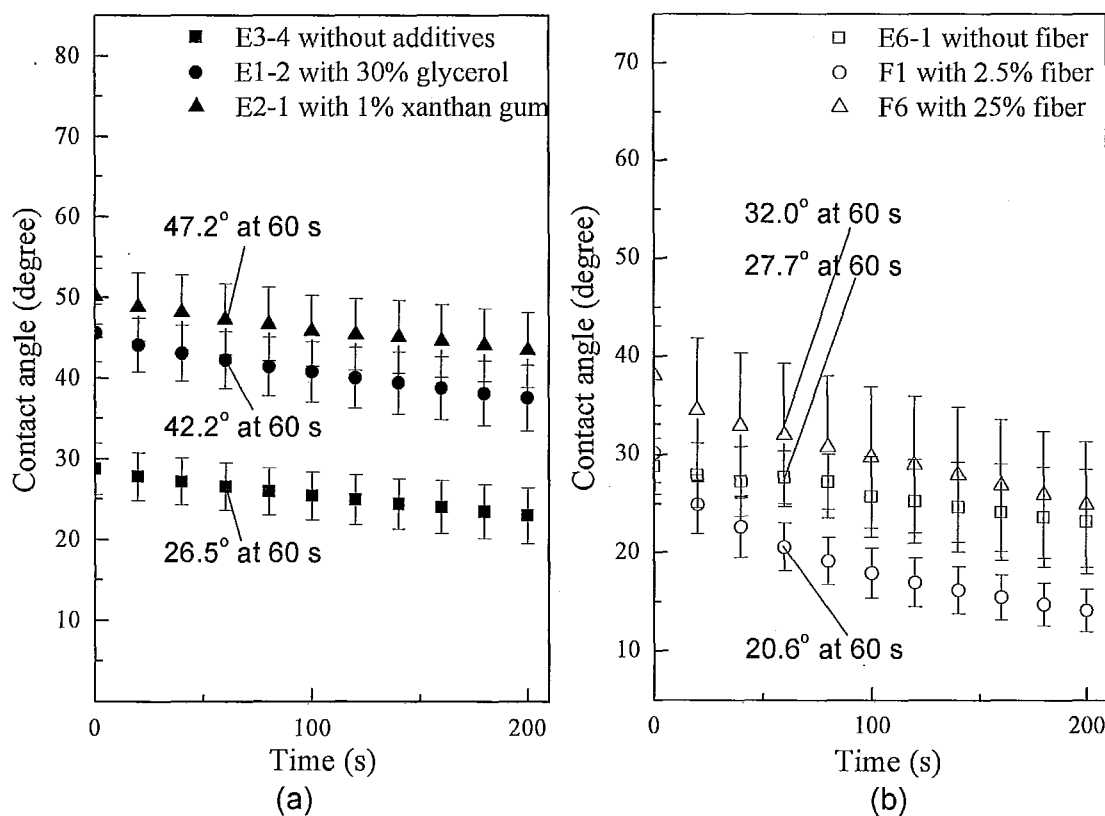
Figure 6.2   Contact angle changing over time of crosslinked starch and its biocomposites.

hydrophilicity of the material changed very little with increasing STMP. In regards to parameter sensitivity in the formulation, the hydrophilicity of the produced material was much more readily altered by the xanthan gum and glycerol (albeit the variance in content for glycerol was far greater than either gum or STMP in the formulations tested). For example, as STMP content increased from 1.6 wt% to 2.7 wt%, the contact angle decreased by only 4° from 28° to 24°; the modified starch experienced increased surface wettability with increased crosslinking similar to the bulk measurement of water absorption. Interestingly, the additives reduced surface wettability in contrast to their effect on the bulk property of moisture absorption. A change of glycerol content from 10 wt% to 30 wt% had much greater effect on contact angle, which increased from 23° to 42°. The contact angle increased from 26° to 31° when xanthan gum content increased from 1 wt% to 2 wt% while the glycerol content remained constant at 30 wt%. Decreasing xanthan gum or glycerol content in the matrix had the opposite effect on the contact angle measurement.

It is evident from these findings that without the inclusion of fibers in the material, the gelatinized partially crosslinked starch materials were not progressing in the desired direction of reduced moisture sensitivity for the final bioplastic. Crosslinkages formed steric hindrance that prevented recrystallization of starch molecular chains. The disruption to the crystal structure of potato starch by crosslinking offered a larger free volume for water absorption despite the greater restriction to chain mobility.

The tensile modulus, tensile strength, and elongation at break for these samples containing different amounts of crosslinking reagents are shown in Figure 6.3. Elongation

at break was the only mechanical factor given in the figure showing correlation with the

reactants, increasing with increased STMP. Elongation at break of crosslinked starch

prepared with 2.7 wt% STMP increased to 16.8% from 9.6 % for uncrosslinked
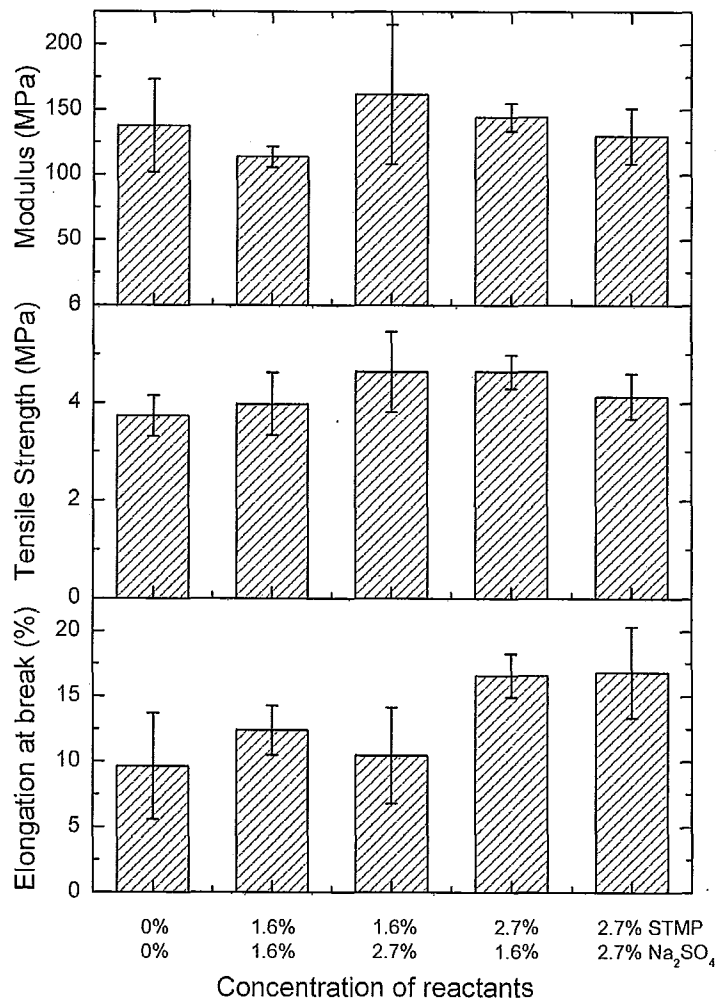
Figure 6.3   Tensile modulus, tensile strength, and elongation at break of extruded crosslinked starch containing different amount of crosslinking agents (based on weight percent of dry starch).

starch (i.e. 0% STMP, 0% Na_2SO_4), showing less brittle behavior. Tensile modulus and strength showed no definitive change for the reactant concentrations examined compared to the gelatinized starch sample. With STMP content varying from 0% to 2.7%, the tensile strength changed from 3.7 MPa to only 4.1 MPa, while the tensile modulus changed from 137.7 MPa to 129.6 MPa, respectively. The extent of crosslinking was evidently too low to reinforce the suprastructure of the thermoplastic starch material though the reduced crystallinity imparted greater drawability without stiffening the matrix, which is agreement with the finding of others (Rioux et al., 2002). From these results, the higher concentrations of the two reactants were used for the subsequent formulation trials.

The influence of the rheological additives, i.e. glycerol and xanthan gum, was considerable more dramatic than found with the crosslinking reactants. The tensile modulus, tensile strength, and elongation at break of extruded crosslinked starch samples (2.7% STMP, 2.7% Na_2SO_4) with differing amounts of glycerol are shown in Figure 6.4. Both tensile modulus and tensile strength values for the modified starch samples decreased with increasing glycerol content, while the elongation at break correspondingly increased. For instance, the tensile strength decreased by 32% from 1.9 MPa to 1.3 MPa, and the tensile modulus decreased by 64% from 27.8 MPa to 10.0 MPa when glycerol content increased from 10 wt% to 30 wt%, while the elongation at break increased by 19 % from 20.8% to 24.8%. The presence of glycerol increased the ductility of the system, reducing brittleness and stiffness. Based on these mechanical data and the fact that the extent of crosslinking remained relatively unchanged for the range of glycerol

concentration tested, it is more than likely that the glycerol acted solely as a plasticizing

agent in the starch matrix (Bergo, Sobral, & Prison, 2010; Sothornvit & Krochta, 2001)

and did not participate in the reaction with trimetaphosphate.
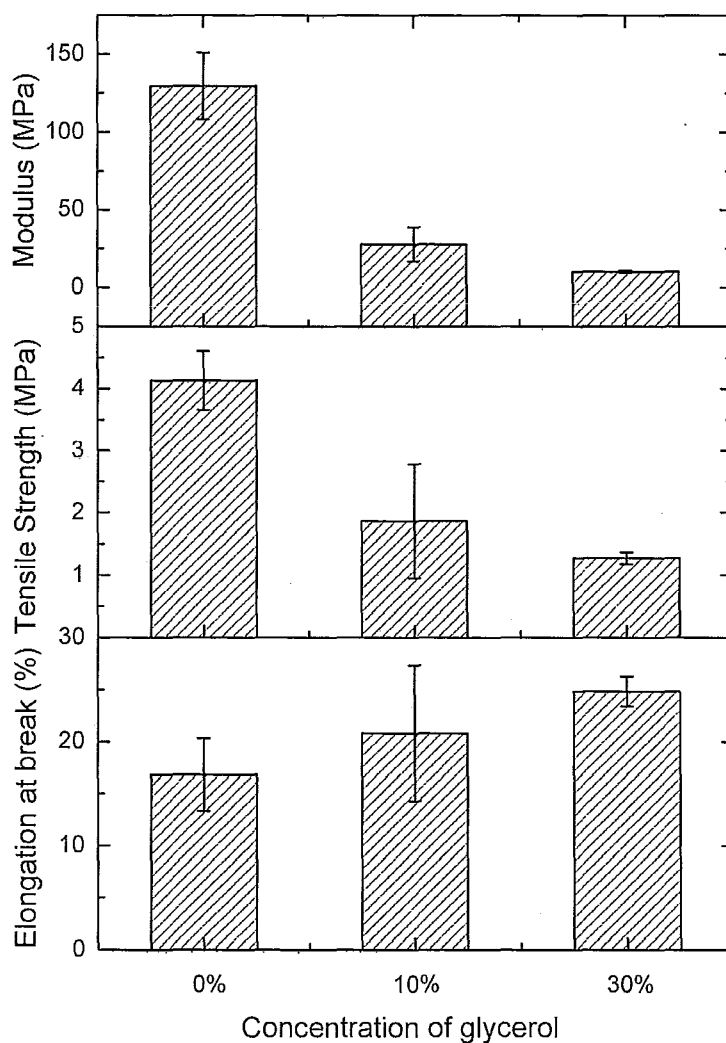
Figure 6.4 Tensile modulus, tensile strength, and elongation at break of crosslinked starch containing the same amount of crosslinking agent (2.7% STMP, 2.7% Na₂SO₄, based on weight percent of dry starch) but different amount of glycerol.

Comparatively, Figure 6.5 shows the effect of differing amounts of xanthan gum

present during the reaction on mechanical properties. The effect of this additive was

opposite to glycerol, naturally acting as a thickening (stiffening) agent in the starch
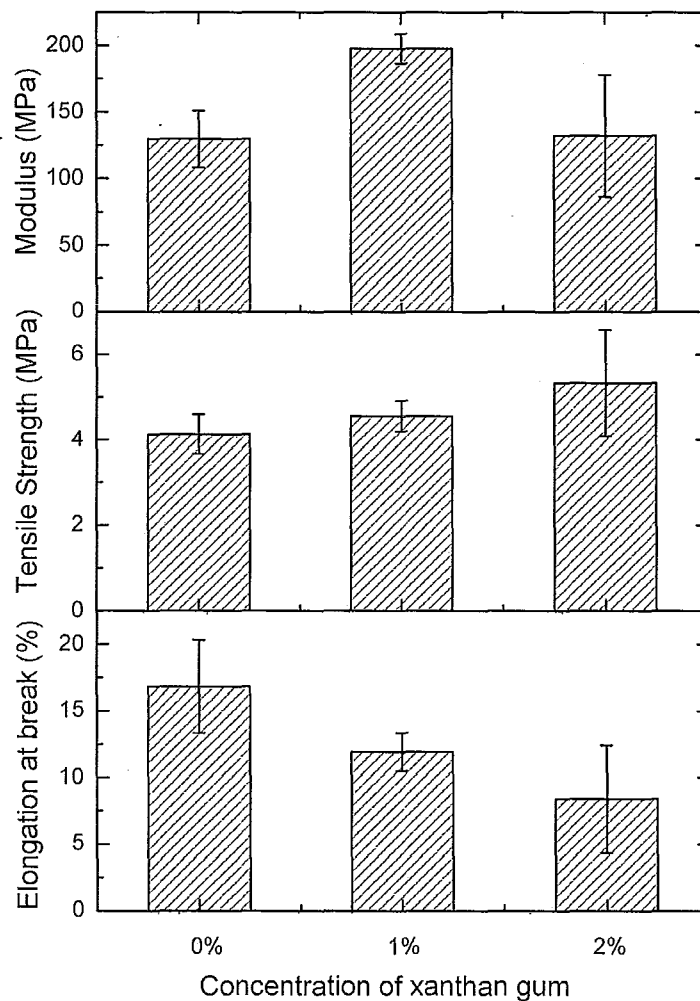
Figure 6.5 Tensile modulus, tensile strength, and elongation at break of crosslinked starch containing same amount of crosslinking agent (2.7% STMP, 2.7% Na$_2$SO$_4$, based on weight percent of dry starch) but different amount of xanthan gum.

matrices. The tensile modulus and strength have been previously reported to increase by inclusion of xanthan gum content in thermoplastic starch films even in the presence of glycerol plasticizer (Flores et al, 2010). In the present study, the tensile modulus and tensile strength increased with addition of the colloidal gum, while the elongation at break decreased as shown in Figure 6.5. The sample with 1% xanthan gum (i.e. sample E2-1) showed the highest stiffness of all samples tested without fibers, having a modulus of 197.6 MPa and a tensile strength of 4.6 MPa. The higher concentration of gum appeared to be less effective, even possibly producing some minor reduction in stiffness. Only elongation at break showed a definitive trend, decreasing from 16.8% to 8.4% as xanthan gum increased from 0% to 2% in the crosslinked starch matrix. Similar to glycerol, xanthan gum had a positive effect on the extent of crosslinking, as seen in Table 6.3, yet again in this case it was not readily apparent whether it had been incorporated into the network structure or simply remained dispersed in the starch matrix.

The additive contributions of these two components, glycerol and xanthan gum, on mechanical properties were observable in Figure 6.6. The stronger plasticizing effect of glycerol was evident in the trends. The stiffness decreased with increasing glycerol content, while xanthan gum content had a lesser opposite effect. The modulus decreased from 136.2 MPa to 21.1 MPa when glycerol content increased from 10 wt% to 30 wt% for a constant concentration of 2% xanthan gum, and the tensile strength decreased from 4.3 MPa to 1.2 MPa. Though glycerol had a negative effect on the material stiffness, it was observed that those samples prepared without glycerol ruptured easily under tension. Therefore, this additive could not be excluded from the composite formulation. A suitable

amount of glycerol was crucial in reducing brittleness of crosslinked product, but excess

glycerol interfered greatly with the hydrogen bonding between the larger molecules of

starch and xanthan gum. As a result, the lower glycerol content of 10% was used in the
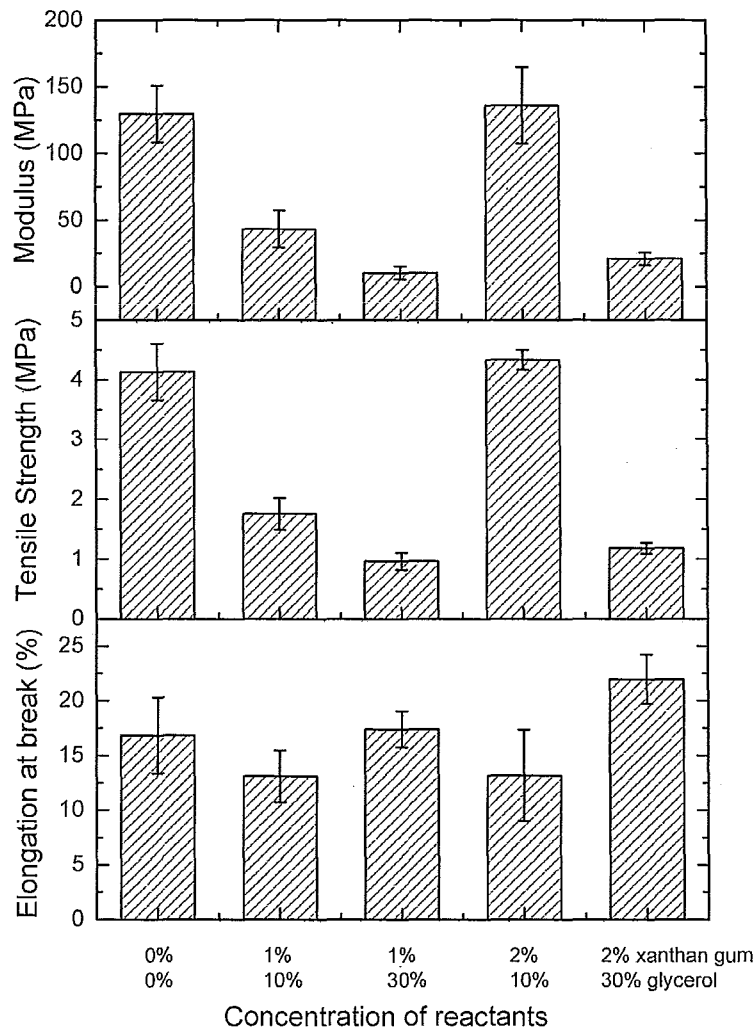
Figure 6.6 Tensile modulus, tensile strength, and elongation at break of crosslinked starch containing same amount of crosslinking agent (2.7% STMP, 2.7% Na$_2$SO$_4$, based on weight percent of dry starch) but different amount of glycerol and xanthan gum.

subsequent testing with sisal fiber reinforcement so as not to diminish the effective

stiffening produced by inclusion of the gum and/or fibers.

6.4.2 Properties of sisal fiber reinforced crosslinked starch biocomposites

Sisal fibers being largely composed of cellulose have ample hydroxyl groups in

comparable electron environments to those found in starch. It is conceivable that these

hydroxyl groups of the fiber and those of starch could competitively seek to crosslink

with STMP during reaction. It was evident from the data above that glycerol does not

participate in the reaction (at least did not lead to crosslinkages) but xanthan gum is

assumed to crosslink to some degree based on its chemical similarity with starch. To test

the effect of sisal fibers on phosphorylation and final properties, sisal fibers were added

at 2.5%, 5.0%, 10%, 15%, 20%, and 25% (w/w, db) into the extruder with starch and the

other reactants. Additives of 2% gum and 10% glycerol were included in the formulations

to balance stiffness and ductility.

From the included data in Table 6.3, the extent of crosslinking for the crosslinked

starch biocomposites was seen to be negatively impacted by inclusion of sisal fibers

during reactive extrusion; a 30% decrease in the extent of crosslinking was observed

from sample E6-1 (no fibers) to sample F1 (2.5 wt% (db) fiber content). However,

increasing sisal fiber loading from 2.5% to 25% increased the extent of crosslinking till it

finally matched the original values found for sample E6-1. The initial inclusion of fibers

in the starch matrix impacted the reaction kinetics by reducing the diffusion rate of

reactants. Increased fiber content should have a corresponding increase on viscosity and

hence, decreased diffusivity. The change in viscosity was noted by a 5.3% increase in

specific mechanical energy demand by the extruder with the inclusion of only 2.5 wt%

fibers compared to the non-reinforced crosslinked starch. The fact that the extent of

crosslinking subsequently increased as the fiber content increased rather points to its

participation in the reaction by making more hydroxyl groups available for reaction. The

reduced extent of crosslinking with only 2.5 wt% fibers had a corresponding effect on the

endotherm transition detected by DSC. The transition temperature decreased from 101°C

for E6-1 to 84°C with the inclusion of 2.5% fiber (F1) and then experienced little change

up till 20% fiber (F5). Only at the highest loading of sisal fibers (F6) was T_m comparable

once again to the non-fiber reinforced crosslinked starch (E6-1). The closer

correspondence of T_m with the extent of crosslinking suggested that the sisal fibers

themselves did not affect the transition. Cyras et al. (Cyras, Kenny, & Vazquez, 2001)

offer an explanation for this outcome as they observed that sisal fibers do not act as

nucleating agents during crystallization.

Table 6.4 includes the moisture absorption content and contact angle data for

these prepared biocomposites. As the mechanical testing that follows examined the

effects of environmental humidity on the biocomposites, the table includes moisture

absorption measurements at both 30% and 95% relative humidity (RH). The moisture

content data at 30 ± 5% RH was found to increase with increasing fiber loading, likely

due to increased crosslinkages, but was notably lower for the fiber-reinforced material

compared to the neat crosslinked starch (E6-1). For instance, the moisture content of the

sample with 25% fiber loading increased from 0.8% to 1.5% compared with the sample

with 2.5% fiber loading at 30 ± 5% RH. The decreasing trend in moisture content at 95 ±

5% RH with increasing fiber loading also correlated well with the extent of crosslinking, pointing to the reduce equilibrium swelling capacity of crosslinked starch. The sensitivity of the biocomposite to water is highlighted more notably by the contact angle data in the table. The fiber-filled materials demonstrated considerably greater moisture sensitivity over the neat crosslinked starch based on both metrics of evaluation (i.e. lower contact angle value and lower contact angle slope). This is readily observed by the plots in Figure 6.2. In fact, changes in contact angle value were much greater between the different fiber-filled samples than had been observed for the neat crosslinked starches over the same range of crosslinking. It was apparent that the hydrophilicity of the fibers themselves had a significant influence on the moisture sensitivity of the biocomposite. The absorption kinetics (based on contact angle slope) was much higher for the fiber-filled materials compared to the neat crosslinked starch. The contact angles of the biocomposites with 2.5 %, 5.0%, 10%, 15%, 20%, and 25% fiber loading were 20.6°, 15.6°, 11.1°, 16.3°, 22.1°, and 32.0°, respectively. A parabolic trend for the contact angle data was noted, going through a minimum at 10% fiber loading, demonstrating the competing contributions by the sisal fibers and the crosslinking reaction. The higher hydrophilicity of the cellulose compared to the modified starch was gradually overcome by crosslinking which reduces the hydroxyl content of both components. Evidently, these composite materials did not achieve the desired reduction in moisture sensitivity sought by this study for their use in structural applications.

Mechanical properties were once again measured using ASTM-type dogbone samples after storing them at $30 \pm 5\%$ RH for 10 days. Tensile modulus, tensile strength

and elongation at break for the crosslinked starch composites are shown in Figure 6.7.

The data shows that the stiffness of the starch matrix increased as much as 600% upon

loadings of 25% fibers (862.2 MPa versus 136.2 MPa for tensile modulus of samples F6
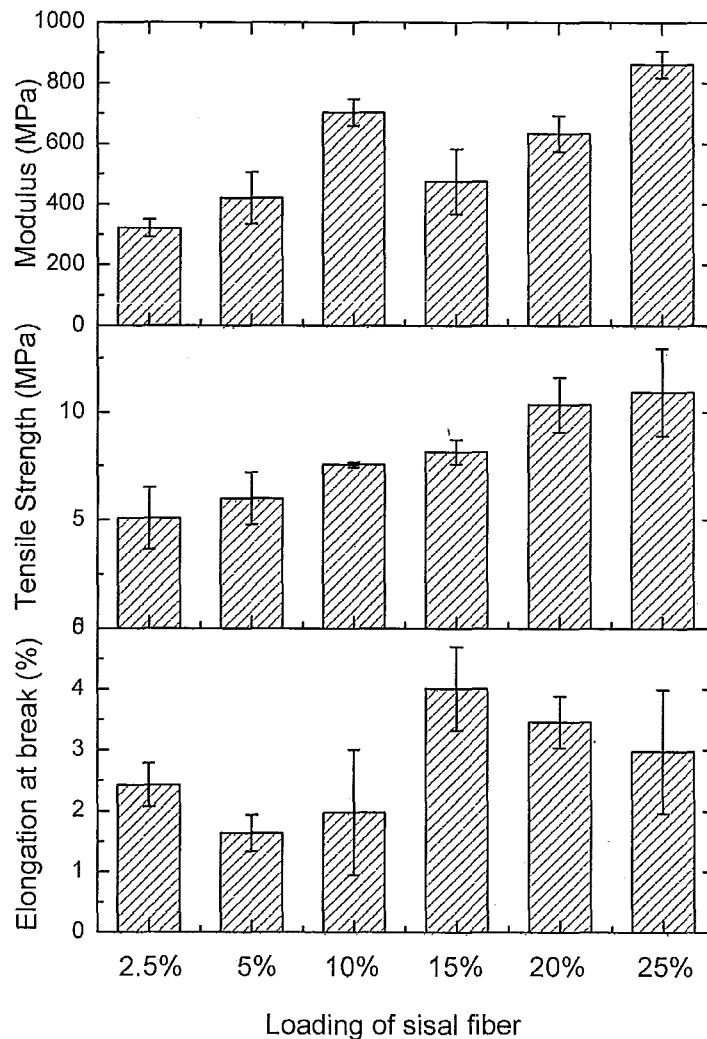
Figure 6.7 Tensile modulus, tensile strength, and elongation at break of crosslinked starch composites containing varying content of sisal fiber, based on weight percentage of dry starch, after storing in 30 ± 5% relative humidity for 10 days.

and E6-1 respectively). The data had some anomalies, though the trend for tensile modulus generally increased with increasing fiber content. The tensile strength data shows a much steadier trend than the modulus data but similarly showed a positive correlation between sisal fiber content and a reduced tendency for plastic yielding. The tensile strength increased by 250% upon loadings of 25 % fiber in the composite. Interestingly, the elongation at break did not show reciprocal correlation with the fiber loading as would be normally expected. At only 2.5% fiber loading the elongation dropped by 84% as expected for a reinforced material but changed very little as higher loadings were used. However, the small variance in value shown does appear to follow inversely with the tensile modulus.

SEM micrographs of the fractured cross-sections for crosslinked starch biocomposites containing 2.5-25 wt% sisal fiber are shown in Figure 6.8. The bare fiber surface exposed under SEM observation looked much smoother than the fiber surface covered with crosslinked starch. The rough sisal fiber surface in the SEM micrographs was observed completely wetted by and adhered to the starch matrix thus allowing effective stress transfer across the interface. The fibers show some retention of orientation occurring from extrusion which persisted after compression molding of the plaques to produce test specimens. The variation in tensile modulus and tensile strength seen in the previous figure was considered mainly due to anisotropic fiber orientation and alteration of the fiber length distribution. Some fiber attrition related to thermomechanical degradation inevitably occurs during shear processing in an extruder; however, for sisal fiber this damage is minor (Belhassen et al., 2009).
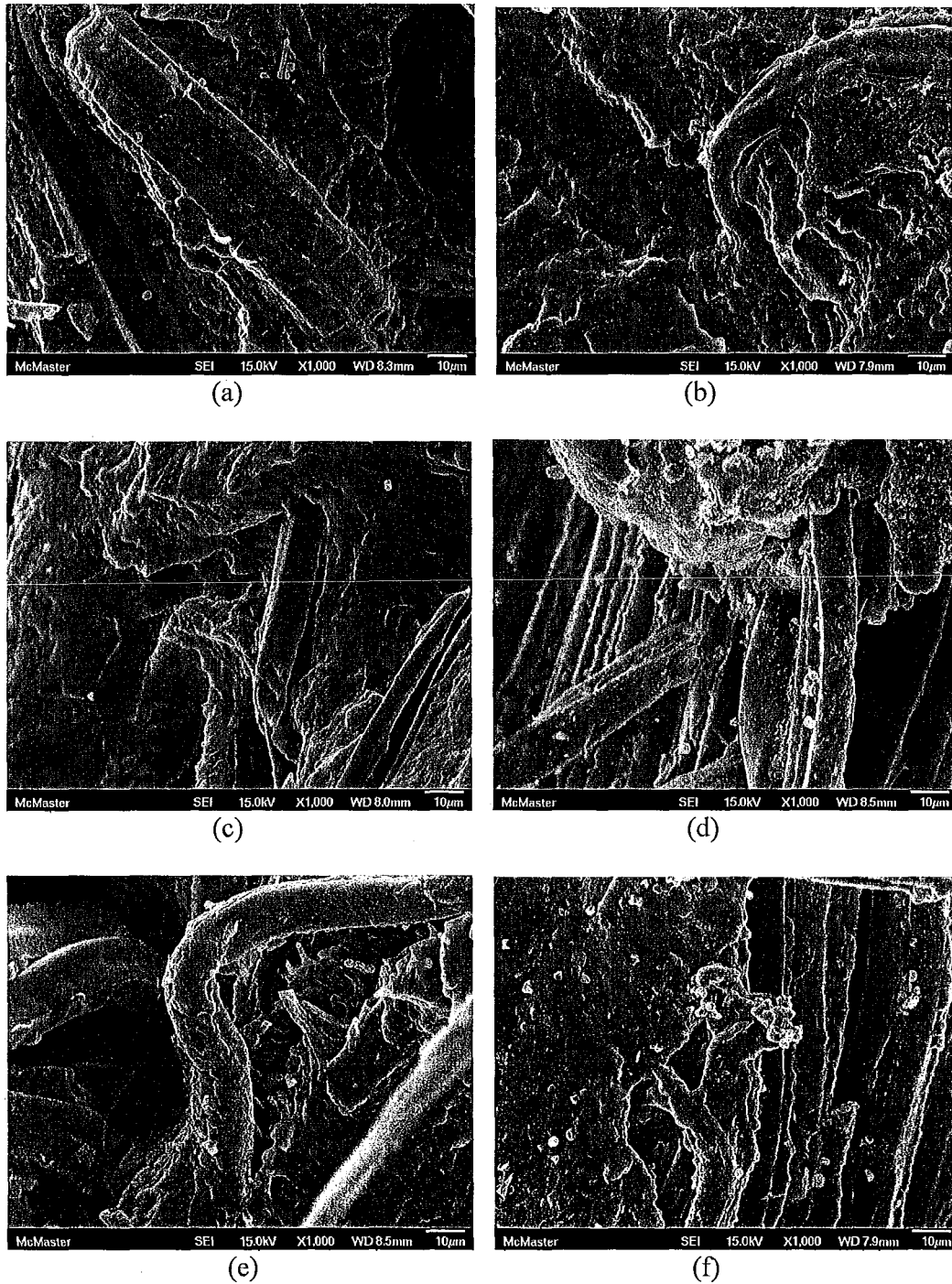
Figure 6.8 SEM micrographs of crosslinked starch biocomposites reinforced by varied loading of sisal fiber: (a) 2.5 wt% (b) 5.0 wt% (c) 10 wt% (d) 15 wt% (e) 20 wt% (f) 25 wt%.

The issue of moisture sensitivity on the mechanical performance for these

biocomposite materials was demonstrated by conditioning the dogbone specimens for 10

days at 95% ± 5% RH in comparison to 30% ± 5% RH. Figure 6.9 shows the tensile
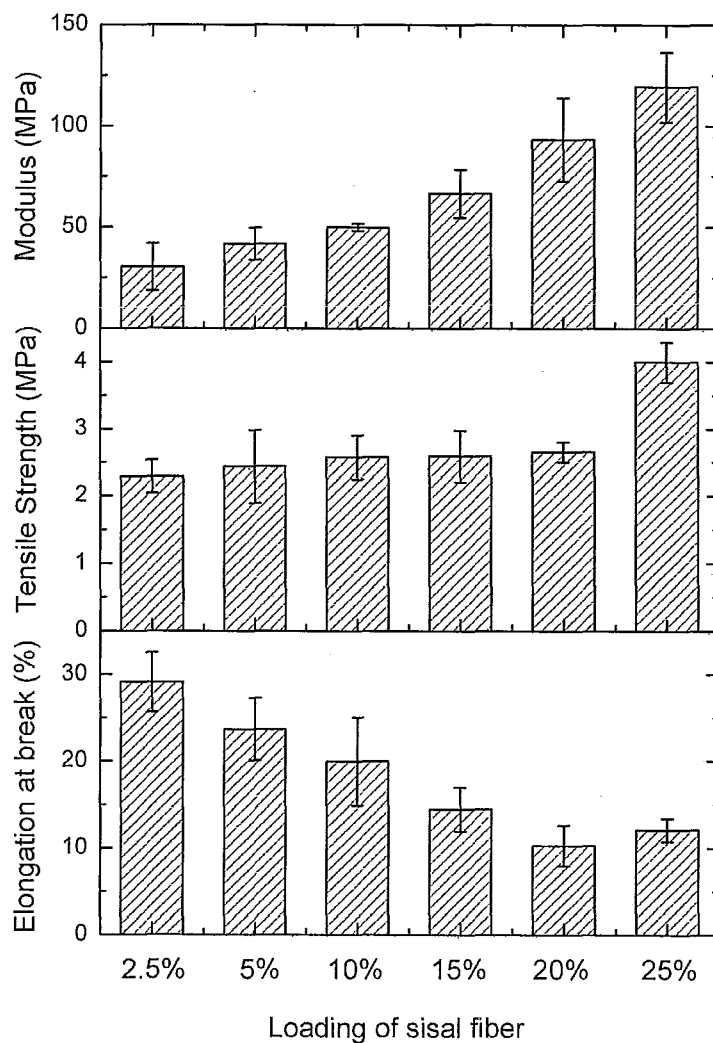
Figure 6.9 Tensile modulus, tensile strength, and elongation at break of crosslinked starch composites containing varying content of sisal fiber, based on weight percentage of dry starch, after storing in 95 ± 5% relative humidity for 10 days.

modulus, tensile strength, and elongation at break values for the same biocomposite species as given in the previous figure but after conditioning at 95% RH. The trends for each measured value versus fiber loading showed much more consistency with none of the anomalies found at lower humidity conditioning. But now it can be observed that the tensile modulus and tensile strength were negatively influenced by the highly humidity environment, while the elongation at break was positively affected. For example, the tensile strength of the biocomposite with 25% fiber loading decreased from 10.9 MPa to 4.0 MPa while the elongation at break increased from 3.0% to 12.1% in surroundings now at 95% RH compared to 30% RH. The materials were plasticized by the water through its association with the hydroxyl groups on starch, gum, glycerol and sisal fibers. The small water molecules increased the free volume of the amorphous regions within these biocomposites allowing higher mobility of the unbound chains, leading to inferior mechanical properties.

6.4.3 Micromechanics modeling

The mechanical data and SEM showed good compatibility between the fibers and starch matrix but did not readily confirm whether the interfacial associations were through hydrogen bonding or covalent attachment. The latter would have a positive effect on the development of the interpenetrating network and increase the stiffness to a much greater degree than the former case. Unfortunately, it was not possible to add fibers into the crosslinked starch matrix once the reaction had completed for comparison to solve the question due to subsequent shear damage of the matrix. However, if the interfacial associations were formed by hydrogen bonding only then the mechanical response of the

system should be additive and could be reasonably predicted by a suitable

micromechanical model such as the modified Tsai-Halpin equation (Nielsen, 1974; Tjong

& Jiang, 1999). The equation is given as:

$$\frac{E_c}{E_m} = \frac{1 + \xi \eta V_f}{1 - \eta V_f} \qquad (2)$$

in which

$$\eta = \frac{E_f - E_m}{E_f + \xi E_m} \qquad (3)$$

where E_c, E_m, and E_f are the moduli of the composites, matrix, and fiber respectively, V_f

is the volume fraction of fiber, and ξ is a constant related to the aspect ratio (L/D) and

orientation of the fiber. The ξ data for discontinuous fiber with random orientation were

given by Nielsen (1974). For example, the ξ value is 2.08, 3.80, and 6.20 when L/D is 4,

8, and 12, respectively. Regression of the data gives $\xi = 0.5738$ (L/D) – 0.5552 with $R^2 =$

0.99. The aspect ratio for the sisal cellulose fibers used in this work was L/D = 108, so an

estimated value of $\xi = 61.4$ was used in the model. The calculated and measured Young's

moduli are compared in Table 6.5, using $E_m = 136.2$ MPa (i.e. sample E6-1) and $E_f =$

700.0 MPa for modulus values of the matrix and fibers, respectively. The calculated

values increased according to fiber loading, following the trend seen in the experimental

data but the modulus was under-predicted by the model in all cases. It is noted that in

some references the modulus of these fibers have been quoted as large as 15 GPa, which

was also tested in the model and still found to under-predict the experimental results (i.e.

392 MPa at 25% fiber loading). More significant was that the deviation grew between

Table 6.5 Comparison of measured and calculated Young's moduli by the modified Tsai-Halpin equation

Sisal fiber content (wt%, db[a])	Measured Young's modulus (MPa)	Calculated Young's modulus (MPa)
2.5	320.4	150.0
5	419.8	163.2
10	703.5	187.7
15	474.9	210.0
20	633.5	230.5
25	862.2	249.4

a. db - dry starch weight basis.

the calculated and experimental data as the sisal fiber content was increased in the starch matrix. The increasingly poor fit by the model with fiber content points to reinforcement features in the composite structure which cannot be readily explained due to interfacial surface area between the fibers and matrix. In combination with the earlier discussed results related to the extent of crosslinking, these findings from the model give reasonable certainty that the fibers were being covalently bound within the starch matrix during reactive compounding in the extruder. The crosslinkages reinforced existing hydrogen bonding between the two domains, providing more effective intra- and intermolecular stress transfer and thus an improved modulus.

6.5 Conclusions

A novel biocomposite based on STMP-crosslinked thermoplastic potato starch and natural sisal fiber was developed by reactive twin screw extrusion in the presence of

hydrocolloidal xanthan gum and glycerol plasticizer. The covalent crosslinkages between the reinforcing fibers and starch matrix significantly enhanced interfacial stress transfer, and thus a corresponding increase in tensile strength and modulus was observed for the prepared biocomposite. Contact angle measurement and water absorption indicated that the moisture sensitivity of the biocomposite increased with increasing fiber loading. Consequently, the mechanical properties were found to readily deteriorate in higher relative humidity surroundings. The increased moisture sensitivity of these materials was attributed to the increased hydroxyl content of the glycerol and xanthan gum additives used as well as losses in matrix crystallinity corresponding to increased crosslinking.

6.6 Acknowledgements

6.7 References

Averous, L., & Boquillon, N. (2004). Biocomposites based on plasticized starch: Thermal and mechanical behaviours. *Carbohydrate Polymers*, 56, 111-122.

Alvarez, V. A., & Vazquez, A. (2006). Influence of fiber chemical modification procedure on the mechanical properties and water absorption of materbi-y/sisal fiber composites. *Composites Part a-Applied Science and Manufacturing*, 37, 1672-1680.

Belhassen, R., Boufi, S., Vilaseca, F., Lopez, J. P., Mendez, J. A., Franco, E., et al. (2009). Biocomposites based on alfa fibers and starch-based biopolymer. *Polymers for Advanced Technologies*, 20, 1068-1075.

Bergo, P., Sobral, P. J. A., & Prison, J. M. (2010). Effect of glycerol on physical properties of cassava starch films. *Journal of Food Processing and Preservation, 34*, 401-410.

Bonacucina, G., Di Martino, P., Piombetti, M., Colombo, A., Roversi, F., & Palmieri, G. F. (2006). Effect of plasticizers on properties of pregelatinised starch acetate (amprac 01) free films. *International Journal of Pharmaceutics, 313*, 72-77.

Canigueral, N., Vilaseca, F., Mendez, J. A., Lopez, J. P., Barbera, L., Puig, J., et al. (2009). Behavior of biocomposite materials from flax strands and starch-based biopolymer. *Chemical Engineering Science, 64*, 2651-2658.

Corradini, E., de Morais, L., Rosa, M. D., Mazzetto, S. E., Mattoso, L. H. C., & Agnelli, J. A. M. (2006). A preliminary study for the use of natural fibers as reinforcement in starch-gluten-glycerol matrix. *Macromolecular Symposia, 245*, 558-564.

Corradini, E., Imam, S. H., Agnelli, J. A. M., & Mattoso, L. H. C. (2009). Effect of coconut, sisal and jute fibers on the properties of starch/gluten/glycerol matrix. *Journal of Polymers and the Environment, 17*, 1-9.

Curvelo, A. A. S., de Carvalho, A. J. F., & Agnelli, J. A. M. (2001). Thermoplastic starch-cellulosic fibers composites: Preliminary results. *Carbohydrate Polymers, 45*, 183-188.

Cyras, V. P., Kenny, J. M., & Vazquez, A. (2001). Crystallization kinetics by differential scanning calorimetry for pcl/starch and their reinforced sisal fiber composites. *Polymer Engineering and Science, 41*, 1521-1528.

Cyras, V. P., Vallo, C., Kenny, J. M., & Vazquez, A. (2004). Effect of chemical treatment on the mechanical properties of starch-based blends reinforced with sisal fibre. *Journal of Composite Materials, 38*, 1387-1399.

de Verney, J. C. K., Lima, M. F. S., & Lenz, D. M. (2008). Properties of sbs and sisal fiber composites: Ecological material for shoe manufacturing. *Materials Research-Ibero-American Journal of Materials, 11*, 447-451.

Demirgoz, D., Elvira, C., Mano, J. F., Cunha, A. M., Piskin, E., & Reis, R. L. (2000). Chemical modification of starch based biodegradable polymeric blends: Effects

on water uptake, degradation behaviour and mechanical properties. *Polymer Degradation and Stability*, 70, 161-170.

Eichhorn, S. J., Baillie, C. A., Zafeiropoulos, N., Mwaikambo, L. Y., Ansell, M. P., Dufresne, A., et al. (2001). Review: Current international research into cellulosic fibres and composites. *Journal of Materials Science*, 36, 2107-2131.

Flores, S. K., Costa, D., Yamashita, F., Gerschenson, L. N., & Grossmann, M. V. (2010). Mixture design for evaluation of potassium sorbate and xanthan gum effect on properties of tapioca starch films obtained by extrusion. *Materials Science & Engineering C-Materials for Biological Applications*, 30, 196-202.

George, J., Sreekala, M. S., & Thomas, S. (2001). A review on interface modification and characterization of natural fiber reinforced plastic composites. *Polymer Engineering and Science*, 41, 1471-1485.

Graupner, N. (2008). Application of lignin as natural adhesion promoter in cotton fibre-reinforced poly(lactic acid) (pla) composites. *Journal of Materials Science*, 43, 5222-5229.

Guimaraes, J. L., Wypych, F., Saul, C. K., Ramos, L. P., & Satyanarayana, K. G. (2010). Studies of the processing and characterization of corn starch and its composites with banana and sugarcane fibers from brazil. *Carbohydrate Polymers*, 80, 130-138.

Huneault, M. A., & Li, H. B. (2007). Morphology and properties of compatibilized polylactide/thermoplastic starch blends. *Polymer*, 48, 270-280.

John, M. J., & Thomas, S. (2008). Biofibres and biocomposites. *Carbohydrate Polymers*, 71, 343-364.

Mohanty, A. K., Misra, M., & Drzal, L. T. (2002). Sustainable bio-composites from renewable resources: Opportunities and challenges in the green materials world. *Journal of Polymers and the Environment*, 10, 19-26.

Nair, K. C. M., Diwan, S. M., & Thomas, S. (1996). Tensile properties of short sisal fiber reinforced polystyrene composites. *Journal of Applied Polymer Science*, 60, 1483-1497.

126

Nielsen, L. E. (1974). Mechanical properties of polymers and composites pp. 453-504. New York: Marcel Dekker.

Rioux, B., Lspas-Szabo, P., Ait-Kadi, A., Mateescu, M. A., & Juhasz, J. (2002). Structure-properties relationship in cross-linked high amylose starch cast films. *Carbohydrate Polymers*, 50, 371-378.

Saiah, R., Sreekumar, P. A., Gopalakrishnan, R., Leblanc, N., Gattin, R., & Saiter, J. M. (2009). Fabrication and characterization of 100% green composite: Thermoplastic based on wheat flour reinforced by flax fibers. *Polymer Composites*, 30, 1595-1600.

Sothornvit, R., & Krochta, J. M. (2001). Plasticizer effect on mechanical properties of beta-lactoglobulin films. *Journal of Food Engineering*, 50, 149-155.

Sreekumar, P. A., Leblanc, N., & Saiter, J. M. (2010). Characterization of bulk agro-green composites: Sisal fiber reinforced wheat flour thermoplastics. *Polymer Composites*, 31, 939-945.

Tjong, S. C., & Jiang, W. (1999). Mechanical and thermal properties of poly(acrylonitrile-butadiene-styrene) copolymer reinforced with potassium titanate whiskers. *Journal of Applied Polymer Science*, 73, 2985-2991.

Trejo-O'Reilly, J. A., Cavaille, J. Y., & Gandini, A. (1997). The surface chemical modification of cellulosic fibres in view of their use in composite materials. *Cellulose*, 4, 305-320.

Vansoest, J. J. G., Dewit, D., Tournois, H., & Vliegenthart, J. F. G. (1994). The influence of glycerol on structural-changes in waxy maize starch as studied by fourier-transform infrared-spectroscopy. *Polymer*, 35, 4722-4727.

Veiga-Santos, P., Oliveira, L. M., Cereda, M. P., Alves, A. J., & Scamparini, A. R. P. (2005). Mechanical properties, hydrophilicity and water activity of starch-gum film: Effect of additives and deacetylated xanthan gum. *Food Hydrocolloids*, 19, 341-349.

Wang, G., Thompson, M. R., & Liu, Q. (2010). Influences of hydrocolloidal gum and glycerol on kinetics of bulk phosphorylation of potato starch. *Carbohydrate Polymers*. Submitted.

Wang, X. L., Yang, K. K., & Wang, Y. Z. (2003). Properties of starch blends with biodegradable polymers. *Journal of Macromolecular Science-Polymer Reviews*, C43, 385-409.

Yoshimura, M., Takaya, T., & Nishinari, K. (1999). Effects of xyloglucan on the gelatinization and retrogradation of corn starch as studied by rheology and differential scanning calorimetry. *Food Hydrocolloids*, 13, 101-111.

CHAPTER 7 SURFACE MODIFICATION OF STARCH BIOCOMPOSITES

7.1 Introduction

As observed in the previous chapter, surroundings with higher relative humidity negatively influences the mechanical properties of crosslinked starch biocomposites reinforced by natural sisal fibers. Therefore, the hydrophobicity of the biocomposite needed to be improved in order to maintain its superior mechanical properties in a humid environment. Surface modification with an alkyl ketene dimer (Hydrores 266MB emulsion) can be employed to achieve this goal. The related literature review is included in Chapter 2.

7.2 Experimental

7.2.1 Materials

The sisal fiber reinforced biocomposites were the samples produced in the experiments described in Chapter 6. The Hydrores 266MB emulsion, an alkyl ketene dimer (AKD) based sizing agent, was obtained from Kemira ChemSolutions b.v. (Tiel, Netherlands).

7.2.2 Characterization

The reinforced biocomposite samples were compression molded into slabs with thickness of 3.2 mm immediately after extrusion and then die-cut into round coupons of

10 mm diameter. The biocomposite coupons were dipped in 12.5wt% Hydrores 266MB/water emulsion in a fume hood for 30 seconds, allowed to dry in a vacuum oven at 80 ℃ for one hour and then sealed in a plastic bag for 24 hours before contact angle measurements.

A Model 100-00-115 goniometer (Rame-hart Inc., Mountain Lakes, NJ, USA) equipped with a Sanyo VCB-3512T NTSC CCD digital camera (Sanyo Electronic LTD, Japan) was employed to measure contact angle for the sessile drop method. FTA 32 software (Version 2.0, Build No.160, First Ten Angstroms Inc.) was used to process images in order to calculate the contact angle of a water droplet. The contact angle was measured once every 20 seconds for 480 seconds. A micro-syringe was used to precisely control the volume of the water droplet. The contact angle between water droplets and selected samples indicated the hydrophobicity of tested samples, higher angles inferring a more apolar surface. The change in contact angle with time also indicated the hydrophobicity of the samples.

Infrared spectra of the sample after surface modification was conducted with a ReactIR™ 1000 infrared system (Mettler-Toledo) scanning the mid-range infrared bands between 600-4000 cm^{-1} at a resolution of 4 cm^{-1}.

7.3 Results and discussion

The ATR/IR spectra of the sample after surface modification with Hydrores 266MB proved chemical bonding occurred between Hydrores 266MB and hydroxyl groups available on the surface of the starch biocomposite. A newly appearing prominent

absorbance peak at 1721 cm^{-1} for the surface-modified sample was assigned to the characteristic C=O stretching vibration of esterification (Figure 7.1), while that peak did not show in ATR/IR spectra of unmodified sample and Hydrores 266MB itself.

The plots of contact angle changing over time of sisal fiber reinforced crosslinked starch biocomposites with different fiber contents after surface modification are included in Appendix B for interested readers. The contact angle value at 60 second was used for comparison in order to allow for droplet stabilization yet minimize absorption by the water into the starch material. As shown in Figure 7.2, the contact angle was improved by at least 112% after surface modification with the Hydrores 266MB emulsion compared to that before the surface treatment, indicating overall hydrophobicity of surface modified samples was significantly enhanced.
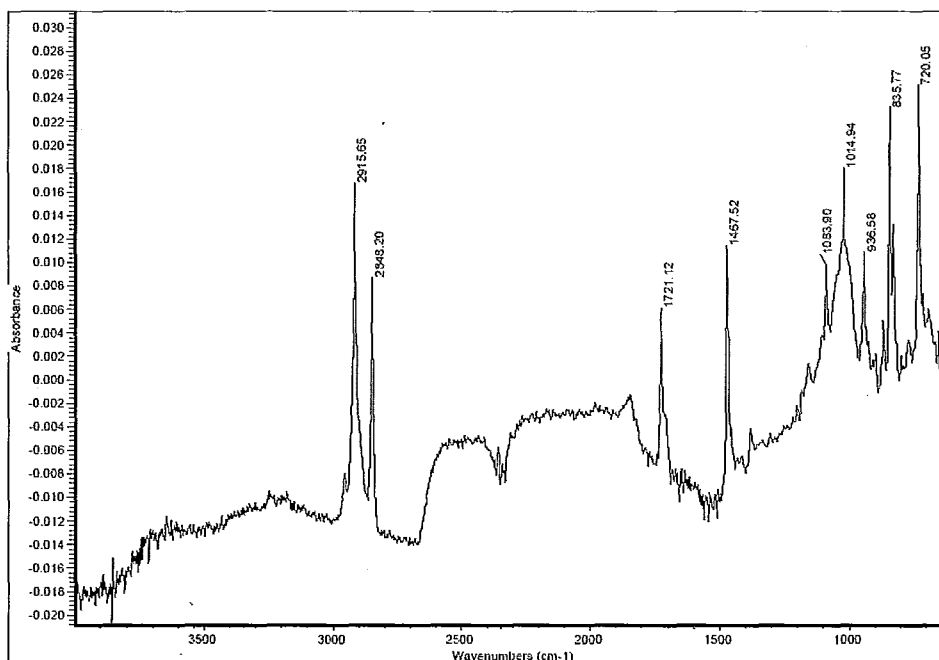
Figure 7.1 ATR/IR spectra of the crosslinked starch biocomposite containing 2.5 % sisal fiber after surface modification by Hydrores 266MB emulsion.

131

Table 7.1 Linear regression results of contact angle changing over time of fiber reinforced crosslinked starch biocomposites after surface treatment

Sample[a]	Fiber content (wt%, db)	Slope	R^2
F1	2.5	-0.0797	0.9891
F2	5.0	-0.0902	0.9711
F3	10	-0.0941	0.9920
F4	15	-0.0968	0.9802
F5	20	-0.0994	0.9756
F6	25	-0.1044	0.9831

a. Sample names correspond to those given in Chapter 6.

b. db - dry starch weight basis.
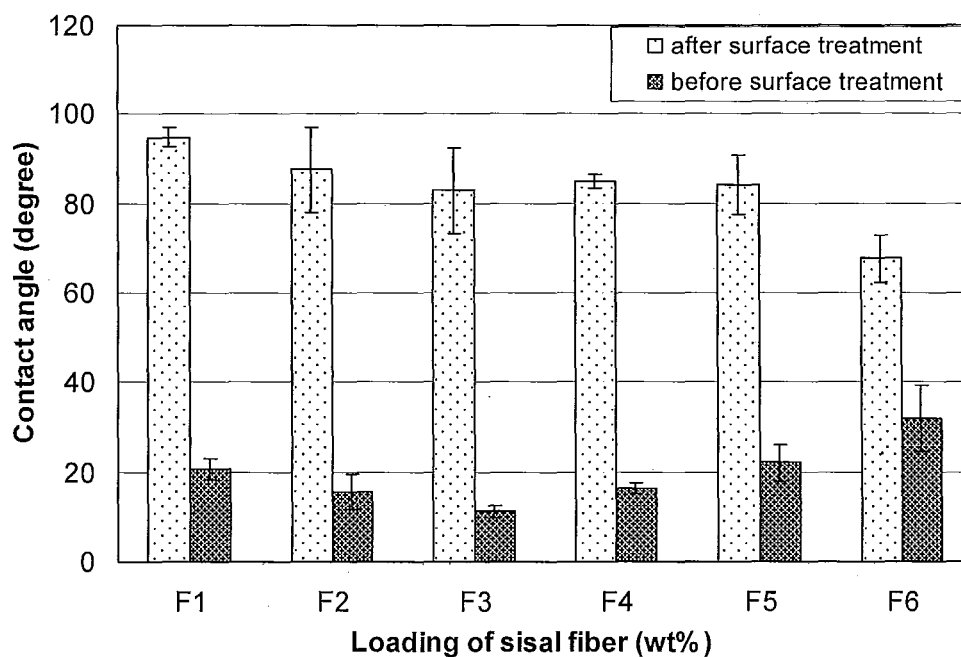
Figure 7.2 Comparison of contact angle at 60 seconds of the biocomposites containing varied sisal fiber contents before and after surface treatment.

The linear regression results of contact angle changing over time of the biocomposites are given in Table 7.1. The slope of linear regression was taken as an indicator of water absorption kinetics. When sisal fiber content increased from 2.5 % to 25 %, the rate of water absorption of the surface treated samples became faster. As discussed in the previous chapter, the extent of crosslinking increased with increasing sisal fiber loading. Therefore, there were less hydroxyl functional groups left for esterification reaction with Hydrores 266MB. The density of hydrophobic hydrocarbon chains on the biocomposite surface decreased with increasing fiber content and crosslink density, leading to higher water absorption rate of biocomposites at higher fiber loading.

7.4 Conclusions

The sisal fiber reinforced crosslinked starch biocomposite surface was modified by Hydrores 266MB emulsion. The chemical bonding between Hydrores 266MB and hydroxyl groups of the biocomposite was confirmed by ATR/IR spectra. The hydrophobicity of sisal fiber reinforced crosslinked starch biocomposite was significantly improved after surface modification with Hydrores 266MB emulsion.

CHAPTER 8 CONCLUSIONS

Granular shape and size affect gelatinization behavior of potato starch. Porosity influences diffusion rate of water and reactants into starch granules. Therefore, investigation of the potato starch granule morphology helps in understanding processing issues with starch gelatinization and crosslinking in a bulk extrusion process. The intra-particle and total porosity of raw potato starch was found to be very low at 1.57% and 2.34%, respectively. Starch gelatinization and the phosphate crosslinking reaction were expected to be impeded by poor reactant diffusivity due to low intra-particle porosity. The optimal composition of plasticizers for potato starch gelatinization was found to be approximately 70 % water and 30 % glycerol (based on dry starch weight).

Based on the statistical analysis result of DSC experiment data, a suitable screw design and operational layout was developed for thermoplastic potato starch extrusion as indicated by steady operation and a stable product output. Screw speed as high as 100 RPM caused degradation and affected rheological and water absorption properties of the final product. No gelatinization transition was observed for the thermoplastic potato starch, suggesting that the semi-crystalline structure of starch was fully disrupted by extrusion.

The industrial usefulness of potato starch was extended by phosphate crosslinking in bulk. The kinetics of crosslinking with STMP was investigated using an in-situ ATR/IR monitoring technique. Multivariate analysis was employed to discover the meaningful vibrational bands related to crosslinking reaction. Conventional rheology

controlling additives such as hydrocolloidal xanthan gum and glycerol had an effect on the reaction rate. It is believed that the phosphoryl reacton was terminated by glycerol and produced a branched microstructure while xanthan gum tend to substitute a starch molecule in crosslinked system. Rheological tests revealed that the additives had only minor effect on the final crosslinked structure. Therefore, the utilization of hydrocolloidal xanthan gum and glycerol is encouraged for the purpose of controlling processability. The actual reaction rate during extrusion was found to be higher than that in batch kinetics study, highlighting the importance of gelatinization to the reaction rate. The finding was explained by eliminated granule wall barrier and thus improved mass transport due to rapid gelatinization in a twin screw extruder.

A novel biocomposite based on STMP-crosslinked thermoplastic potato starch and natural sisal fiber was developed by reactive twin screw extrusion in the presence of hydrocolloidal xanthan gum and glycerol plasticizer. The covalent crosslinkages between the reinforcing fibers and crosslinked starch matrix significantly enhanced interfacial stress transfer, and thus a corresponding increase in tensile strength and modulus was observed for the prepared biocomposite. Contact angle measurement and water absorption indicated that the moisture sensitivity of the biocomposite increased with increasing fiber loading. Consequently, the mechanical properties were found to readily deteriorate in higher relative humidity surroundings. The increased moisture sensitivity of these materials was attributed to the increased hydroxyl content of the glycerol and xanthan gum additives used as well as losses in matrix crystallinity corresponding to increased crosslinking.

To reduce moisture sensitivity, the sisal fiber reinforced crosslinked starch biocomposite surface was modified by Hydrores 266MB emulsion, an alkyl ketene dimer. The chemical bonding between Hydrores 266MB and hydroxyl groups of the biocomposite was confirmed by ATR/IR spectra as an esterification reaction. Contact angle measurements indicted that the hydrophobicity of the biocomposite was significantly improved after surface modification with the emulsion.

CHAPTER 9 RECOMMENDATIONS FOR FUTURE WORK

Suggested future work would be in the area of increasing fiber content and introducing tertiary component such as PLA or PHA in natural fiber reinforced crosslinked starch biocomposites, in which the interpenetrating network (IPN) would greatly enhance the mechanical properties of the crosslinked system.

Another suggestion for future work would be biocomposites reinforced by nano-scaled cellulose fiber. Though natural cellulose fiber helps lower the cost of producing crosslinked starch biocomposites, the improvement of mechanical properties is limited. The incorporation of nano-scaled cellulose fiber into crosslinked starch biocomposites could expand our research horizon. Cellulose nano-whiskers could be obtained from sisal fibers via acid hydrolysis (Kamel, 2007), which could be employed to reinforce crosslinked starch biocomposite through nano-scaled interfacial interaction. The nano-scaled control over biocomposite microstructure and interfacial interaction could effectively improve overall mechanical properties of the biocomposites (Yu *et al.*, 2007).

REFERENCES

Achayuthakan, P., & Suphantharika, M. (2008). Pasting and rheological properties of waxy corn starch as affected by guar gum and xanthan gum. *Carbohydrate Polymers, 71*, 9-17.

Atichokudomchai, N., & Varavinit, S. (2003). Characterization and utilization of acid-modified cross-linked tapioca starch in pharmaceutical tablets. *Carbohydrate Polymers, 53*, 263-270.

Averous, L., & Boquillon, N. (2004). Biocomposites based on plasticized starch: Thermal and mechanical behaviours. *Carbohydrate Polymers, 56*, 111-122.

Beckermann, G. W., & Pickering, K. L. (2008). Engineering and evaluation of hemp fibre reinforced polypropylene composites: Fibre treatment and matrix modification. *Composites Part a-Applied Science and Manufacturing, 39*, 979-988.

Belhassen, R., Boufi, S., Vilaseca, F., Lopez, J. P., Mendez, J. A., Franco, E., et al. (2009). Biocomposites based on alfa fibers and starch-based biopolymer. *Polymers for Advanced Technologies, 20*, 1068-1075.

BeMiller, J. N., & Whistler, R. L. (1996). Carbohydrates. In O. R. Fennema (Ed) *Food Chemistry, 3rd Edition* pp. 157-225. New York: Marcel Dekker, INC.

Bertoft, E. (2004). On the nature of categories of chains in amylopectin and their connection to the super helix model. *Carbohydrate Polymers, 57*, 211-224.

Biliaderis, C. G., & Zawistowski, J. (1990). Viscoelastic behavior of aging starch gels - effects of concentration, temperature, and starch hydrolysates on network properties. *Cereal Chemistry, 67*, 240-246.

Bledzki, A. K., & Faruk, O. (2006). Injection moulded microcellular wood fibre-polypropylene composites. *Composites Part a-Applied Science and Manufacturing, 37*, 1358-1367.

Bonacucina, G., Di Martino, P., Piombetti, M., Colombo, A., Roversi, F., & Palmieri, G. F. (2006). Effect of plasticizers on properties of pregelatinised starch acetate (amprac 01) free films. *International Journal of Pharmaceutics*, 313, 72-77.

Braz, R., Hechenleitner, A. A. W., & Cavalcanti, O. A. (2007). Extraction, structural modification and characterization of lotus roots polysaccharides (nelumbo nucifera gaertn). Excipient with potential application in modified drug delivery systems. *Latin American Journal of Pharmacy*, 26, 706-710.

Canigueral, N., Vilaseca, F., Mendez, J. A., Lopez, J. P., Barbera, L., Puig, J., et al. (2009). Behavior of biocomposite materials from flax strands and starch-based biopolymer. *Chemical Engineering Science*, 64, 2651-2658.

Corradini, E., Imam, S. H., Agnelli, J. A. M., & Mattoso, L. H. C. (2009). Effect of coconut, sisal and jute fibers on the properties of starch/gluten/glycerol matrix. *Journal of Polymers and the Environment*, 17, 1-9.

Curvelo, A. A. S., de Carvalho, A. J. F., & Agnelli, J. A. M. (2001). Thermoplastic starch-cellulosic fibers composites: Preliminary results. *Carbohydrate Polymers*, 45, 183-188.

Cury, B. S. F., Castro, A. D., Klein, S. I., & Evangelista, R. C. (2009). Modeling a system of phosphated cross-linked high amylose for controlled drug release. Part 2: Physical parameters, cross-linking degrees and drug delivery relationships. *International Journal of Pharmaceutics*, 371, 8-15.

Cury, B. S. F., Klein, S. A., & Evangelista, R. C. (2008). Modeling a system of phosphated cross-linked high amylose for controlled drug release. Part 1: Synthesis and polymer characterization. *Reactive & Functional Polymers*, 68, 1200-1206.

deGraaf, R. A., Broekroelofs, G. A., Janssen, L., & Beenackers, A. (1995). The kinetics of the acetylation of gelatinised potato starch. *Carbohydrate Polymers*, 28, 137-144.

DellaValle, G., Boche, Y., Colonna, P., & Vergnes, B. (1995). The extrusion behaviour of potato starch. *Carbohydrate Polymers*, 28, 255-264.

Delval, F., Crini, G., Bertini, S., Morin-Crini, N., Badot, P. M., Vebrel, J. L., et al. (2004). Characterization of crosslinked starch materials with spectroscopic techniques. *Journal of Applied Polymer Science*, 93, 2650-2663.

Demirgoz, D., Elvira, C., Mano, J. F., Cunha, A. M., Piskin, E., & Reis, R. L. (2000). Chemical modification of starch based biodegradable polymeric blends: Effects on water uptake, degradation behaviour and mechanical properties. *Polymer Degradation and Stability*, 70, 161-170.

Denardin, C. C., & da Silva, L. P. (2009). Starch granules structure and its regards with physicochemical properties. *Ciencia Rural*, 39, 945-954.

Doan, T. T. L., Gao, S. L., & Mader, E. (2006). Jute/polypropylene composites i. Effect of matrix modification. *Composites Science and Technology*, 66, 952-963.

Dubois, I., Picton, L., Muller, G., Audibert-Hayet, A., & Doublier, J. L. (2001). Structure/rheological properties relations of crosslinked potato starch suspensions. *Journal of Applied Polymer Science*, 81, 2480-2489.

Dulong, V., Lack, S., Le Cerf, D., Picton, L., Vannier, J. P., & Muller, G. (2004). Hyaluronan-based hydrogels particles prepared by crosslinking with trisodium trimetaphosphate. Synthesis and characterization. *Carbohydrate Polymers*, 57, 1-6.

Dumitriu, S., Vidal, P. F., & Chornet, E. (1996). Hydrogels based on polysaccharides. In S. Dumitriu (Ed) *Polysaccharides in medicinal applications* pp. 125-243. New York: Marcel Dekker Inc.

Dumoulin, Y., Alex, S., Szabo, P., Cartilier, L., & Mateescu, M. A. (1998). Cross-linked amylose as matrix for drug controlled release. X-ray and ft-ir structural analysis. *Carbohydrate Polymers*, 37, 361-370.

Eichhorn, S. J., Baillie, C. A., Zafeiropoulos, N., Mwaikambo, L. Y., Ansell, M. P., Dufresne, A., et al. (2001). Review: Current international research into cellulosic fibres and composites. *Journal of Materials Science*, 36, 2107-2131.

FAO/WHO (1999). Compendium of food additive specifications, issue 52, addendum 7. Rome: Joint FAO/WHO Committee on Food Additives, 53rd session.

Garcia-Ochoa, F., Santos, V. E., Casas, J. A., & Gomez, E. (2000). Xanthan gum: Production, recovery, and properties. *Biotechnology Advances*, 18, 549-579.

George, J., Sreekala, M. S., & Thomas, S. (2001). A review on interface modification and characterization of natural fiber reinforced plastic composites. *Polymer Engineering and Science*, 41, 1471-1485.

Govindasamy, S., Campanella, O. H., & Oates, C. G. (1997). Enzymatic hydrolysis and saccharification optimisation of sago starch in twin-screw extruder. *Journal of Food Engineering*, 32, 427-446.

Graupner, N. (2008). Application of lignin as natural adhesion promoter in cotton fibre-reinforced poly(lactic acid) (pla) composites. *Journal of Materials Science*, 43, 5222-5229.

Guimaraes, J. L., Wypych, F., Saul, C. K., Ramos, L. P., & Satyanarayana, K. G. (2010). Studies of the processing and characterization of corn starch and its composites with banana and sugarcane fibers from brazil. *Carbohydrate Polymers*, 80, 130-138.

Huda, M. S., Mohanty, A. K., Drzal, L. T., Schut, E., & Misra, M. (2005). "Green" Composites from recycled cellulose and poly(lactic acid): Physico-mechanical and morphological properties evaluation. *Journal of Materials Science*, 40, 4221-4229.

Hundhausen, U., Militz, H., & Mai, C. (2009). Use of alkyl ketene dimer (akd) for surface modification of particleboard chips. *European Journal of Wood and Wood Products*, 67, 37-45.

Huneault, M. A., & Li, H. B. (2007). Morphology and properties of compatibilized polylactide/thermoplastic starch blends. *Polymer*, 48, 270-280.

Jenkins, J. P. J., Cameron, R. E., & Donald, A. M. (1993). A universal feature in the structure of starch granules from different botanical sources. *Starch-Starke*, 45, 417-420.

Jenkins, P. J., & Donald, A. M. (1995). The influence of amylose on starch granule structure. *International Journal of Biological Macromolecules*, 17, 315-321.

John, M. J., & Thomas, S. (2008). Biofibres and biocomposites. *Carbohydrate Polymers*, 71, 343-364.

Kajita, H., & Imamura, Y. (1991). Improvement of physical and biological properties of particleboards by impregnation with phenolic resin. *Wood Science and Technology*, 26, 63-70.

Kamel, S. (2007). Nanotechnology and its applications in lignocellulosic composites, a mini review. *Express Polymer Letters*, 1, 546-575.

Kim, Y. S., Wiesenborn, D. P., & Grant, L. A. (1997). Pasting and thermal properties of potato and bean starches. *Starch-Starke*, 49, 97-102.

Le Bail, P., Morin, F. G., & Marchessault, R. H. (1999). Characterization of a crosslinked high amylose starch excipient. *International Journal of Biological Macromolecules*, 26, 193-200.

Li, B. Z., Wang, L. J., Li, D., Chiu, Y. L., Zhang, Z. J., Shi, J., et al. (2009). Physical properties and loading capacity of starch-based microparticles crosslinked with trisodium trimetaphosphate. *Journal of Food Engineering*, 92, 255-260.

Lim, S., & Seib, P. A. (1993). Preparation and pasting properties of wheat and corn starch phosphates. *Cereal Chemistry*, 70, 137-144.

Luo, F. X., Huang, Q., Fu, X., Zhang, L. X., & Yu, S. J. (2009). Preparation and characterisation of crosslinked waxy potato starch. *Food Chemistry*, 115, 563-568.

Mao, G. J., Wang, P., Meng, X. S., Zhang, X., & Zheng, T. (2006). Crosslinking of corn starch with sodium trimetaphosphate in solid state by microwave irradiation. *Journal of Applied Polymer Science*, 102, 5854-5860.

Marques, P. T., Lima, A. M. F., Blanco, G., Laurindo, J. B., Borsali, R., Le Meins, J. F., et al. (2006). Thermal properties and stability of cassava starch films cross-linked with tetraethylene glycol diacrylate. *Polymer Degradation and Stability*, 91, 726-732.

Martin, C., & Smith, A. M. (1995). Starch biosynthesis. *Plant Cell*, 7, 971-985.

Miladinov, V. D., & Hanna, M. A. (1995). Apparent viscosity of starch and xanthan gum extruded with crosslinking agents. *Industrial Crops and Products*, 4, 261-271.

Mohanty, A. K., Misra, M., & Drzal, L. T. (2002). Sustainable bio-composites from renewable resources: Opportunities and challenges in the green materials world. *Journal of Polymers and the Environment*, 10, 19-26.

Moss, G. E. (1976). The microscopy of starch. In J. A. Radley (Ed) *Examination and analysis of starch and starch products*. London: Applied science publishers LTD.

Murua-Pagola, B., Beristain-Guevara, C. I., & Martinez-Bustos, F. (2009). Preparation of starch derivatives using reactive extrusion and evaluation of modified starches as shell materials for encapsulation of flavoring agents by spray drying. *Journal of Food Engineering*, 91, 380-386.

Nabeshima, E. H., & Grossmann, M. V. E. (2001). Functional properties of pregelatinized and cross-linked cassava starch obtained by extrusion with sodium trimetaphosphate. *Carbohydrate Polymers*, 45, 347-353.

Nagano, T., Tamaki, E., & Funami, T. (2008). Influence of guar gum on granule morphologies and rheological properties of maize starch. *Carbohydrate Polymers*, 72, 95-101.

Nayouf, M., Loisel, C., & Doublier, J. L. (2003). Effect of thermomechanical treatment on the rheological properties of crosslinked waxy corn starch. *Journal of Food Engineering*, 59, 209-219.

Neimo, L. (1999). Papermaking chemistry. In L. Neimo (Ed) *Papermaking Science and Technology* p. 330. Fapet Oy Helsinki: TAPPI.

Park, J. W., Im, S. S., Kim, S. H., & Kim, Y. H. (2000). Biodegradable polymer blends of poly(l-lactic acid) and gelatinized starch. *Polymer Engineering and Science*, 40, 2539-2550.

Parker, R., & Ring, S. G. (2001). Aspects of the physical chemistry of starch. *Journal of Cereal Science*, 34, 1-17.

Pongsawatmanit, R., & Srijunthongsiri, S. (2008). Influence of xanthan gum on rheological properties and freeze-thaw stability of tapioca starch. *Journal of Food Engineering*, 88, 137-143.

Ptaszek, P., & Grzesik, M. (2007). Viscoelastic properties of maize starch and guar gum gels. *Journal of Food Engineering*, 82, 227-237.

Puncha-Arnon, S., Pathipanawat, W., Puttanlek, C., Rungsardthong, V., & Uttapap, D. (2008). Effects of relative granule size and gelatinization temperature on paste and gel properties of starch blends. *Food Research International*, 41, 552-561.

Qiu, W. L., Zhang, F. R., Endo, T., & Hirotsu, T. (2003). Preparation and characteristics of composites of high-crystalline cellulose with polypropylene: Effects of maleated polypropylene and cellulose content. *Journal of Applied Polymer Science*, 87, 337-345.

Rioux, B., Lspas-Szabo, P., Ait-Kadi, A., Mateescu, M. A., & Juhasz, J. (2002). Structure-properties relationship in cross-linked high amylose starch cast films. *Carbohydrate Polymers*, 50, 371-378.

Romhany, G., Karger-Kocsis, J., & Czigany, T. (2003). Tensile fracture and failure behavior of thermoplastic starch with unidirectional and cross-ply flax fiber reinforcements. *Macromolecular Materials and Engineering*, 288, 699-707.

Rosentrater, K. A., & Otieno, A. W. (2006). Considerations for manufacturing bio-based plastic products. *Journal of Polymers and the Environment*, 14, 335-346.

Saiah, R., Sreekumar, P. A., Gopalakrishnan, R., Leblanc, N., Gattin, R., & Saiter, J. M. (2009). Fabrication and characterization of 100% green composite: Thermoplastic based on wheat flour reinforced by flax fibers. *Polymer Composites*, 30, 1595-1600.

Sang, Y., Prakash, O., & Seib, P. A. (2007). Characterization of phosphorylated cross-linked resistant starch by 31p nuclear magnetic resonance (p-31 nmr) spectroscopy. *Carbohydrate Polymers*, 67, 201-212.

Seker, M., & Hanna, M. A. (2005). Cross-linking starch at various moisture contents by phosphate substitution in an extruder. *Carbohydrate Polymers*, 59, 541-544.

Seker, M., & Hanna, M. A. (2006). Sodium hydroxide and trimetaphosphate levels affect properties of starch extrudates. *Industrial Crops and Products*, 23, 249-255.

Seo, J. A., Kim, J. C., Koh, J. K., Ahn, S. H., & Kim, J. H. (2009). Preparation and characterization of crosslinked cellulose/sulfosuccinic acid membranes as proton conducting electrolytes. *Ionics*, 15, 555-560.

Shalviri, A., Liu, Q., Abdekhodaie, M. J., & Wu, X. Y. (2010). Novel modified starch-xanthan gum hydrogels for controlled drug delivery: Synthesis and characterization. *Carbohydrate Polymers*, 79, 898-907.

Siddique, R., Khatib, J., & Kaur, I. (2008). Use of recycled plastic in concrete: A review. *Waste Management*, 28, 1835-1852.

Simkovic, I., Hricovini, M., Mendichi, R., & van Soest, J. J. G. (2004). Cross-linking of starch with 1, 2, 3, 4-diepoxybutane or 1, 2, 7, 8-diepoxyoctane. *Carbohydrate Polymers*, 55, 299-305.

Singh, J., & Singh, N. (2003). Studies on the morphological and rheological properties of granular cold water soluble corn and potato starches. *Food Hydrocolloids*, 17, 63-72.

Singh, N., & Kaur, L. (2004). Morphological, thermal, rheological and retrogradation properties of potato starch fractions varying in granule size. *Journal of the Science of Food and Agriculture*, 84, 1241-1252.

Steeneken, P. A. M., & Woortman, A. J. J. (2009). Identification of the thermal transitions in potato starch at a low water content as studied by preparative dsc. *Carbohydrate Polymers*, 77, 288-292.

Takatani, M., Ikeda, K., Sakamoto, K., & Okamoto, T. (2008). Cellulose esters as compatibilizers in wood/poly(lactic acid) composite. *Journal of Wood Science*, 54, 54-61.

Thomas, D. J., & Atwell, W. A. (1999). Starches. St. Paul, Minn.; Eagan Press.

Trejo-O'Reilly, J. A., Cavaille, J. Y., & Gandini, A. (1997). The surface chemical modification of cellulosic fibres in view of their use in composite materials. *Cellulose*, 4, 305-320.

VanderBurgt, M. C., VanderWoude, M. E., & Janssen, L. (1996). The influence of
    plasticizer on extruded thermoplastic starch. *Journal of Vinyl & Additive
    Technology*, 2, 170-174.

Wang, N., Yu, J. G., & Ma, X. F. (2007). Preparation and characterization of
    thermoplastic starch/pla blends by one-step reactive extrusion. *Polymer
    International*, 56, 1440-1447.

Wang, X. L., Yang, K. K., & Wang, Y. Z. (2003). Properties of starch blends with
    biodegradable polymers. *Journal of Macromolecular Science-Polymer Reviews*,
    C43, 385-409.

Weber, F. H., Queiroz, F. P. C., & Chang, Y. K. (2008). Freeze-thaw stability of normal,
    waxy and high amylose corn starch gels with added guar and xanthan gums.
    Ciencia E Tecnologia De Alimentos, 28, 413-417.

White, P. J., Abbas, I. R., & Johnson, L. A. (1989). Freeze-thaw stability and
    refrigerated-storage retrogradation of starches. *Starch-Starke*, 41, 176-180.

Woo, K., & Seib, P. A. (1997). Cross-linking of wheat starch and hydroxypropylated
    wheat starch in alkaline slurry with sodium trimetaphosphate. *Carbohydrate
    Polymers*, 33, 263-271.

Xie, F. W., Liu, H. S., Chen, P., Xue, T., Chen, L., Yu, L., et al. (2006). Starch
    gelatinization under shearless and shear conditions. *International Journal of Food
    Engineering*, 2.

Xie, S. X., Liu, Q., & Cui, S. W. (2005). Starch modifications and applications. In S. W.
    Cui (Ed) *Food carbohydrates: chemistry, physical properties, and applications* pp.
    359-382. Boca Raton: CRC press.

Xu, X., Jayaraman, K., Morin, C., & Pecqueux, N. (2008). Life cycle assessment of
    wood-fibre-reinforced polypropylene composites. *Journal of Materials
    Processing Technology*, 198, 168-177.

Yu, L., Dean, K., & Li, L. (2006). Polymer blends and composites from renewable
    resources. *Progress in Polymer Science*, 31, 576-602.

Yu, L., Petinakis, S., Dean, K., Bilyk, A., & Wu, D. Y. (2007). Green polymeric blends and composites from renewable resources. *Macromolecular Symposia*, 249, 535-539.

Zhang, J., & Wang, Z. W. (2009). Optimization of reaction conditions for resistant canna edulis ker starch phosphorylation and its structural characterization. *Industrial Crops and Products*, 30, 105-113.

APPENDICES

Appendix A.   DSC thermograms of starch gelatinization
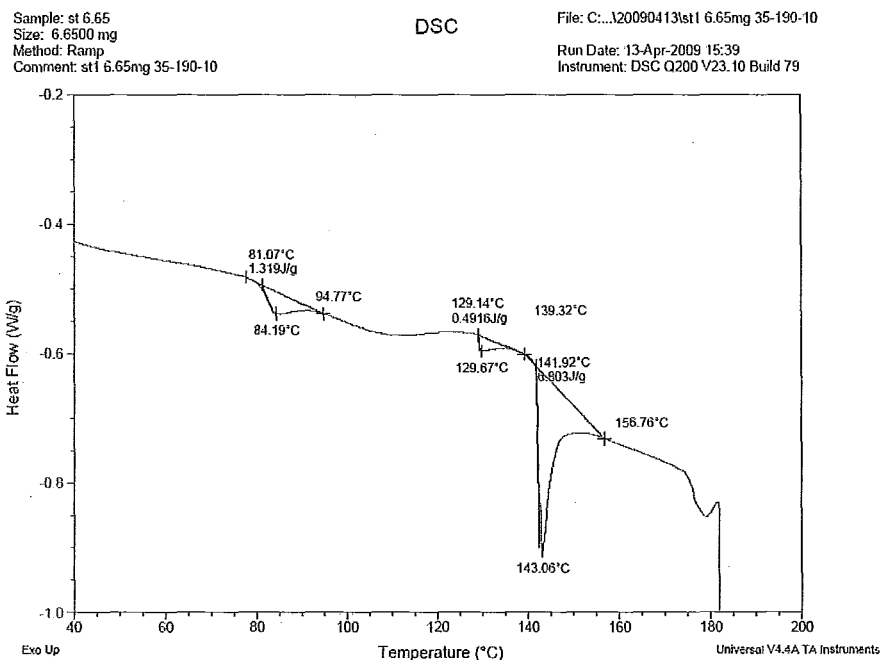
Figure A. 1 DSC thermogram of starch gelatinization containing 35.6 wt % water and 33.9 wt % glycerol (percentage based on dry starch weight).
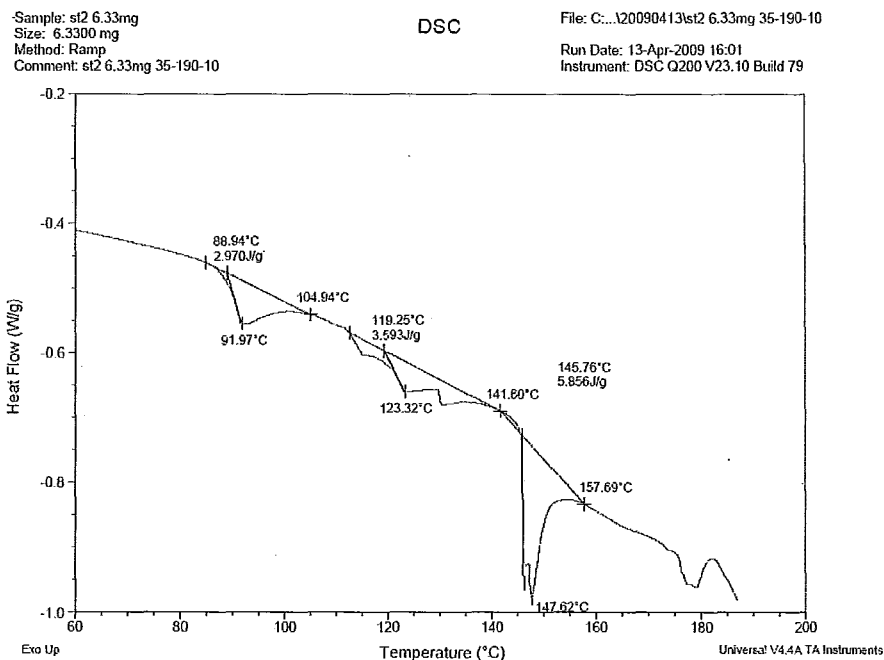
Figure A. 2 DSC thermogram of starch gelatinization containing 35.6 wt % water and 56.5 wt % glycerol (percentage based on dry starch weight).
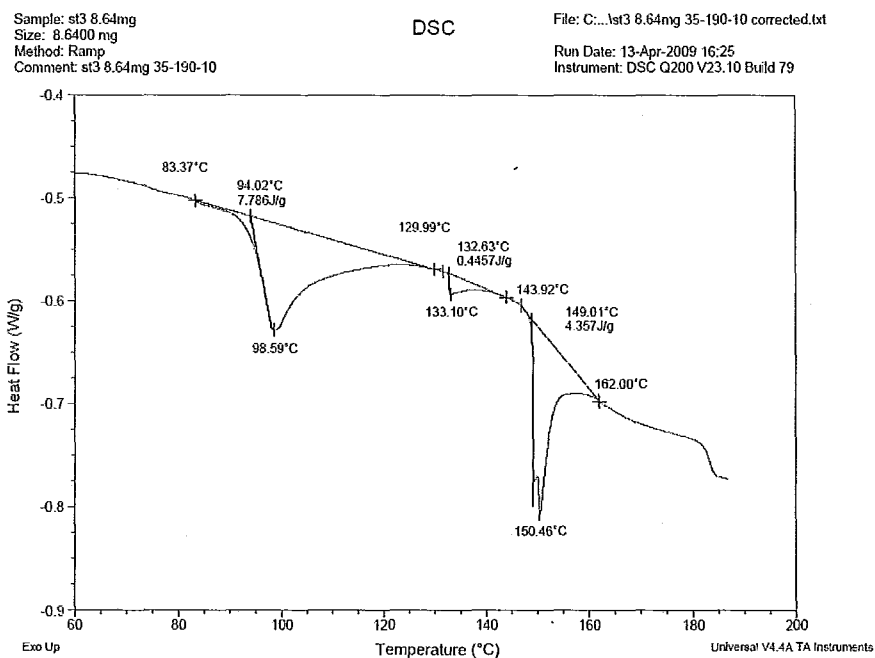
Figure A. 3 DSC thermogram of starch gelatinization containing 35.6 wt % water and 79.1wt % glycerol (percentage based on dry starch weight).
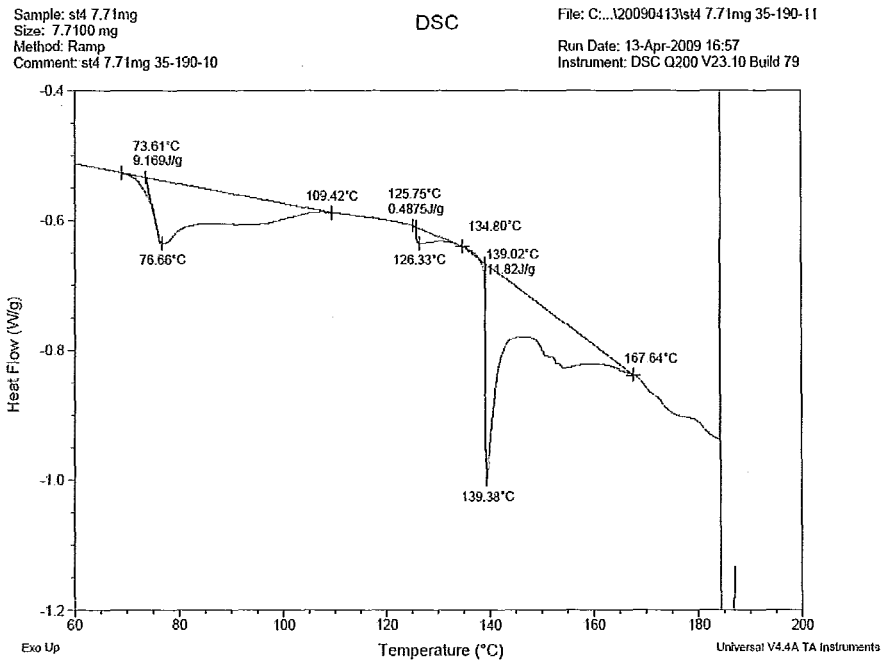
Figure A. 4 DSC thermogram of starch gelatinization containing 58.2 wt % water and 33.9 wt % glycerol (percentage based on dry starch weight).
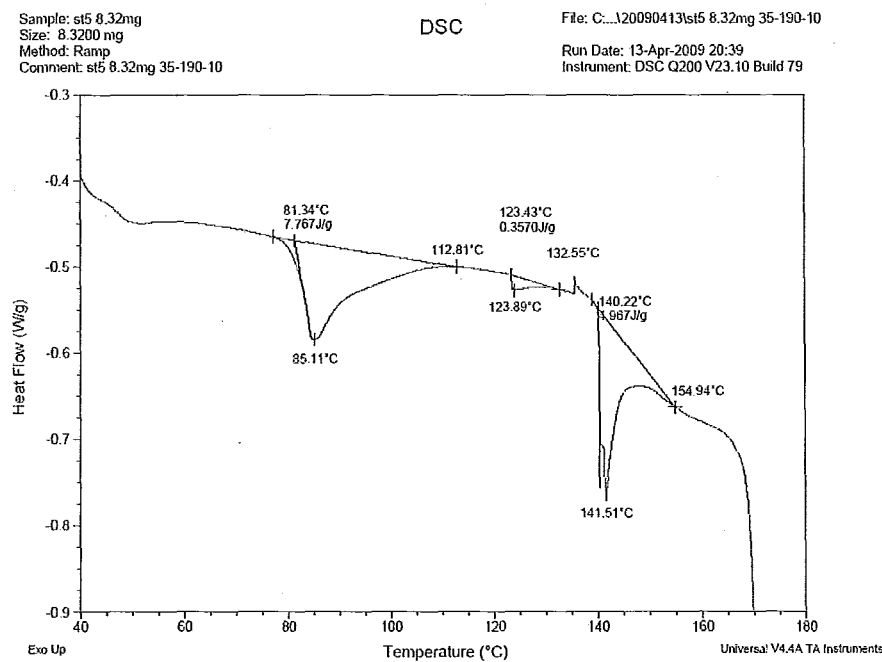
Figure A. 5 DSC thermogram of starch gelatinization containing 58.2 wt % water and 56.5 wt % glycerol (percentage based on dry starch weight).
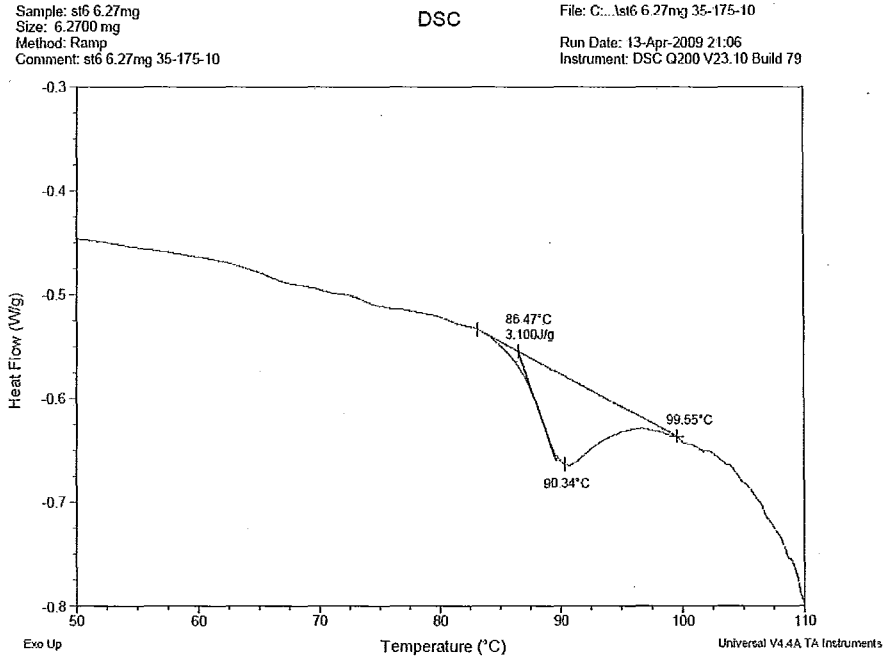
Figure A. 6   DSC thermogram of starch gelatinization containing 58.2 wt % water and 79.1wt % glycerol (percentage based on dry starch weight).
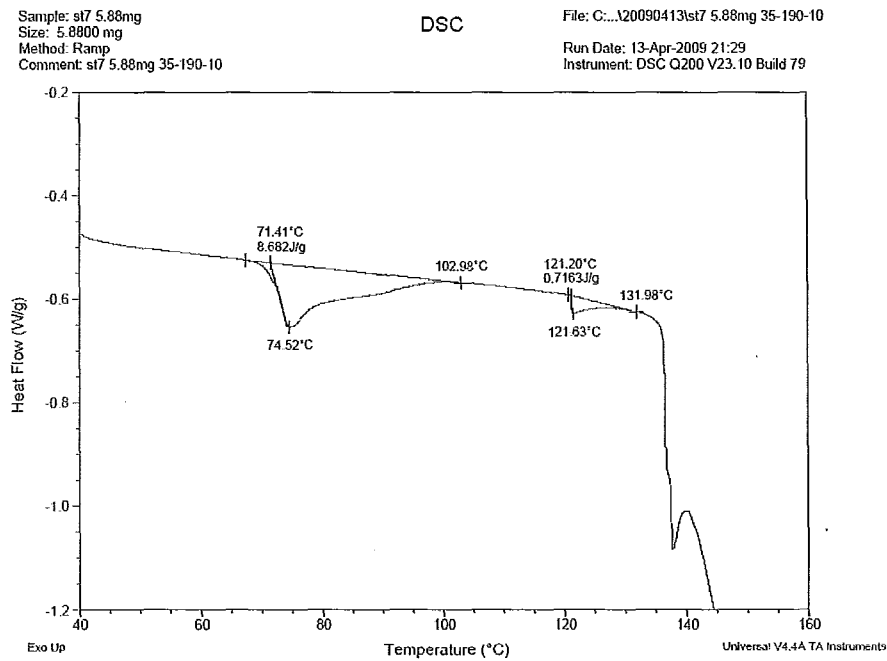
Figure A. 7   DSC thermogram of starch gelatinization containing 80.8 wt % water and 33.9 wt % glycerol (percentage based on dry starch weight).

151
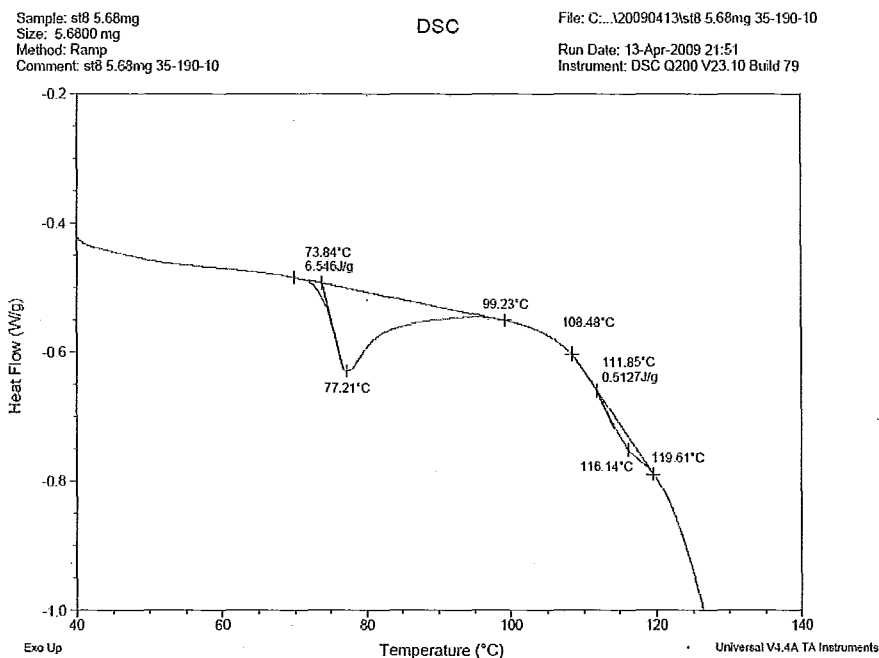
Figure A. 8 DSC thermogram of starch gelatinization containing 80.8 wt % water and 56.5 wt % glycerol (percentage based on dry starch weight).
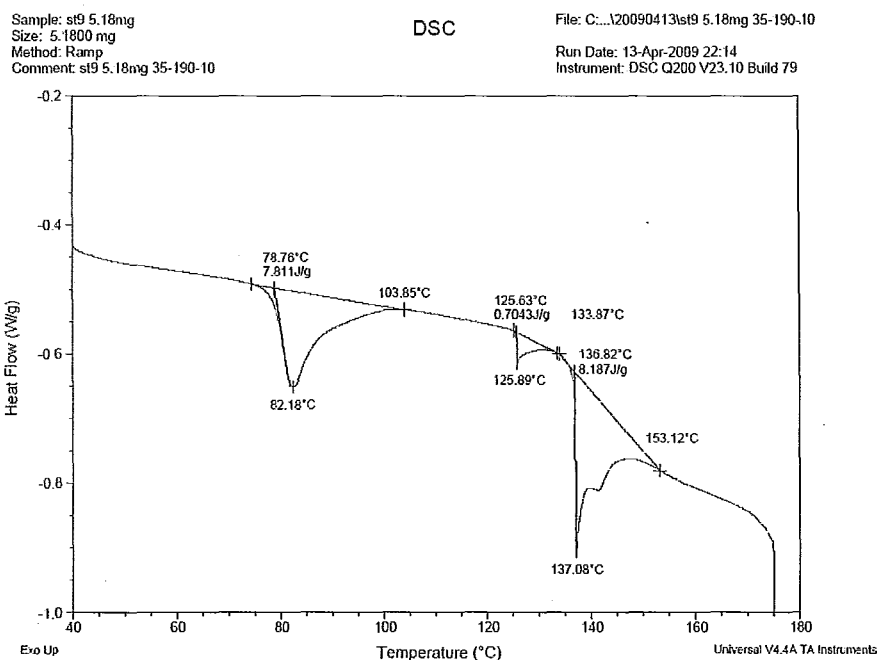
Figure A. 9 DSC thermogram of starch gelatinization containing 80.8 wt % water and 79.1 wt % glycerol (percentage based on dry starch weight).

Appendix B.   Contact angle plots of sisal fiber reinforced crosslinked starch biocomposites after surface modification

$y = -0.0797x + 100.79$

$R^2 = 0.9891$
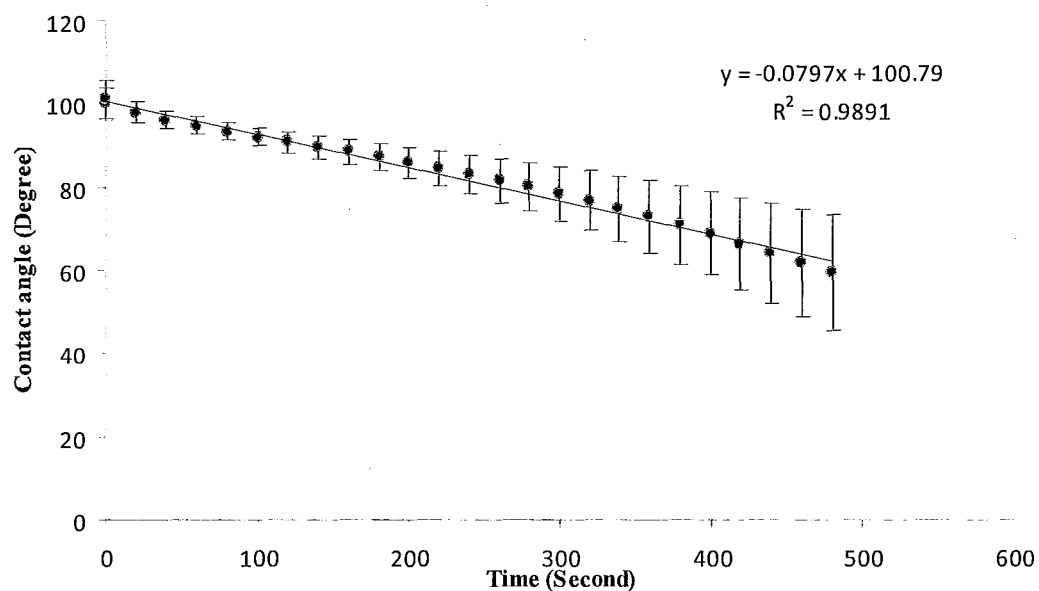
Figure B. 1 The contact angle changing over time of sisal fiber reinforced crosslinked starch with 2.5 wt% fiber content based on dry starch weight after surface treatment.
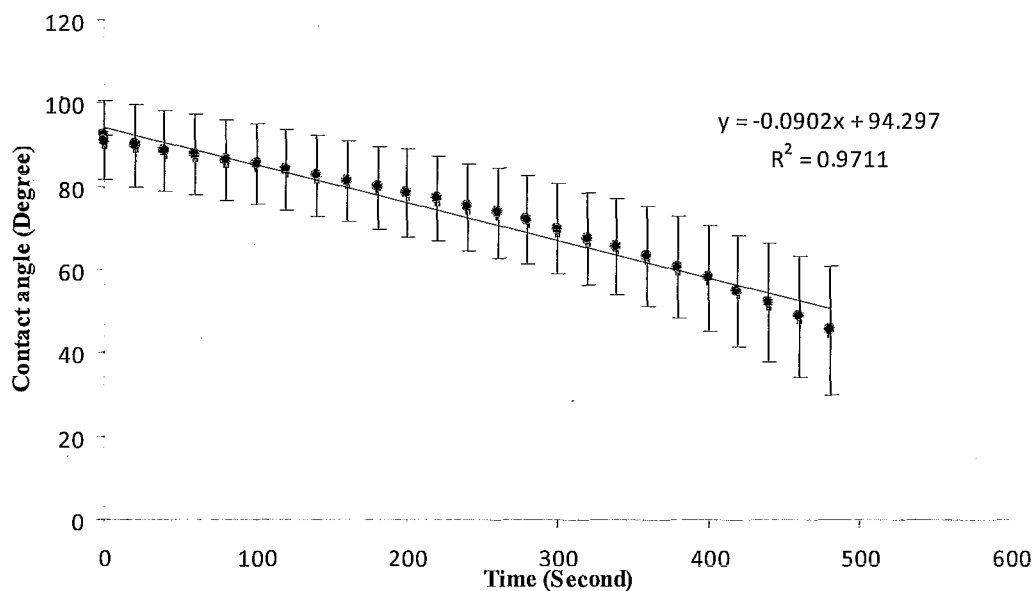
Figure B. 2 The contact angle changing over time of sisal fiber reinforced crosslinked starch with 5.0 wt% fiber content based on dry starch weight after surface treatment.
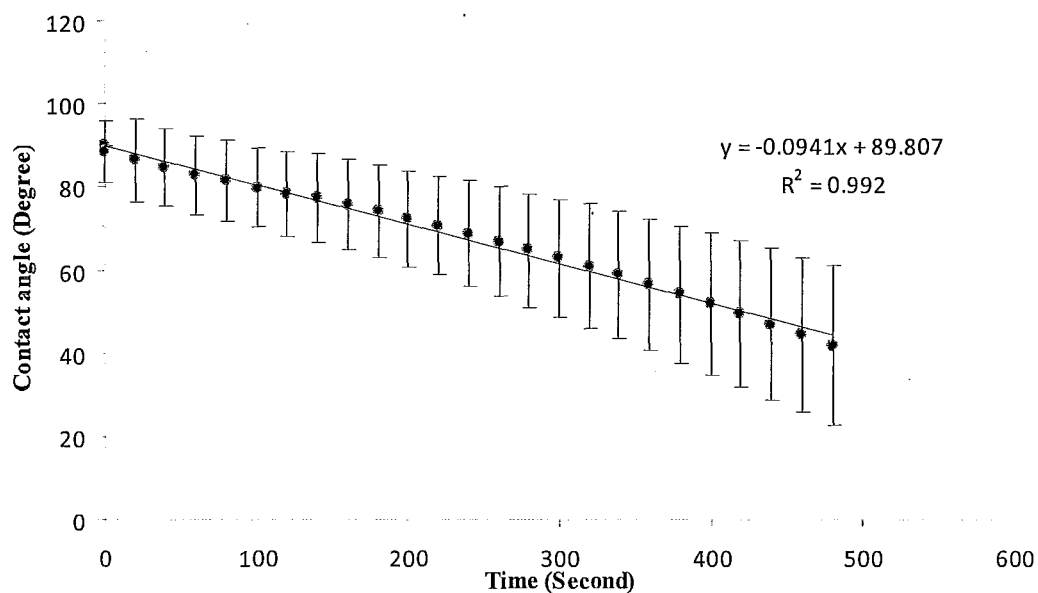
Figure B. 3 The contact angle changing over time of sisal fiber reinforced crosslinked starch with 10 wt% fiber content based on dry starch weight after surface treatment.
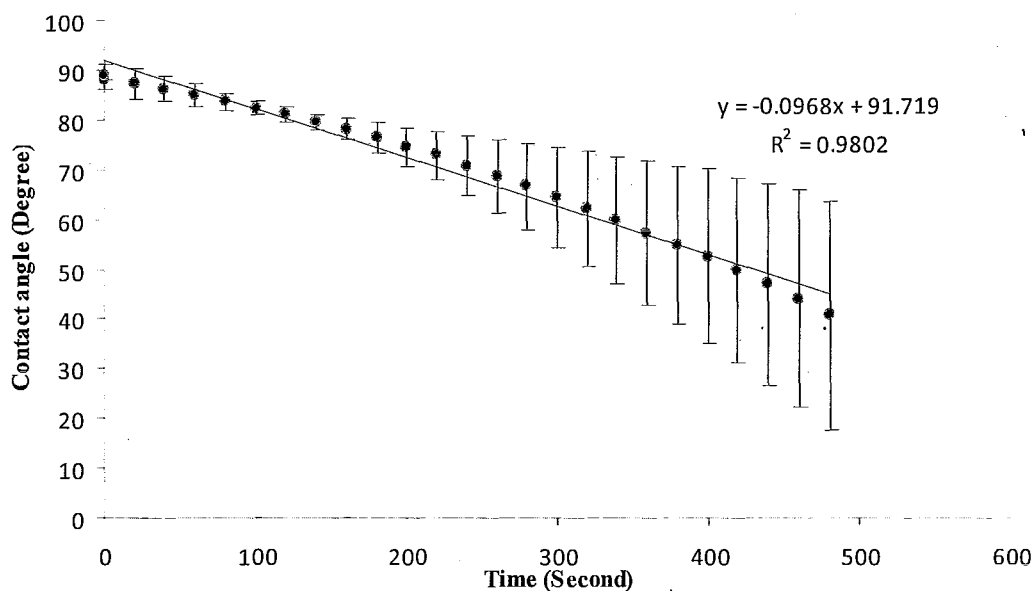
Figure B. 4 The contact angle changing over time of sisal fiber reinforced crosslinked starch with 15 wt% fiber content based on dry starch weight after surface treatment.
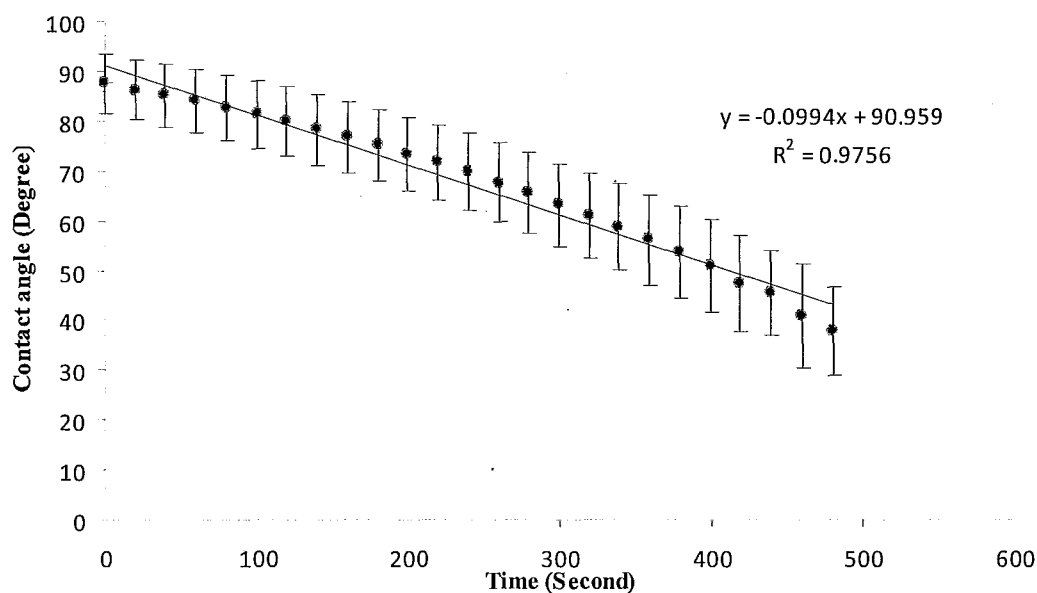
Figure B. 5 The contact angle changing over time of sisal fiber reinforced crosslinked starch with 20 wt% fiber content based on dry starch weight after surface treatment.

The chart shows contact angle (Degree) on the y-axis from 0 to 90 and Time (Second) on the x-axis from 0 to 600.

$$y = -0.1044x + 74.999$$
$$R^2 = 0.9831$$
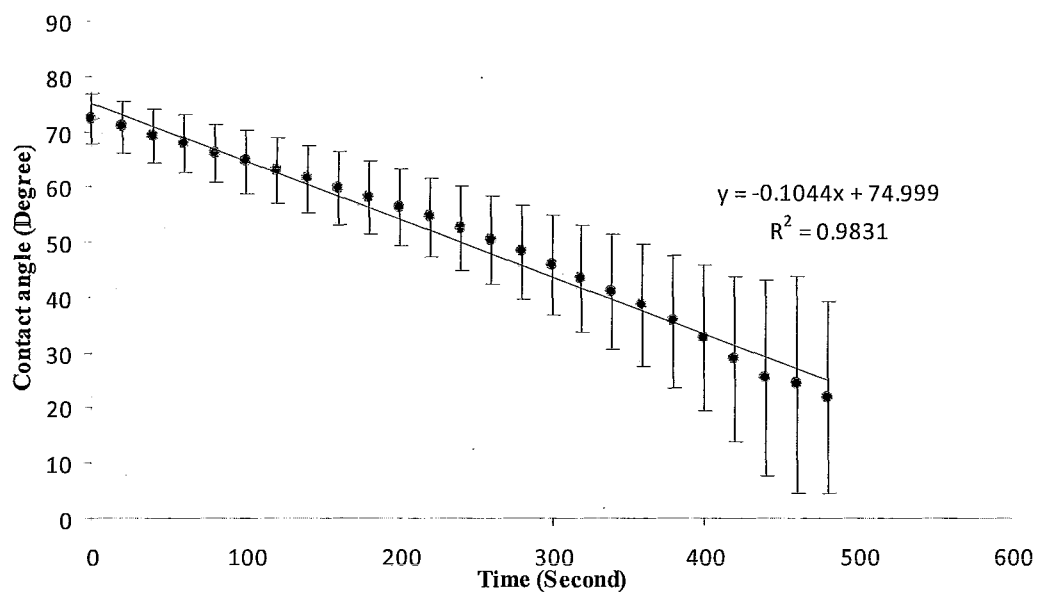
Figure B. 6 The contact angle changing over time of sisal fiber reinforced crosslinked starch with 25 wt% fiber content based on dry starch weight after surface treatment.

156